DISTINCT SENSORY REPRESENTATIONS OF WIND AND NEAR-FIELD SOUND IN THE *DROSOPHILA* BRAIN

Thesis by

Suzuko Yorozu

In Partial Fulfillment of the Requirements

for the Degree of

Doctor of Philosophy

California Institute of Technology

Pasadena, California

2010

(Defended May 10, 2010)

Acknowledgements

I am grateful for the support and advice of many people who helped me to complete the work in this thesis. Firstly, and most importantly, I wish to thank my advisor, David Anderson, who taught me to be a creative but careful thinker, an effective communicator, and a better scientist. His intellectual rigor together with his creativity and dedication for science make him a great mentor and an exceptional scientist. His curiosity and clear thinking has always been an inspiration and guidance for my research work. I will always be grateful for his advice and support.

I was incredibly lucky to have the chance to interact with other exceptional scientists as my committee members, including Seymour Benzer, Paul Sternberg, Kai Zinn, and Michael Dickenson. I greatly appreciate their support and helpful suggestions during my graduate work. I also greatly enjoyed interacting with Seymour who truly loved science, food, culture, and life.

The Anderson lab houses a wealth of knowledge and talent. I deeply appreciate the time that Allan Wong spent to train me and introduce me to the calcium response imaging technique, which allowed me to obtain many interesting results in my work. I appreciated Anne Hergarden for being a friendly colleague. I enjoyed sharing our office together, and talking about science and life in general. I also would like to thank other lab members, Heiko Dankert, Tim Tayler, Tim Lebestky, Kiichi Watanabe, Liming Wang, Hidehiko Inagaki, Haijiang Cai, Dayu Lin, Hyosang Lee, Todd Anthony, Sophia Vrontou, Wulf Haubensak, Prabhat Kunwar, and Li-ching Lo for their support and advice.

My graduate experience was blessed by the support of exceptional lab managers, Gaby Mosconi and Gina Moncuso. They not only helped me carry out the project efficiently, but their caring characters brought lots of smiles and comfort to the lab. I also don't want to forget to thank Gaby for bringing us weekly delicious treats, which made our weekend work so much easier.

I would like to thank Mark Konishi and his former post-doc fellow, Brian J. Fischer, for their advice and support, and for letting me use their lab space and equipment. I also thank Gilles Laurent for inviting me to carry out a rotation project in his lab. I would especially like to thank Stijn Cassenaer, Glenn Turner, and Vivek Jayaman for introducing me to electrophysiological recording techniques, which became very handy for this thesis project.

I also met wonderful people outside the lab Caltech. I am grateful to Peter Lee, whose wisdom and encouragement helped me through some difficult times. Also, countless thanks goes to my boot camp class members at the Caltech gym: Candice, Tina, Gordon, Michelle, Monica, and other girls. Their energy and friendly faces made me forget all the insignificant worries and doubts that I had in me. I truly enjoyed their company. I also thank HeeJu Kim, Monica Martinez, and Jung Sook Chang for their emotional support.

Foremost, I thank my family for continuous support throughout my life. The confidence and strength that I gained from them cannot be quantified.

ABSTRACT

Behavioral responses to wind are thought to play a critical role in controlling the dispersal and population genetics of wild *Drosophila* species, as well as their navigation in flight, but their underlying neurobiological basis is unknown. I show that *Drosophila melanogaster*, like wild-caught *Drosophila* strains, exhibits robust wind-induced suppression of locomotion (WISL), in response to air currents delivered at speeds normally encountered in nature. Furthermore, I identify wind-sensitive neurons in the Johnston's organ (JO), an antennal mechanosensory structure previously implicated in near-field sound detection. Using Gal4 lines targeted to different subsets of JO neurons, and a genetically encoded calcium indicator, I show that wind and near-field sound (courtship song) activate distinct JO populations, which project to different regions of the antennal and mechanosensory motor center (AMMC) in the central brain. Selective genetic ablation of wind-sensitive JO neurons in the antenna abolishes WISL behavior, without impairing hearing. Different neuronal sub-populations within the wind-sensitive population, moreover, respond to different directions of arista deflection caused by airflow and project to different regions of the AMMC, providing a rudimentary map of wind direction in the brain. Importantly, sound- and wind-sensitive JO neurons exhibit different intrinsic response properties: the former are phasically activated by small, bidirectional displacements of the aristae, while the latter are tonically activated by unidirectional, static deflections of larger magnitude. These different intrinsic properties are well suited to the detection of oscillatory pulses of near-field sound and laminar airflow, respectively. These data identify wind-sensitive neurons in JO, a structure that

has been primarily associated with hearing, and reveal how the brain can distinguish different types of air particle movements, using a common sensory organ.

TABLE OF CONTENTS

LIST OF ILLUSTRATIONS

Chapter 1

Chapter 2

Chapter 3

Chapter 1

Introduction

Introduction

All animals have evolved to respond rapidly to various sensory stimuli that threaten or enhance their survival and reproduction. At any moment in nature, animals have to figure out details about various aspects of stimuli surrounding them to make a judgment about the current status of the environment, whether the stimuli pose a threat or an opportunity to feed or mate. For example, animals may need to figure out whether the predator in the far distance is moving or stationary. How fast is it moving? At the same time, they might have to figure out from which direction a conspecific calling song is coming, and whether it is getting louder or quieter. They need to be able to detect and discriminate biologically relevant stimuli accurately and quickly to maximize their survival. So, how did the animal's nervous system evolve to facilitate rapid and accurate sensory information processing? Are there common strategies used by many sensory systems from various organisms for efficient sensory information processing?

One of the goals in neurobiology is to understand how sensory information is processed, from its initial detection in the periphery to the eventual generation of percepts that drive behavioral outputs. There are many types of mechanisms and strategies that may be involved in sensory information processing. Some mechanisms might be specific for processing certain types of sensory stimuli, while others might be common to all sensory systems, since they are essential for efficient sensory information processing. Among all mechanisms and strategies used by various sensory systems, which are the critical components for accurate and rapid sensory information processing? To provide insight into these questions, I will discuss first the general mechanisms involved in sensory systems, and second the common mechanisms used by various systems to

facilitate efficient sensory information processing, by comparing three types of mammalian sensory systems. Finally, I will also compare mammalian and insect sensory systems to discuss whether there are common strategies used for efficient and accurate sensory information processing by different organisms across phylogeny.

The sensory nervous system

Our brain receives sensory information about sight, sound, taste, touch, smell, temperature, balance, and limb position, among other stimuli from specialized sensory organs in the peripheral nervous system. Each sensory organ contains specialized sensory receptor cells whose major function is to transform physical or chemical stimuli into a code of neural impulses and transmit these electrical signals to neurons in the higher-order processing centers for further computations and transformations (Bloom and Lazerson, 1988; Kandel et al., 2000). In some systems, the receptor cells have the afferent fibers projecting to the second-order processing center (i.e., olfaction), while in other systems (i.e., hearing and gustation), the receptor cells do not have fibers, but they communicate to other fiber-bearing cells that project to the central nervous system (Norgren, 1983; Rusznak and Szucs, 2009; Sullivan et al., 1995). After multiple transformations in the higher order processing centers, the brain pieces together all of the information it receives from various sensory modalities at any given moment to construct a coherent percept of the external world (Bloom and Lazerson, 1988; Kandel et al., 2000).

Sensory receptor cells convey four basic types of information about the stimulus: modality, time, intensity, and location (Fechner, [1860] 1966). All four of these

elementary attributes of stimuli influence our sensory perception in important ways, and how our sensory systems encode these elements impacts their efficiency. We will now briefly look at the four basic attributes of stimuli encoded by the sensory receptors.

Encoding modality

Modality defines the general classes of stimulus that receptors are specialized to recognize. For example, vision, audition, olfaction, gustation, and somesthesia (which includes tactile, pain, temperature, itch, proprioception, and visceral sense) are the major modalities that humans experience. Each modality is encoded by a specific class of receptors, and usually no overlapping usage of receptors is observed between modalities (Kandel et al., 2000). For each modality, there are several constituent qualities or submodalities, which are encoded by different receptors. For example, gustation has five constituent qualities: sweet, sour, salty, bitter, and Umami, and are encoded by different gustatory receptors (Chandrashekar et al., 2006; Montell, 2009). Thus, each modality is represented by the ensemble of receptors that belong to a specific class.

Encoding stimulus intensity

Sensory receptors also encode information about the intensity of stimulus. The intensity of a stimulus refers to its magnitude or strength, which contributes to the salience of the stimulus under certain circumstances. For example, the louder the sound of a predator or the stronger the scent of a predator, the closer the danger is for many animals in nature. Thus, accurate knowledge of the intensity of a stimulus directly relates to the survival of animals in nature.

The encoding of stimulus intensity is usually achieved by varying the firing frequency of the sensory afferent fibers (Adrian and Zotterman, 1926). When the stimulus magnitude increases, the firing frequency of the afferent fibers also increases. Moreover, the stronger the stimulus, the greater the number of afferent fibers (and receptors) that are activated; thus, intensity of stimulus is coded by the firing frequency of an ensemble of afferent fibers (and sensory receptor cells).

The lowest possible stimulus magnitude that an organism can detect is reflected in the activation threshold of the sensory receptors, and is related to the sensitivity of the system. In order to truly increase the sensitivity of the system, the receptors should be able to detect both low stimulus intensities and a wide dynamic range of stimulus intensities. Different sensory systems have developed different mechanisms to improve sensitivity, as will be discussed later in this chapter.

Encoding stimulus time

The duration and temporal properties of a stimulus (i.e., the rate at which the stimulus intensity increases or decreases) are encoded by various types of receptors with different response properties (i.e., adaptation rate and activation threshold). In the mammalian glabrous skin, there are several types of mechanoreceptor structures, including the slowly adapting Merkel discs, rapidly adapting Meissner's corpuscles and Pacinian corpuscles, that encode different temporal aspects of light touch stimulation (Johnson, 2001; Johnson and Hsiao, 1992). For example, when a probe touches the skin for several seconds, the initial spike discharge reflects both the total amount of pressure applied to the skin and the speed at which the skin is indented. The acceleration and

velocity of skin indentation are encoded by the rapidly adapting Meissner's corpuscles and Pacinian's corpuscles, which respond only at the beginning and end of the stimulus, and are specialized to encode the rate at which stimulus is applied or removed (Loewenstein and Mendelson, 1965; Torre et al., 1995). In contrast, the stimulus duration is encoded by the slowly adapting Merkel discs, which are able to respond throughout continuous prolonged stimulation (Vallbo and Johansson, 1984). The activation of rapidly adapting receptors at the beginning and end of stimulation provide a information about the changing sensory environment while the activation of slowly adapting receptors provide a information about the presence of a prolonged stimulus.

Encoding stimulus location

The location of the stimulus conveys important spatial information about the stimulus, such as its size and directionality (Kandel et al., 2000). For example, animals in nature have to figure out the size of an approaching object (i.e., predator), from which direction the object is approaching, or from which direction a con-specific calling song is coming. The accurate representation of the location and size of a stimulus is thus obviously an important aspect of sensory coding. For many modalities, such as vision, audition, touch, pain, and temperature, the spatial location of a stimulus is represented by the spatial arrangement of the ensembles of activated receptors in a sense organ, which is called a receptive field (Hubel, 1963; Hubel and Wiesel, 1968; Kandel et al., 2000).

The size of a receptive field influences how well a sensory system can resolve small details of the stimulus. Denser populations of receptors have smaller receptive fields, which allows finer resolution of spatial details of the stimulus (Cleland et al.,

1979; Vallbo and Johansson, 1978). The size of receptive fields is not uniform within a given sensory organ. For example, mechanoreceptors are not uniformly distributed across our body parts. Our fingertips contain smaller receptive fields with more densely populated receptors, compared to our thoracic region, which allows us to discriminate fine details of objects that we touch (Weinstein, 1968). Similarly, the fovea of the retina has a better ability to resolve small details of the visual stimulus compared to the retinal periphery, because the fovea contains a denser population of cone photoreceptors with smaller receptive fields (Hubel, 1988). Thus the size of a receptive field is related to the acuity of a given sensory system.

As we have discussed so far, receptors transform physical stimuli into a code of neural impulses, which contains basic information about stimulus modality, intensity, time, and location. These four elementary attributes of stimuli influence our perception of the salience of stimuli and percepts in different ways.

Accumulating evidence suggests that there are common strategies used by many sensory systems to improve their sensitivity, acuity, and speed of information processing. For the improvement of sensitivity, most sensory systems seem to modify either the structure or circuit organization in the periphery. For the improvement of acuity (or ability to resolve small differences), many sensory systems utilize inhibitory mechanisms in both the periphery and higher order processing centers of the brain. Finally, to improve the speed of information processing, many systems modify the circuit organization. To illustrate these points, I will mainly focus on the sensory systems that are activated by physical stimuli (pressure, sound waves, and photons), and compare

three mammalian sensory systems, which are located in bilaterally symmetrical organs- the visual, auditory, and tactile systems.

Common mechanisms to improve sensitivity

The sensitivity of most sensory systems is primarily determined by the property of the sensory receptor cells; however, it can be improved by different amplification mechanisms. Some sensory systems make use of structure-based amplification, while others make use of circuit-based amplification.

Many nocturnal animals have exquisite nighttime vision due to the tapetum lucidum, an extra layer of tissue behind the retina, which contains reflective material such as zinc-cysteine and riboflavin (Ollivier et al., 2004). The tapetum lucidum allows light to pass through the photoreceptors twice to increase the sensitivity of the eyes in a dim light environment. Although there are variations among different organisms regarding the structure, location, and choice of reflective materials, the tapetum lucidum represents a remarkable example of a sensory organ that achieves structure-based amplification as an adaptation to a dim light environment.

Our hearing organs also utilize a structure-based amplification mechanism. Most mammalian cochlea contain two types of hair cells, inner and outer hair cells (Moller, 2003). The inner hair cell is the auditory receptor, which transforms acoustic energy into electrical signals, while outer hair cells are involved in gain control. The outer hair cells, together with the stapedius muscle in the middle ear that controls how hard the stapes hits the oval window, are capable of both amplifying faint sound to increase our hearing range and reducing the energy of loud sound to protect our ears from damage (Moller,

2003). This gain control by the outer hair cells is due to the motion of the outer hair cell body in response to changes in the cell membrane potential, called electromotility (Holley and Ashmore, 1988; Liberman et al., 2002). When an isolated outer hair cell is depolarized, its cell body shortens. Conversely, when an isolated outer hair cell is hyperpolarized, its cell body elongates (Holley and Ashmore, 1988). At low sound intensities, the outer hair cells improve the mechanical performance of the cochlea by increasing the magnitude of electromotility, which in turn, amplifies the basilar membrane motion to increase hearing sensitivity (Ashmore, 2008; Dallos, 2008).

In contrast to nocturnal animals, diurnal animals do not have a tapetum lucidum, thus their nighttime vision is nowhere near as sensitive as that of nocturnal animals. Nevertheless, they also utilize sensitivity amplification mechanisms to improve their nighttime vision. However, in this case the mechanism is circuit-based rather than structure-based. The retina of diurnal mammals, including humans, contains two major types of photoreceptors, rods and cones. Rods contain more photosensitive visual pigments than cones, thus, rods function well in nighttime vision, while cones function better in high illumination conditions (Kandel et al., 2000; Moller, 2003). Thus sensitivity is an issue for rods rather than cones. While rods are sensitive enough to respond to a single photon of light (Baylor et al., 1979; Baylor et al., 1984), their signals are further amplified by converging axons of multiple rods onto a single target bipolar cell. However, improved sensitivity with high convergence of rods onto a single ganglion cell comes at a cost of visual acuity, since a high convergence of rods increases the size of the ganglion cell receptive fields, which causes reduced acuity (Kandel et al., 2000). This is why it is difficult to resolve small differences in dim light conditions. The

circuit-based amplification using a high convergence of receptors onto the target neuron is also observed in the olfactory system (Masse et al., 2009; Mori et al., 1999; Sullivan et al., 1995). Multiple olfactory receptor neurons expressing the same odorant receptor converge on the same glomerulus in the olfactory bulb.

Cones, in contrast, require more acuity than sensitivity, since they function in high illumination conditions. Cones, especially in the fovea, do not show high convergence onto a single bipolar cell; rather, they synapse on multiple bipolar cells, and achieve high acuity by increasing the receptor density in the fovea, where receptive fields are very small. Similar to the cones of the eyes, the tactile system requires more acuity than sensitivity. The high acuity is achieved by increasing the receptor density in certain areas of the body surface (i.e., fingertips and tongue) and by making the receptive fields smaller to increase their acuity (Johansson and Vallbo, 1983).

Thus, most sensory systems seem to have a mechanism to improve sensitivity (or acuity), however, the mechanisms used are different depending on the system.

Lateral inhibition is a general mechanism to improve acuity

The interaction between the excitation and inhibition is the basis for many kinds of computational processes that occur in the nervous system (Kandel et al., 2000; von Bekesy, 1967b). Lateral inhibition is an inhibitory mechanism that arises from the activities of local inhibitory interneurons to modulate the activities of the neighboring excitatory neurons. The Nobel Prize–winning work by Haldan Keffer Hartline demonstrated that lateral inhibition (in the retina) is a neural mechanism that most animals, including humans, use to better discriminate borders by increasing the contrast

(Hartline et al., 1956; Ratliff et al., 1959). The effect of lateral inhibition in the retina can be best illustrated by the phenomenon called "Mach band," which was discovered by Ernst Mach (Ratliff, 1965). Figure 1 shows seven gray rectangular bands next to each other. Each of the seven bands is a fixed shade of gray but the area around the left edge appears lighter than the center area, and the area around the right edge appears darker than the center. The Mach band illusion is caused by lateral inhibition of the photoreceptor cells by the horizontal (inhibitory) cells in the retina (Fig. 1a–b). Lateral inhibition in the retina is an example of how sensory information processing begins in the periphery. In addition, the Mach band effect demonstrates that what we see is not exactly "what is out there." It is an excellent illustration of how the brain is organized to "actively" construct our perception rather than to reproduce a faithful replication of the physical world in order to facilitate our sensory interpretation.

The use of inhibitory mechanisms to improve acuity is a general phenomenon that applies to other sensory systems (von Bekesy, 1967a). For example, lateral inhibition is particularly important for fine tactile discrimination involved in Braille reading (DiCarlo and Johnson, 2002; DiCarlo et al., 1998; von Bekesy, 1960). When two Braille dots strike our fingertip, two populations of Merkel cells are activated. When two dots are far apart, two non-overlapping Merkel cell populations are activated on the skin. In contrast, when two dots are closer together, two overlapping populations are activated. If there is no lateral inhibition between the two overlapping populations, we will not be able to discriminate the two closely positioned dots. Lateral inhibition enhances the separation of the two active populations, which allows us to discriminate two closely positioned dots in space.

Lateral inhibition is also used to enhance pitch discrimination in mammalian auditory systems (Ma and Suga, 2004; Paolini et al., 2005; Paolini et al., 1998; Suga, 1995). The transformation of acoustic energy into electrical impulses involves the displacement of the basilar membrane, which causes the inner hair cells to bend against the tectorial membrane. The mechanical bending of the hair cells thus allows us to hear sound, and our ability to hear different sound frequencies depends on the location of the basilar membrane displacement, since the basilar membrane of the cochlea is organized into a tonotopic map: Higher frequency sound causes maximum displacement of the basilar membrane closer to its base near the stapes, while lower frequency sound produces maximum displacement of the basilar membrane closer to its apex near the helicotrema (Kandel et al., 2000; Moller, 2003). Our ability to discriminate similar frequencies is due to the lateral inhibition that occurs in the medulla. Each inner hair cell is innervated by multiples of spiral ganglion cells that project to the cochlear nuclei of the medulla. In the rat cochlear nuclei, there are three interconnected sub-nuclei that receive tonotopically organized inputs from the cochlea. Paolini et al. (1998) showed that lateral inhibition between these sub-nuclei sharpens the frequency discrimination.

Strategies for fast information processing

The visual environment consists of enormous amounts of information, which is extracted by our visual system. Color, depth, shape, orientation direction, and motion are just a few of the many features through which we interpret our visual environment. To achieve efficient processing for large amounts of information, the visual system utilizes a combination of parallel and hierarchical processing, which is also facilitated by the

layered structural organization of the cortex (Kandel et al., 2000; Nassi and Callaway, 2009). Distinct features, such as color, depth, shape, and motion, are processed in parallel channels, and within each channel, hierarchical processing takes place in such a manner that simpler properties emerge first in the periphery, and more sophisticated properties emerge later at higher processing centers in the cortex. At each information relay along the hierarchical processing centers, selective filtering of visual information occurs via complex interactions between inhibitory and excitatory neurons (e.g. lateral inhibition) to extract specific properties. Interestingly, the parallel processing of distinct features starts as early as the first synapse of the retina, because ganglion cells in the retina exhibit feature selectivity (Masland, 2001; Nassi and Callaway, 2009; Wassle, 2004). For example, there are object motion-selective ganglion cells called Brisk transient-Y cells (Olveczky et al., 2003), direction-selective ganglion cells (Barlow and Hill, 1963; Barlow and Levick, 1965; Fried et al., 2002), and color-selective ganglion cells called Midget (Diller et al., 2004; Wassle, 2004). The feature selective ganglion cells project to specific layers of the lateral geniculate nucleus. Color-selective ganglion cells project to layers 3–6 via the parvocellular pathway, while the direction-selective and object motion-sensitive ganglion cells project to layers 1–2 via the magnocellular pathway (Merigan and Maunsell, 1993). The information for color vision and motion detection is further processed by different layers of the primary visual cortex (Fitzpatrick et al., 1985; Hawken et al., 1988; Livingstone and Hubel, 1984; Ts'o and Gilbert, 1988). Thus, the visual system speeds up the information processing time by processing different features of visual information in the separate channels simultaneously. It is important to note that information from the parallel pathways is eventually unified to

generate a coherent visual image.

Parallel processing is not a unique property of the visual system; it is also found in most sensory modalities in the mammalian brain. The somatosensory system of rodents also utilizes parallel processing. In rats and other rodents, whiskers are highly sensitive and specialized sensory organs that allow the animals to navigate and recognize objects; thus whiskers convey both tactile and spatial information. Three parallel pathways from the periphery to the thalamus exist for processing object identity, object location, and the temporal information of whisking for motor control (Yu et al., 2006). The information regarding object identity is conveyed by the lemniscal pathway, while the spatial information regarding the location of an object is conveyed by the extralemniscal pathway (Pierret et al., 2000; Yu et al., 2006). Finally, the temporal information regarding the motor control of whisking is conveyed by the paralemniscal pathway. Thus, the whisking system in rats also utilizes layered structures to facilitate parallel processing of different features of whisking information.

In the auditory system, similar parallel pathways for sound localization and temporal pattern discrimination have been identified in the auditory cortex of humans (Courtney et al., 1996; Ungerleider and Haxby, 1994), monkeys (Romanski et al., 1999; Tian et al., 2001), and cats (Lomber and Malhotra, 2008). Therefore, parallel processing of different features within a modality seems to be a general principle used by most sensory systems for speedy information processing.

It is noteworthy that in most sensory systems, there are topographic representations of sensory maps associated with information processing centers in the periphery, cortex, and intervening relay nuclei. For example, in the visual and

somatosensory systems, the topographic arrangement of receptors in the periphery is maintained in the cortex, as retinotopic and somatopic maps. Some maps are simple and well organized, such as the tonotopic map in the basilar membrane and auditory cortex (Merzenich and Brugge, 1973) and somatotopic maps in the somatosensory cortex (Penfield and Rasmussen, 1950), while other maps, such as orientation columns and ocular dominance columns in the primary visual cortex, are organized into a complex pattern (Blasdel and Salama, 1986; Hubel et al., 1978). The fact that orderly maps of the periphery are maintained throughout the chain of hierarchical nuclei up to the primary cortex makes us wonder what functional advantage, if any, such sensory maps might serve? It is plausible that sensory maps facilitate circuit operation, such as lateral inhibition, which benefits from topographic organization of functionally related areas (Kaas, 1997). It is also plausible that the sensory map in the cortex is required for the process of piecing together information from the parallel pathways to generate a coherent percept. Whatever the reasons, the presence of sensory maps seems to indicate a presence of some forms of information processing in the pathway.

Based on the mammalian visual, tactile, and auditory systems, there are emerging common mechanisms and circuit organization that are required to build an efficient sensory system. First, most systems seem to have mechanisms to improve sensitivity using either structure-based or circuit-based amplification. Second, most sensory systems seem to use some inhibitory mechanisms (i.e., lateral inhibition) to improve their ability to discriminate small differences. Third, most systems use a combination of parallel and hierarchical processing to speed up the information processing time. Fourth, the cortex of many sensory systems is layered to facilitate parallel information processing. Finally,

many sensory systems seem to have sensory maps at the cortex and relay nuclei, which seem to provide some functional advantages. These strategies seem reasonable, but are they conserved across evolution? Are these strategies the only way to build an efficient sensory system? To provide insights into the potential evolutionary conservation of mechanisms for efficient sensory information processing, I will now discuss examples of invertebrate sensory systems.

Insect visual systems

Bees navigate the natural world much as we do, and they must also similarly cope with all the challenges of processing visual cues in order to respond to biologically relevant stimuli. Although bees have smaller brains, with a smaller number of neurons, compared to mammals, they still have to perform visual information processing. Thus, their visual system must be more efficient in order to cope with the challenges imposed by small brains. What mechanisms and structural organizational features allow small insect brains to perform efficient visual information processing? Do insects with small brains also use similar mechanisms and circuit organizations as mammals with large brains? Or do they use different strategies to compensate for their small nervous system?

The flow of visual information in the bee's visual system begins from the retina to the lamina, and to the medulla, and then to the lobula, which has a similar functional role as the primary visual cortex (Paulk et al., 2008). Neurons in the lobula exhibit a variety of functional properties similar to those observed in the mammalian visual system, such

as orientation selectivity, direction specific and non-direction-specific motion sensitivity, color opponency, and spatially antagonistic receptive fields (DeVoe et al., 1982; Hertel, 1980; Maddess and Yang, 1997; Menzel, 1973; Yang et al., 2004). Interestingly, the lobula also has six layers, much like the primary visual cortex of mammals, and these six layers are engaged in parallel processing of different features of visual stimuli (Paulk et al., 2009; Paulk et al., 2008). Layers 1–4 show achromatic motion sensitivity, while layers 5–6 show color sensitivity. Furthermore, color and motion-selective information is further processed in parallel channels by the anterior portion of the lateral protocerebrum for colors, and the posterior portion of lateral protocerebrum for motion (Paulk et al., 2009). Thus, the visual system of bumblebees also possesses parallel visual pathways that are comparable to the magnocellular (for motion) and parvocellular (for color) subsystems of primates.

Interestingly, evidence suggests that this parallel segregation of pathways for color and visual-motion processing begins at the level of specialized receptors with distinct response properties in the retina. Paulk et al. (2008) showed that there are four major types of receptors in the bumblebee's retina. The first group shows tonic responses, the second group shows phasic responses only at the onset of the stimulus (referred as "phasic"), the third group shows phasic responses at both onset and offset of the stimulus (referred as "ON-OFF"), and the fourth group shows tonic responses with phasic bursting at the onset of stimulus (referred as "phasic-tonic"). They found that the majority of the "phasic" receptors exhibit habituation for repeated stimuli and are involved in encoding color sensitivity, while the majority of the "ON-OFF" receptors exhibit a high accuracy of spike timing and are involved in achromatic motion sensitivity.

Thus, receptors with specific response properties seem to be involved in specific feature processing in bees.

Similar to the mammalian visual systems, bees also utilize a layered structure to facilitate parallel processing for different features of visual stimuli. These mechanisms seem to be a general rule that also applies to other insect species, such as the blowfly *Phaenicia sericata* (Okamura and Strausfeld, 2007), Mantis shrimp (Cronin and Marshall, 2001), and *Drosophila* (Borst, 2009; Douglass and Strausfeld, 1996). Thus, these similarities between the mammalian and various insects' visual systems suggest that these mechanisms are evolutionarily conserved, and seem to follow general rules for achieving rapid information processing, at least in the visual system.

Insect auditory systems

The hearing organs of insects have evolved many times independently, under different environmental and evolutionary contexts (Yack, 2004). Consequently, there are many variations among different insect species as to where the hearing organ is located, what type of hearing organ they have (i.e., tympanal membrane, Johnston's organ, subgenual organ), and the mechanisms and neural circuitry underlying auditory information processing (Yager, 1999). The obvious difference between mammalian ears and the ears of insect species is reflected in the type of auditory receptors they have. The mammalian auditory receptor, the inner hair cell, in itself does not have a specific frequency tuning; instead the location of the basilar membrane displacement determines the frequency tuning of the inner hair cells (Moller, 2003). In contrast, the auditory receptors of most insect species with tympanal membranes (except moths) have intrinsic,

specific frequency tuning properties. They normally have two or more types of receptors with slightly different frequency tuning curves to cover the entire range of audible frequencies. The discrimination of frequencies requires the comparisons of relative levels of excitation across a group of receptors with different preferred frequency tuning (Esch et al., 1980; Hutchings and Lewis, 1981; Michelsen, 1966; Michelsen, 1968; Oldfeld, 1982).

What is common between mammalian and insect auditory systems is the presence of tonotopic representations (Kaas, 1997). In many insects, such as bushcrickets and grasshoppers, the central projections of the sensory receptor neurons are organized into a tonopotic map (Hennig et al., 2004; Imaizumi and Pollack, 2005; Mason and Faure, 2004; Stolting and Stumpner, 1998). In bushcrickets, for example, receptor cells that are tuned to lower frequencies project towards the anterior portion of the prothoracic ganglion, while receptor cells that are tuned to higher frequencies project towards the posterior portion of the prothoracic ganglion. Interestingly, the receptor cells that are tuned to sound frequencies of the conspecific calling song have a larger representation in the tonotopic map compared to the frequencies outside of the conspecific calling song (Oldfeld, 1983; Romer, 1983). This is reminiscent of the homunculus, in which more sensitive body surfaces, such as the fingertips and lips, are represented in a much larger areas of the cortex compared to less sensitive body surface areas, such as the trunk (Penfield and Rasmussen, 1950). Interestingly, the sharpening of frequency tuning takes place at the prothoracic ganglion, where a tonotopic map exists (Atkins et al., 1989; Boyan, 1981; Romer, 1987). In addition, crickets and grasshoppers also utilize inhibitory mechanisms to sharpen the frequency tuning. It was shown that when such inhibition is

eliminated by the application of picrotoxin, the frequency tuning broadens (Romer and Seikowski, 1985; Stumpner, 1998; Stumpner, 2002).

The segregation into separate parallel channels dedicated to processing directional and temporal patterns of sound stimuli is well documented in the vertebrate auditory systems (Covey and Casseday, 1991; Oertel, 1999; Takahashi et al., 1984; Viete et al., 1997). Interestingly, grasshoppers also process directional and temporal patterns of sound stimuli in parallel pathways, in much the same way as vertebrates. Grasshoppers determine the direction of sound sources using the interaural intensity differences between the right and left tympanal ears on their first abdominal segments (Hennig et al., 2004; Mason and Faure, 2004). It is important to note that vertebrates with large heads use both interaural intensity and interaural time differences for sound localization; However, insects with a small body sizes mainly rely on interaural intensity differences, since it is difficult to resolve small differences in the arrival time of a sound stimulus between the right and left ears of a small body.

Crickets, in contrast, process the direction and temporal patterns of sound stimuli in a serial order instead of processing in parallel pathways (Schul, 1998; Stabel et al., 1989; von Helversen and von Helversen, 1995). In bushcrickets, information regarding both directional and temporal patterns of the sound stimuli converges on a pair of interneurons called ascending interneuron-1 and -2 (AN1 and AN2) (Schildberger and Horner, 1988), while in grasshoppers, the ascending interneurons are functionally separated in two parallel pathways to process directional and temporal information (Franz and Ronacher, 2002; Schildberger and Horner, 1988).

So what are the costs and benefits of parallel vs. serial processing of directional and temporal patterns of sound stimuli in grasshoppers and crickets, respectively? In both grasshoppers and crickets, information regarding the frequency, direction, and temporal pattern is used for positive phonotaxis behavior in such a way that they orient towards louder and more attractive patterns of sound stimuli (Stabel et al., 1989; von Helversen and von Helversen, 1997). Interestingly, crickets, with serial processing, exhibit positive phonotaxis with better angular resolution than grasshoppers, with parallel processing (Hennig et al., 2004). Grasshoppers tend to either over- or under estimate the angles of sound sources; however, under complex circumstances in which the direction and temporal patterns of two competing sound stimuli are ambiguous, crickets (with serial processing) fail to exhibit a positive phonotaxis behavior (Stabel et al., 1989). Thus, it seems that crickets (with serial processing) have an advantage in angular resolution, but this gain is opposed by a loss in fidelity for pattern processing under complex circumstances. Although more detailed analyses with various organisms are required for informative generalization, there seems to exist a trade-off between the serial and parallel processing strategies, and this might explain why higher-order organisms with larger brains use the combination of serial and parallel processing for efficiency and accuracy of sensory information processing.

So, what is the best strategy to build the most efficient and accurate sensory system? We do not have a clear answer but there are general trends. Based on the comparisons between different sensory systems in mammals and other organisms across phylogeny, there are several strategies and mechanisms that are commonly used for efficient information processing. First, most sensory systems use amplification

mechanisms to improve sensitivity of the system, whether structure-based or circuit-based. Second, most sensory systems use inhibitory mechanisms, such as lateral inhibition, to improve the ability to discriminate small differences. Third, most sensory systems preserve topographic representations of peripheral sensory information at the multiple levels of information processing centers, which seems to argue that topographic representation of sensory stimuli is beneficial for sensory information processing. Fourth, the example of insect auditory systems suggests that both serial and parallel processing have a cost and benefit. This might be the reason why many sensory systems, especially in higher organisms, use a combination of parallel and serial processing for speed and accuracy, and these separate channels are later combined in the association areas of the brain to generate a coherent percept. Finally, the use of layered structures, such as the cortex, seems extremely efficient for parallel processing. Layered structures are utilized by many sensory systems in many organisms, from insects to humans.

What is most striking of all is that the brain acquires and processes information using separate channels first. This is evident from the fact that sensory information from different modalities is acquired and processed via different sensory systems. Furthermore, different features of stimuli (or submodalities) are also processed in separate parallel channels. It is only at the later stages of information processing that all information from different modalities (and submodalities) is pieced together to generate a coherent percept. Is this a general theme used by the brain? Are all modalities acquired and processed by the separate sensory organs with distinct classes of sensory receptors?

When I started my project, I was investigating the neural circuitry underlying wind detection in *Drosophila* with a simple curiosity to identify the mechanisms and

neural circuits involved in wind detection. However, in the course of my study, I found that *Drosophila* detect wind using a mechanosensory organ called Johnston's organ, which is known to be implicated in sound detection (Bennet-Clark, 1971; Boekhoff-Falk, 2005; Eberl, 1999; Tauber and Eberl, 2003). This dual role in sound and wind detection seems contrary to the central concept that different modalities are processed by distinct pathways via distinct sensory organs each equipped with specialized set of receptors. Is *Drosophila* an unusual case in which both wind and sound are processed using a common sensory organ? Do other insects have separate sensory organs to process wind and sound? Most insect species including cockroaches and crickets, wind and sound information are processed via separate sensory organs. For example, the cockroach detects wind using the filiform sensilla of the cercal system, located at the posterior end of the abdomen, while sound is detected by the subgenual organ, which is located on its proximal tibia (Keegan and Comer, 1993; Kondoh et al., 1993; Moran and Rowley, 1975; Rinberg and Davidowitz, 2003; Shaw, 1994). Crickets also detect wind using the cercal system located at the posterior end of their abdomen, while they use a tympanal membrane on their forelegs to detect sound (Hedwig, 2006; Kanou et al., 2006; Mason and Faure, 2004). Thus, *Drosophila* might be considered unusual in using a single sensory organ to detect both wind and sound. The question is how. The fact that the receptor subtypes and neural circuits implicated in sound or wind pathways in *Drosophila* were unknown, and the unique arrangement of the wind/sound detector in the common sensory organ, antennae, therefore raises several interesting questions: How do flies distinguish wind from sound using a common sensory organ? Do the same population of receptors encode wind and sound? How are wind and sound pathways organized in the

Johnston's organ and in the brain? Are wind and sound processed by separate pathways or by the same pathway?

To gain insight into these issues, I investigated the following questions using a combination of behavioral and electrophysiological analyses, and *in-vivo* calcium response imaging: 1) Which receptor neurons are implicated in sound and wind detection? Do the receptor neurons implicated in sound and wind detection belong to the same or to different populations? 2) If distinct populations of receptor neurons are implicated in sound vs. wind detection, then do they differ in their intrinsic response properties? 3) Are wind and sound processed in separate or the same pathways, and 4) Is there a sensory map of wind or sound?

In this project, I will focus on the mechanisms and information processing in the periphery. The understanding of the peripheral organization of a sensory system is an essential first step, and also provides insights into how these circuits are organized in the brain. A comprehensive circuit analysis beyond the primary sensory neurons is however, beyond the scope of this project. I will lay out the peripheral organization of these pathways for the future comprehensive analysis of the circuits involved in wind and sound information processing in *Drosophila*.

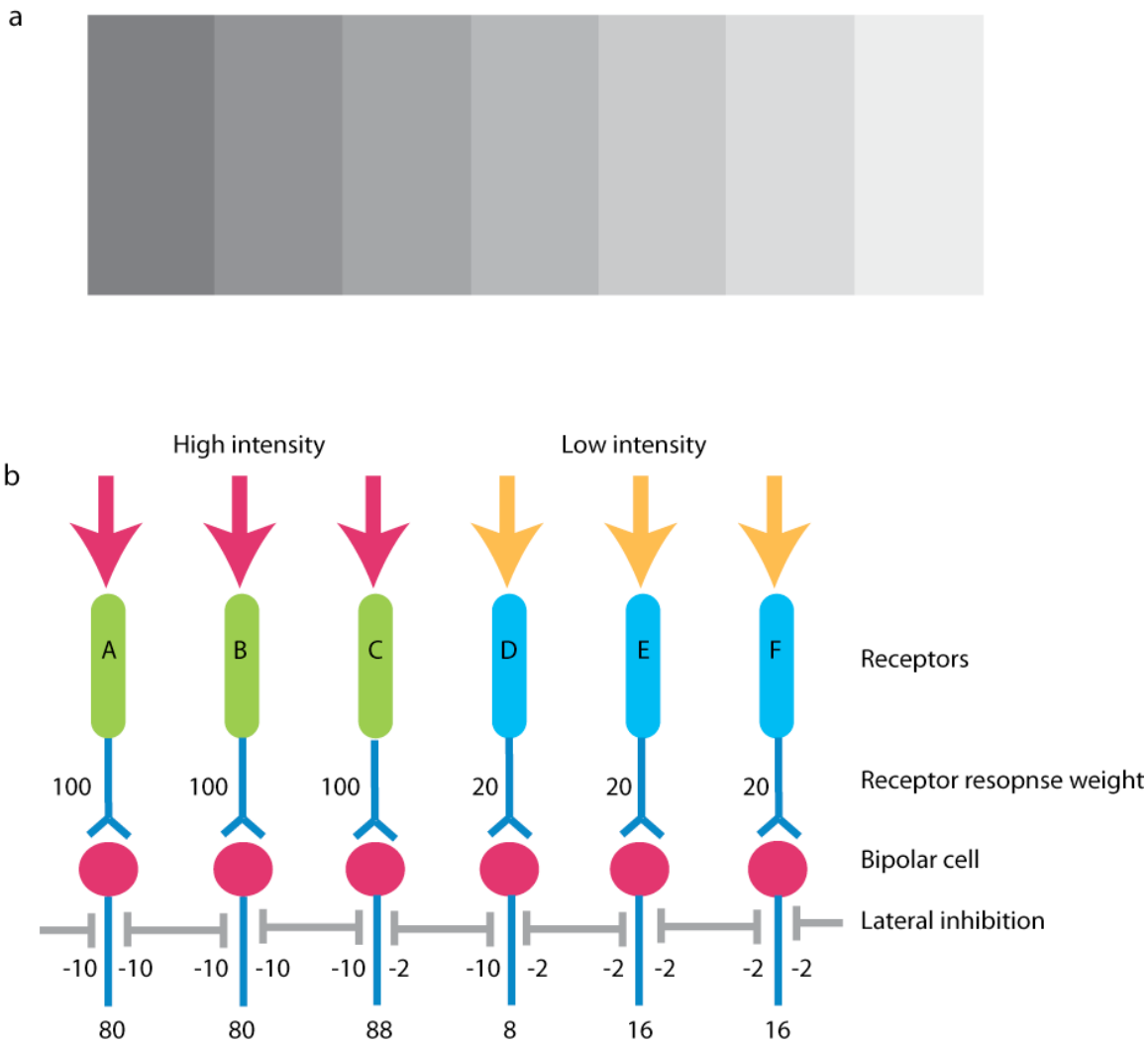

Figure 1: The Mach band effect can be explained by lateral inhibition.

(a) The Mach band illusion: Seven rectangular bands are placed next to each other. Each band is a fixed shade of gray but the area around the left edge appears lighter than the area around the right edge. (b) The Mach band illusion is caused by lateral inhibition in the retina. The bipolar cell that is post-synaptic to the receptor-C, receiving high intensity light, transmits stronger intensity compared to other bipolar cells receiving high intensity light. In contrast, the bipolar cell that is post-synaptic to the receptor-D, receiving low intensity light, transmits lower intensity compared to other bipolar cells receiving low intensity light.

REFERENCES

Adrian, E. D., and Zotterman, Y. (1926). The impulses produced by sensory nerve-endings: part II. The response of a single end-organ. J Physiol *61*, 151-171.

Ashmore, J. (2008). Cochlear outer hair cell motility. Physiol Rev *88*, 173-210.

Atkins, S., Atkins, G., Rhodes, M., and Stout, J. (1989). Influence of syllable period on song encoding properties of an ascending auditory interneuron in the cricket *Acheta domestica*. J Comp Physiol A Neuroethol Sens Neural Behav Physiol *165*, 827-836.

Barlow, H. B., and Hill, R. M. (1963). Selective sensitivity to direction of movement in ganglion cells of the rabbit retina. Science *139*, 412-414.

Barlow, H. B., and Levick, W. R. (1965). The mechanism of directionally selective units in the rabbit's retina. J Physiol *178*, 447-504.

Baylor, D. A., Lamb, T. D., and Yau, K. W. (1979). Responses of retinal rods to single photons. J Physiol *288*, 613-634.

Baylor, D. A., Nunn, B. J., and Schnapf, J. L. (1984). The photocurrent, noise and spectral sensitivity of rods of the monkey *Macaca fascicularis*. J Physiol *357*, 575-607.

Bennet-Clark, H. (1971). Acoustics of insect song. Nature *234*, 255-259.

Blasdel, G. G., and Salama, G. (1986). Voltage-sensitive dyes reveal a modular organization in monkey striate cortex. Nature *321*, 579-585.

Bloom, F. E., and Lazerson, A., eds. (1988). Brain, mind, and behavior, 2 edn (New York: Freeman).

Boekhoff-Falk, G. (2005). Hearing in *Drosophila*: development of Johnston's organ and emerging parallels to vertebrate ear development. Dev Dyn *232*, 550-558.

Borst, A. (2009). *Drosophila*'s view on insect vision. Curr Biol *19*, R36-47.

Boyan, G. (1981). Two-tone suppression of an identified auditory neurone in the brain of the cricket *Gryllus bimaculatus* (De Geer). J Comp Physiol A Neuroethol Sens Neural Behav Physiol *144*, 117-125.

Chandrashekar, J., Hoon, M. A., Ryba, N. J., and Zuker, C. S. (2006). The receptors and cells for mammalian taste. Nature *444*, 288-294.

Cleland, B. G., Harding, T. H., and Tulunay-Keesey, U. (1979). Visual resolution and receptive field size: examination of two kinds of cat retinal ganglion cell. Science *205*, 1015-1017.

Courtney, S. M., Ungerleider, L. G., Keil, K., and Haxby, J. V. (1996). Object and spatial visual working memory activate separate neural systems in human cortex. Cereb Cortex *6*, 39-49.

Covey, E., and Casseday, J. (1991). The monaural nuclei of the lateral lemniscus in an echolocating bat: parallel pathways for analyzing temporal features of sound. J Neurosci *11*, 3456-3470.

Cronin, T. W., and Marshall, J. (2001). Parallel processing and image analysis in the eyes of mantis shrimps. Biol Bull *200*, 177-183.

Dallos, P. (2008). Cochlear amplification, outer hair cells and prestin. Curr Opin Neurobiol *18*, 370-376.

DeVoe, R., Kaiser, W., Ohm, J., and Stone, L. (1982). Horizontal movement detectors of honeybees: directionally-selective visual neurons in the lobula and brain. J Comp Physiol A Neuroethol Sens Neural Behav Physiol *147*, 155-170.

DiCarlo, J. J., and Johnson, K. O. (2002). Receptive field structure in cortical area 3b of the alert monkey. Behav Brain Res *135*, 167-178.

DiCarlo, J. J., Johnson, K. O., and Hsiao, S. S. (1998). Structure of receptive fields in area 3b of primary somatosensory cortex in the alert monkey. J Neurosci *18*, 2626-2645.

Diller, L., Packer, O. S., Verweij, J., McMahon, M. J., Williams, D. R., and Dacey, D. M. (2004). L and M cone contributions to the midget and parasol ganglion cell receptive fields of macaque monkey retina. J Neurosci *24*, 1079-1088.

Douglass, J. K., and Strausfeld, N. J. (1996). Visual motion-detection circuits in flies: parallel direction- and non-direction-sensitive pathways between the medulla and lobula plate. J Neurosci *16*, 4551-4562.

Eberl, D. F. (1999). Feeling the vibes: chordotonal mechanisms in insect hearing. Curr Opin Neurobiol *9*, 389-393.

Esch, H., Huber, F., and Wohlers, D. (1980). Primary auditory neurons in crickets: Physiology and central projections. J Comp Physiol A Neuroethol Sens Neural Behav Physiol *137*, 27-38.

Fechner, G., ed. ([1860] 1966). Elements of psychophysics (New York: Holt, Rinehart and Winston).

Fitzpatrick, D., Lund, J. S., and Blasdel, G. G. (1985). Intrinsic connections of macaque striate cortex: afferent and efferent connections of lamina 4C. J Neurosci *5*, 3329-3349.

Franz, A., and Ronacher, B. (2002). Temperature dependence of temporal resolution in an insect nervous system. J Comp Physiol A Neuroethol Sens Neural Behav Physiol *188*, 261-271.

Fried, S. I., Munch, T. A., and Werblin, F. S. (2002). Mechanisms and circuitry underlying directional selectivity in the retina. Nature *420*, 411-414.

Hartline, H. K., Wagner, H. G., and Ratliff, F. (1956). Inhibition in the eye of Limulus. J Gen Physiol *39*, 651-673.

Hawken, M. J., Parker, A. J., and Lund, J. S. (1988). Laminar organization and contrast sensitivity of direction-selective cells in the striate cortex of the Old World monkey. J Neurosci *8*, 3541-3548.

Hedwig, B. (2006). Pulses, patterns and paths: neurobiology of acoustic behaviour in crickets. J Comp Physiol A Neuroethol Sens Neural Behav Physiol *192*, 677-689.

Hennig, R. M., Franz, A., and Stumpner, A. (2004). Processing of auditory information in insects. Microsc Res Tech *63*, 351-374.

Hertel, H. (1980). Chromatic properties of identified interneurons in the optic lobes of the bee. J Comp Physiol A Neuroethol Sens Neural Behav Physiol *137*, 215-231.

Holley, M. C., and Ashmore, J. F. (1988). On the mechanism of a high-frequency force generator in outer hair cells isolated from the guinea pig cochlea. Proc R Soc Lond B Biol Sci *232*, 413-429.

Hubel, D. H. (1963). The Visual Cortex of the Brain. Sci Am *209*, 54-62.

Hubel, D. H. (1988). Eye, brain, and vision, Vol 22 (New York: Scientific American Library series).

Hubel, D. H., and Wiesel, T. N. (1968). Receptive fields and functional architecture of monkey striate cortex. J Physiol *195*, 215-243.

Hubel, D. H., Wiesel, T. N., and Stryker, M. P. (1978). Anatomical demonstration of orientation columns in macaque monkey. J Comp Neurol *177*, 361-380.

Hutchings, M., and Lewis, B. (1981). Response properties of primary auditory fibers in the cricket *Teleogryllus oceanicus*. J Comp Physiol A Neuroethol Sens Neural Behav Physiol *143*, 129-134.

Imaizumi, K., and Pollack, G. S. (2005). Central projections of auditory receptor neurons of crickets. J Comp Neurol *493*, 439-447.

Johansson, R. S., and Vallbo, A. B. (1983). Tactile sensory coding in the glabrous skin of the human hand. Trends Neurosci *6*, 27-32.

Johnson, K. O. (2001). The roles and functions of cutaneous mechanoreceptors. Curr Opin Neurobiol *11*, 455-461.

Johnson, K. O., and Hsiao, S. S. (1992). Neural mechanisms of tactual form and texture perception. Annu Rev Neurosci *15*, 227-250.

Kaas, J. H. (1997). Topographic maps are fundamental to sensory processing. Brain Res Bull *44*, 107-112.

Kandel, E., Schwartz, J., and Jessell, T., eds. (2000). Principles of neural science, 4 edn (McGraw-Hill).

Kanou, M., Nawae, M., and Kuroishi, H. (2006). Cercal sensory system and giant interneurons in *Gryllodes sigillatus*. Zoolog Sci *23*, 365-373.

Keegan, A. P., and Comer, C. M. (1993). The wind-elicited escape response of cockroaches (*Periplaneta americana*) is influenced by lesions rostral to the escape circuit. Brain Res *620*, 310-316.

Kondoh, Y., Arima, T., Okuma, J., and Hasegawa, Y. (1993). Response dynamics and directional properties of nonspiking local interneurons in the cockroach cercal system. J Neurosci *13*, 2287-2305.

Liberman, M. C., Gao, J., He, D. Z., Wu, X., Jia, S., and Zuo, J. (2002). Prestin is required for electromotility of the outer hair cell and for the cochlear amplifier. Nature *419*, 300-304.

Livingstone, M. S., and Hubel, D. H. (1984). Anatomy and physiology of a color system in the primate visual cortex. J Neurosci *4*, 309-356.

Loewenstein, W. R., and Mendelson, M. (1965). Components of Receptor Adaptation in a Pacinian Corpuscle. J Physiol *177*, 377-397.

Lomber, S. G., and Malhotra, S. (2008). Double dissociation of "what" and "where" processing in auditory cortex. Nat Neurosci *11*, 609-616.

Ma, X., and Suga, N. (2004). Lateral inhibition for center-surround reorganization of the frequency map of bat auditory cortex. J Neurophysiol *92*, 3192-3199.

Maddess, T., and Yang, E. (1997). Orientation-sensitive Neurons in the Brain of the Honey Bee (*Apis mellifera*). J Insect Physiol *43*, 329-336.

Masland, R. H. (2001). The fundamental plan of the retina. Nat Neurosci *4*, 877-886.

Mason, A. C., and Faure, P. A. (2004). The physiology of insect auditory afferents. Microsc Res Tech *63*, 338-350.

Masse, N. Y., Turner, G. C., and Jefferis, G. S. (2009). Olfactory information processing in *Drosophila*. Curr Biol *19*, R700-713.

Menzel, R. (1973). Spectral responses of moving detecting and "sustaining" fibres in the optic lobe of the bee. J Comp Physiol A Neuroethol Sens Neural Behav Physiol *82*, 135-150.

Merigan, W. H., and Maunsell, J. H. (1993). How parallel are the primate visual pathways? Annu Rev Neurosci *16*, 369-402.

Merzenich, M. M., and Brugge, J. F. (1973). Representation of the cochlear partition of the superior temporal plane of the macaque monkey. Brain Res *50*, 275-296.

Michelsen, A. (1966). Pitch discrimination in the locust ear: observations on single sense cells. J Insect Physiol *12*, 1119-1131.

Michelsen, A. (1968). Frequency discrimination in the locust ear by means of four groups of receptor cells. Nature *220*, 585-586.

Moller, A. R. (2003). Sensory systems: anatomy and physiology: Academic Press).

Montell, C. (2009). A taste of the *Drosophila* gustatory receptors. Curr Opin Neurobiol *19*, 345-353.

Moran, D. T., and Rowley, J. C., 3rd (1975). The fine structure of the cockroach subgenual organ. Tissue Cell *7*, 91-105.

Mori, K., Nagao, H., and Yoshihara, Y. (1999). The olfactory bulb: coding and processing of odor molecule information. Science *286*, 711-715.

Nassi, J. J., and Callaway, E. M. (2009). Parallel processing strategies of the primate visual system. Nat Rev Neurosci *10*, 360-372.

Norgren, R. (1983). The gustatory system in mammals. Am J Otolaryngol *4*, 234-237.

Oertel, D. (1999). The role of timing in the brain stem auditory nuclei of vertebrates. Annu Rev Physiol *61*, 497-519.

Okamura, J. Y., and Strausfeld, N. J. (2007). Visual system of calliphorid flies: motion- and orientation-sensitive visual interneurons supplying dorsal optic glomeruli. J Comp Neurol *500*, 189-208.

Oldfeld, B. (1982). Tonotopic organisation of auditory receptors in *Tettigoniidae Orthoptera Ensifera*. J Comp Physiol A Neuroethol Sens Neural Behav Physiol *147*, 461-470.

Oldfeld, B. (1983). Central projections of primary auditory fibres in *Tettigoniidae Orthoptera Ensifera*. J Comp Physiol A Neuroethol Sens Neural Behav Physiol *151*, 389-395.

Ollivier, F., Samuelson, D., Brooks, D., Lewis, P., Kallberg, M., and Komaromy, A. (2004). Comparative morphology of the tapetum lucidum (among selected species). Veterinary Ophthalmology *7* 11-22.

Olveczky, B. P., Baccus, S. A., and Meister, M. (2003). Segregation of object and background motion in the retina. Nature *423*, 401-408.

Paolini, A. G., Clarey, J. C., Needham, K., and Clark, G. M. (2005). Balanced inhibition and excitation underlies spike firing regularity in ventral cochlear nucleus chopper neurons. Eur J Neurosci *21*, 1236-1248.

Paolini, A. G., Cotterill, E. L., Bairaktaris, D., and Clark, G. M. (1998). Muscimol suppression of the dorsal cochlear nucleus modifies frequency tuning in rats. Brain Res *785*, 309-316.

Paulk, A. C., Dacks, A. M., Phillips-Portillo, J., Fellous, J. M., and Gronenberg, W. (2009). Visual processing in the central bee brain. J Neurosci *29*, 9987-9999.

Paulk, A. C., Phillips-Portillo, J., Dacks, A. M., Fellous, J. M., and Gronenberg, W. (2008). The processing of color, motion, and stimulus timing are anatomically segregated in the bumblebee brain. J Neurosci *28*, 6319-6332.

Penfield, W., and Rasmussen, T. (1950). The cerebral cortex of man: a clinical study of localization of function (New York: Macmillan).

Pierret, T., Lavallee, P., and Deschenes, M. (2000). Parallel streams for the relay of vibrissal information through thalamic barreloids. J Neurosci *20*, 7455-7462.

Ratliff, F. (1965). Mach Bands: quantitative studies on neural network in the retina (San Francisco: Holden-Day).

Ratliff, F., Miller, W. H., and Hartline, H. K. (1959). Neural interaction in the eye and the integration of receptor activity. Ann N Y Acad Sci *74*, 210-222.

Rinberg, D., and Davidowitz, H. (2003). Wind spectra and the response of the cercal system in the cockroach. J Comp Physiol A Neuroethol Sens Neural Behav Physiol *189*, 867-876.

Romanski, L. M., Tian, B., Fritz, J., Mishkin, M., Goldman-Rakic, P. S., and Rauschecker, J. P. (1999). Dual streams of auditory afferents target multiple domains in the primate prefrontal cortex. Nat Neurosci *2*, 1131-1136.

Romer, H. (1983). Tonotopic organization of the auditory neuropile in the bushcricket *Tettigonia viridissima*. Nature *306*, 60-62.

Romer, H. (1987). Representation of auditory distance within a central neuropil of the bushcricket *Mygalopsis marki*. J Comp Physiol A Neuroethol Sens Neural Behav Physiol *161*, 33-42.

Romer, H., and Seikowski, U. (1985). Responses to model songs of auditory neurons in the thoracic ganglia and brain of the locust. J Comp Physiol A Neuroethol Sens Neural Behav Physiol *156*, 845-860.

Rusznak, Z., and Szucs, G. (2009). Spiral ganglion neurones: an overview of morphology, firing behaviour, ionic channels and function. Pflugers Arch *457*, 1303-1325.

Schildberger, K., and Horner, M. (1988). The function of auditory neurons in cricket phonotaxis. J Comp Physiol A Neuroethol Sens Neural Behav Physiol *163*, 621-631.

Schul, J. (1998). Song recognition by temporal cues in a group of closely related bushcricket species (genus *Tettigonia*). J Comp Physiol A Neuroethol Sens Neural Behav Physiol *183*, 401-410.

Shaw, S. (1994). Detection of Airborne Sound by a Cockroach "Vibration Detector": a Possible Missing Link in Insect Auditory Evolution. J Exp Biol *193*, 13-47.

Stabel, J., Wendler, G., and Scharstein, H. (1989). Cricket phonotaxis: localization depends on recognition of the calling song pattern. J Comp Physiol A Neuroethol Sens Neural Behav Physiol *165*, 165-177.

Stolting, H., and Stumpner, A. (1998). Tonotopic organization of auditory receptors of the bushcricket *Pholidoptera griseoaptera* (*Tettigoniidae, decticinae*). Cell Tissue Res *294*, 377-386.

Stumpner, A. (1998). Picrotoxin eliminates frequency selectivity of an auditory interneuron in a bushcricket. J Neurophysiol *79*, 2408-2415.

Stumpner, A. (2002). A species-specific frequency filter through specific inhibition, not specific excitation. J Comp Physiol A Neuroethol Sens Neural Behav Physiol *188*, 239-248.

Suga, N. (1995). Sharpening of frequency tuning by inhibition in the central auditory system: tribute to Yasuji Katsuki. Neurosci Res *21*, 287-299.

Sullivan, S. L., Ressler, K. J., and Buck, L. B. (1995). Spatial patterning and information coding in the olfactory system. Curr Opin Genet Dev *5*, 516-523.

Takahashi, T., Moiseff, A., and Konishi, M. (1984). Time and intensity cues are processed independently in the auditory system of the owl. . J Neurosci *4*, 1781-1786.

Tauber, E., and Eberl, D. F. (2003). Acoustic communication in Drosophila. Behav Processes *64*, 197-210.

Tian, B., Reser, D., Durham, A., Kustov, A., and Rauschecker, J. P. (2001). Functional specialization in rhesus monkey auditory cortex. Science *292*, 290-293.

Torre, V., Ashmore, J. F., Lamb, T. D., and Menini, A. (1995). Transduction and adaptation in sensory receptor cells. J Neurosci *15*, 7757-7768.

Ts'o, D. Y., and Gilbert, C. D. (1988). The organization of chromatic and spatial interactions in the primate striate cortex. J Neurosci *8*, 1712-1727.

Ungerleider, L. G., and Haxby, J. V. (1994). "What" and "where" in the human brain. Curr Opin Neurobiol *4*, 157-165.

Vallbo, A. B., and Johansson, R. S. (1978). The tactile sensory innervation of the glabrous skin of the human hand, In Active touch, G. Gordon, ed. (New York: Pergamon), pp. 29-54.

Vallbo, A. B., and Johansson, R. S. (1984). Properties of cutaneous mechanoreceptors in the human hand related to touch sensation. Hum Neurobiol *3*, 3-14.

Viete, S., Pena, J. L., and Konishi, M. (1997). Effects of interaural intensity difference on the processing of interaural time difference in the owl's nucleus laminaris. J Neurosci *17*, 1815-1824.

von Bekesy, G. (1960). Neural inhibitory units of the eye and skin: quantitative description of contrast phenomena. J Opt Soc Am *50*, 1060-1070.

von Bekesy, G. (1967a). Mach band type lateral inhibition in different sense organs. J Gen Physiol *50*, 519-532.

von Bekesy, G. (1967b). Sensory inhibition (Princeton, NJ: Princeton University Press).

von Helversen, D., and von Helversen, O. (1995). Acoustic pattern recognition and orientation in orthopteran insects: parallel or serial processing? J Comp Physiol A Neuroethol Sens Neural Behav Physiol *177*, 767-774.

von Helversen, D., and von Helversen, O. (1997). Recognition of sex in the acoustic communication of the grasshopper *Chorthippus biguttulus* (*Orthoptera, Acrididae*). J Comp Physiol A Neuroethol Sens Neural Behav Physiol *4*, 373-386.

Wassle, H. (2004). Parallel processing in the mammalian retina. Nat Rev Neurosci *5*, 747-757.

Weinstein, S. (1968). The skin senses, Paper presented at: International Symposium on Skin Senses (IL: Thomas: Springfield).

Yack, J. E. (2004). The structure and function of auditory chordotonal organs in insects. Microsc Res Tech *63*, 315-337.

Yager, D. D. (1999). Structure, development, and evolution of insect auditory systems. Microsc Res Tech *47*, 380-400.

Yang, E. C., Lin, H. C., and Hung, Y. S. (2004). Patterns of chromatic information processing in the lobula of the honeybee, *Apis mellifera L.* J Insect Physiol *50*, 913-925.

Yu, C., Derdikman, D., Haidarliu, S., and Ahissar, E. (2006). Parallel thalamic pathways for whisking and touch signals in the rat. PLoS Biol *4*, e124.

Chapter 2

Distinct populations of Johnston's organ neurons detect wind and near-field sound in the *Drosophila* brain

Suzuko Yorozu, Allan Wong, Brian J. Fischer, Heiko Dankert, Maurice J. Kernan, Azusa Kamikouchi, Kei Ito, and David J. Anderson.

ABSTRACT

Behavioral responses to wind are thought to play a critical role in controlling the dispersal and population genetics of wild *Drosophila* species (Johnston and Heed, 1976; Johnston and Templeton, 1982), as well as their navigation in flight (Budick et al., 2007), but their underlying neurobiological basis is unknown. I show that *Drosophila melanogaster*, like wild-caught *Drosophila* strains (Richardson and Johnston, 1975), exhibits robust wind-induced suppression of locomotion (WISL), in response to air currents delivered at speeds normally encountered in nature (Johnston and Heed, 1976; Johnston and Templeton, 1982). Furthermore, I identify wind-sensitive neurons in the Johnston's organ (JO), an antennal mechanosensory structure previously implicated in near-field sound detection (Caldwell and Eberl, 2002; Kernan, 2007). Using Gal4 lines targeted to different subsets of JO neurons (Kamikouchi et al., 2006), and a genetically encoded calcium indicator, I show that wind and near-field sound (courtship song) activate distinct JO populations, which project to different regions of the antennal and mechanosensory motor center (AMMC) in the central brain. Selective genetic ablation of wind-sensitive JO neurons in the antenna abolishes WISL behavior, without impairing hearing. Different neuronal subsets within the wind-sensitive population, moreover, respond to different directions of arista deflection caused by airflow and project to different regions of the AMMC, providing a rudimentary map of wind direction in the brain. Importantly, sound- and wind-sensitive JO neurons exhibit different intrinsic response properties: the former are phasically activated by small, bidirectional, displacements of the aristae, while the latter are tonically activated by unidirectional, static deflections of larger magnitude. These different intrinsic properties are well suited

to the detection of oscillatory pulses of near-field sound and laminar airflow, respectively. These data identify wind-sensitive neurons in the JO, a structure that has been primarily associated with hearing, and reveal how the brain can distinguish different types of air particle movements, using a common sensory organ.

Introduction

Gene flow is a fundamental determinant of genetic diversification in sexual organisms. Levels of gene flow between populations influence the degree to which closely related interbreeding organisms will either share a common evolutionary trajectory, or will diverge over time through genetic drift and natural selection (Slatkin, 1985; Slatkin, 1987; Wright, 1943). There are a number of factors that affect the rate of gene flow between populations. Evolutional biologists argue that dispersal ability is a highly significant predictor of gene flow and play an important role in speciation (Smith and Farrell, 2006).

Johnston and his colleagues have studied wind-induced behavioral responses of various wild Hawaiian *Drosophila* species and show that many *Drosophila* species exhibit suppression of locomotor activities at high-speed wind within their natural habitat (Johnston and Heed, 1976; Johnston and Templeton, 1982). For example, *D. mercatorum*, *D. hydei*, and *D. minica* inhabit environments where trade winds blow in the range of 5–25 km/hr (1.4–6.9 m/s). Wild-caught *D. mercatorum* and *D. hydei* exhibit locomotor arrest at wind speeds of >10 km/hr (2.8 m/s), while wild-caught *D. minica* exhibited locomotor arrest at air speeds between 6 and 7 km/hr (1.67–1.94 m/s). Johnston and colleagues therefore, argue that wind induced suppression of locomotion may be the dominant environmental influence affecting dispersal of wild *Drosophila* populations and thereby an important determinant of their "genoclines," geographic gradients in gene frequencies.

While many *Drosophila* species exhibit wind-induced suppression of locomotion during high-speed wind, they also exhibit anemotaxis, orientation towards or away from the wind source, during low-speed wind. It is believed that the anemotaxis behavior is important for many insect species to locate and identify a wide variety of resources important for survival, such as food, potential mates, and predators (Willis and Avondet, 2005; Willis et al., 2008). Successful resource localization requires their ability to detect odor and direction of wind bearing that odor. They use the wind direction as the primary directional cue that enables them to steer their movements toward or away from the odor source (Willis and Avondet, 2005; Willis et al., 2008).

Therefore, the ability to detect wind and wind-induced behavior, such as anemotaxis and wind-induced suppression of locomotion, have important consequences for flies' survival and implication in shaping their population genetics; however, the underlying neurobiological bases of wind detection in *Drosophila* is unknown. In this project, I investigated which sensory organ is implicated in wind detection, and how wind information is represented in the brain.

RESULTS

Drosophila exhibit wind-induced suppression of locomotion

When *Drosophila* is exposed to a constant flow of gentle air current (0.7–1.6 m/s), it exhibits a rapid and reversible suppression of walking activity (Fig. 1a–b; Supplementary Movie 1). We call this behavior wind-induced suppression of locomotion (WISL). The WISL behavior is also exhibited by wild-caught Hawaiian *Drosophila* species, at wind speeds (1.7 m/s–2.8 m/s) within the range measured in their natural

habitats (Johnston and Heed, 1976; Johnston and Templeton, 1982; Richardson and Johnston, 1975) (J. S. Johnston, personal communication; Supplementary Footnote S1). To test whether the WISL is a stable and repeatable general phenotype, we tested WISL in various conditions including different times of day, genders, lighting, and arousal level. To test the effect of arousal level, we introduced mechanical startle prior to the introduction of airflow (Fig. 1b–d). None of these variables affected the WISL behavior, suggesting that WISL is a stable and repeatable general phenotype.

Drosophila detect wind using the Johnston's organ

Recent antennal-gluing experiments have implicated the antennae, and by extension the JO, in wind-sensation in *Drosophila* (Bennet-Clark, 1971; Budick et al., 2007). Surgical removal of the third antennal segment (a3), or gluing of a3 to the second antennal segment (a2) causes a functional impairment of the JO (Manning, 1967), since both a2 and a3 segments (including the aristae) form a functional unit of the JO. Interestingly, both of these surgical manipulations eliminated WISL (Fig. 1c–d). Furthermore, genetic ablation of JO neurons using nanchung-Gal4 (Kim et al., 2003) and *UAS-hid*, a *Drosophila* pro-apoptotic gene (Wang et al., 1999), also eliminated WISL (Fig. 2a–c). A similar result was also obtained from a "deaf" mutant called *nanchung*. The *nanchung* mutant has a loss-of-mutation in the *nanchung* gene encoding the TRPV channel normally expressed in JO neurons. The *nanchung* mutants show no electrophysiological responses to courtship song (Kim et al., 2003), thus they are defined as deaf, and they also fail to exhibit WISL (data not shown). Therefore, these results seem to suggest that the JO is implicated in both sound and wind detection.

This result is rather surprising in the sense that a single sensory organ is implicated in the detection of both sound and wind, because sensory information from different modalities is normally processed by distinct sensory organs in most animals. This potentially unique arrangement of *Drosophila* sound/wind detector in the JO begs the question, How do flies distinguish wind from sound using a common sensory organ? An equally important question is how these neural circuits underlying wind and sound pathways are arranged in the brain. It is important to note that flies are capable of distinguishing wind from sound, since these stimuli elicit distinct behavioral outputs. For example, the presentation of wind elicits WISL but wind does not induce courtship behavior (Fig 1, Supplementary Movie 1). Conversely, the presentation of courtship song elicits courtship behavior but it does not elicit suppression of locomotion (Fig. 2d).

In order to give insight into wind and sound information processing and their underlying neural circuits in the brain, we first need to determine whether JO neurons are generalist or specialist. If JO neurons are specialist, there must be distinct populations of sound- and wind-sensitive JO neurons, and it also suggests that wind and sound could be processed separately by distinct neural circuits. On the other hand, if JO neurons are generalist, they are versatile neurons that respond to both wind and sound, which suggests that the processing of wind and sound information involves population coding.

Distinct populations of wind- and sound-sensitive neurons in the Johnston's organ

To investigate the tuning properties of JO neurons for wind and sound stimulus, we next performed extracellular recordings from the antennal nerve (Eberl et al., 2000). Consistent with previous data, we observed robust JO neurons responses to courtship

song (pulse song, 75 dB) (Fig. 3a, 3c). We also observed robust wind-induced responses (Fig 3b, 3d), and noticed that the amplitude of wind-induced responses are much larger (0.45 mV) than that of sound-induced responses (0.1 mV), suggesting that wind- and sound-sensitive neurons might belong to two different populations. It is important to note that the short duration of the wind-evoked action potentials (<1 msec) is consistent with neuronal, rather than muscle, action potentials (Tanouye and Wyman, 1980). Interestingly, when we recorded from a slightly different location that is a few microns away from the original recording site, we observed robust sound-induced responses, but no wind-induced responses were observed, except at the onset and offset of the wind stimulus (Fig 3e–f). We also noticed that the amplitude of these transient responses at the onset and offset of the wind stimulus were very similar to that of sound-induced responses. In other recording sites, we observed the reverse situation where there were robust wind-induced responses but no sound-induced responses (Fig 3g–h). Taken together, these results suggested that: 1) JO neurons are responsive to both wind and sound, and 2) there are distinct populations of sound- and wind-sensitive JO neurons.

Although extracellular recordings allowed us to identify the presence of separate populations of wind- and sound-sensitive JO neurons, extracellular recordings lack spatial resolution, thus they are not useful for characterizing the spatial distribution of these sub-populations. Therefore, we decided to carry out calcium response imaging to identify the spatial distribution of these sub-populations.

The axons of the Johnston's organ neurons project to the AMMC of the central brain

According to Kamikouchi et al (2006), axons of the JO neurons project to the central brain region called AMMC, which is located ventro-laterally to the antennal lobes, the olfactory glomeruli (Fig. 4a). Within the AMMC, there are five distinct axon termination zones called zones A, B, C, D, and E (Fig. 4a, inset), and mosaic analysis has revealed that individual JO neurons innervate only one of the five zones (Kamikouchi et al., 2006), which suggests that there are potentially five distinct populations of JO neurons. Since it is difficult to distinguish the cell bodies of these five groups of neurons in the JO itself, we decided to image the calcium responses in JO axon terminals in the AMMC, where the five zones are easily discriminated. In addition, imaging the activity in JO axon terminals in the AMMC would allow us to visualize the spatial distributions of wind- and sound-sensitive JO neurons in the brain.

Distinct populations of sound- and wind-sensitive Johnston's organ neurons

To determine the spatial distribution of wind- and sound-sensitive JO neurons in the brain, we performed functional calcium response imaging experiments, using a genetically encoded calcium sensor (GCaMP-1.3 (Nakai et al., 2001), controlled by different Gal4 enhancer trap lines, which are expressed in specific sub-populations of JO neurons (Kamikouchi et al., 2006). To do this, we mounted a live *Drosophila* in an inverted orientation under a two-photon microscope, while airflow and/or near-field sound were delivered from a tubing and a speaker, respectively (Fig. 4b).

First, we examined the activity of A and B neurons using an enhancer trap line (JO-AB-GAL4) that selectively labels neurons in zones A and B by the presentation of courtship song (pulse song; 400 Hz, 90 dB SPL (Bennet-Clark, 1971), but not by the presentation of wind (0.9 m/s) (Fig.4 c–g). We next evaluated the activity of C and E neurons using a different enhancer trap line (JO-CE-GAL4) that selectively labels neurons in zones C and E (Kamikouchi et al., 2006). We observed robust responses to wind in zone E, but not to courtship song (Fig. 4h–l). Therefore, these results suggest that neurons in zones A and B are sound-sensitive, while neurons in the zone E are wind-sensitive.

To directly compare the activity of wind- and sound-sensitive zones in the same preparation, we employed a third enhancer trap line (JO-ACE-GAL4), which labels neurons in zones A, C, and E (Kamikouchi et al., 2006) (Fig. 5a). These experiments confirmed that zone A was activated by sound but not by wind, while zone E was activated by wind but not by sound (Fig. 5b–g, and Supplementary Movie 2a, b). The same selective responses were observed when the two stimuli were presented sequentially or simultaneously (Fig. 5h–m, and Supplementary Movie 2c, d). Together, these data indicated that the JO contains distinct populations of sound- and wind-responsive neurons that project to different regions of the AMMC (Kamikouchi et al., 2006) (Supplementary Footnote S2).

The tuning specificity of sound-sensitive neurons

Calcium response imaging data suggested that both A and B JO neurons respond to sound (courtship song), however it is not clear whether there is tuning specificity

between these neurons. To test if there are differences in frequency sensitivity between A and B JO neurons, we compared their response sensitivity to different frequencies of sound stimuli. We used frequency-modified courtship song as our sound stimuli in this experiment. The central frequency of original courtship song (pulse song) is around 280 Hz. We used Fourier transformation to modify the central frequency of courtship song to create various frequencies of sound stimuli between 100 Hz and 2,000 Hz (see method for more details).

Calcium response imaging was used to test the frequency sensitivity of A and B neurons. The zone A JO neurons were sensitive to frequency range between 100–1,800 Hz (Fig. 6a). The maximal responses of JO-A neurons were observed at 400 Hz, which matches the resonance frequency of aristae at 400 Hz (Gopfert and Robert, 2002). The zone B neurons were sensitive to narrower range of frequencies compared to that of zone A neurons, and they responded best between 100–400 Hz (Fig 6a). Thus these results suggest that A and B neurons have frequency tuning specificity.

Wind-sensitive neurons respond to wide range of wind speed

To give insight into the tuning specificity of wind-sensitive neurons, we first evaluated the range of wind speed that E neurons can respond to. The E neurons responded to a wide range of wind speed between 0.005–15 m/s (Fig. 6b). The maximal responses were observed at the wind speed between 0.5 and 1 m/s, which is the wind speed that flies normally encounter during their flight (personal communication with Michael Dickenson). Thus these experiments suggest that wind-sensitive neurons can respond to wind speed varying over at least five orders of magnitude.

Sensory map of wind direction in the *Drosophila* brain

We reasoned that wind-sensitive sensory neurons have to encode at least three aspects of wind qualities including speed, acceleration, and direction in order to accurately represent the wind stimulus in the brain. Here we evaluated if and how wind-sensitive neurons encode directionality of wind stimulus. To test the sensitivity of wind-sensitive neurons to different wind directions, we presented wind from four different directions, 0^o (from the front), 45^o, 90^o, and 180^o (from the rear) (Fig. 7a–c).

When airflow was applied from the front of the head (0^o), or at 45^o, there was strong activation in zone E, and little or no activation in zone C (Fig. 7d–f, and Supplementary Movie 3a–b). Conversely, airflow applied from the rear (180^o) activated zone C, and slightly inhibited zone E (Fig. 7d–f, and Supplementary Movie 3c). Interestingly, airflow applied to the side of the head (90^o) activated zone C ipsilaterally, and zone E contralaterally (Fig. 7d–f, 90^o; Supplementary Movie 3d). Therefore, these experiments suggest that both C and E neurons are sensitive to wind and they are differentially sensitive to wind directionality. In addition, there is a rudimentary map of wind directions within the AMMC. However, the underlying logic for this map of wind directions is not evident from these experiments.

Directions of atistae displacement explains the sensory map of wind direction

To give insight into the underlying logic of the map of wind directions, we decided to examine the direction of aristae displacement during wind stimulation from different directions using high magnification video analyses.

We observed from the calcium response imaging that wind from either 0^o or 45^o causes bilateral activation of zone E neurons in the brain, and was correlated with posterial aristae displacement in both antennae (Fig. 7d–f, 8a, Supplementary Movie 4b–c). Conversely, wind from the rear (180^o) causes bilateral activation of zone C neurons in the brain, and was correlated with anterial aristae displacement in both antennae (Fig. 7d–f, 8a, Supplementary Movie 4a). For wind 90^o, which activated zone C neurons in the ipsilateral hemisphere and zone E neurons in the contralateral hemisphere, elicited anterial and posterial aristae displacements in the ipsilateral and contralateral antennae respectively (Fig, 7d–f, 8a, Supplementary Movie 4d).

A combination of calcium response imaging and high magnification video analyses (Supplementary Movie 4a–c) suggested a simple hypothesis to account for the underlying logic for the map of wind directions: Airflow from either 0^o or 45^o causes posterial arista deflection and activates zone E neurons, while airflow from the 180^o causes anterial arista deflection and activates zone C neurons. It is important to note that arista ablation experiments indicated that the activation of wind-sensitive JO neurons, like that of sound-sensitive JO neurons (Ewing, 1978; Manning, 1967), is dependent upon this structure (Fig. 8).

To test the hypothesis directly, we moved the aristae in either anterior or posterior directions using a probe controlled by a DC motor (Fig. 9b). As hypothesized, displacing the arista posteriorly with a probe activated the zone E neurons almost as strongly as wind delivered from the front, and weakly inhibited the zone C neurons (Fig. 9c–d, “Push back”), while displacing it anteriorly activated the zone C neurons and inhibited the zone E neurons (Fig. 9c–d, “Push forward”).

These data demonstrate a direct causal link between the direction of aristae deflection and the activation of C vs. E neurons: C neurons are activated by anterial deflection of aristae, while E neurons are activated by posterial deflection of aristae. Thus, this model can explain the asymmetric activation of zones C and E neruons in ipsi and contrallateral hemi-brains during wind stimulation from 90^o (Fig. 7f, 90^o), because this stimulus produces opposite deflection of the aristae on the ipsi- and contra-lateral sides of the antennae (Fig. 9a, 90^o, Supplementary Movie 4d). We hypothesize that an internal comparison of activity between zones C and E neurons, both within and between each hemi-brain, could provide a basis for computing wind direction (Budick et al., 2007) in *Drosophila* brain.

Wind-sensitive C and E neurons are required for WISL behavior but not for courtship behavior

To determine whether the wind-sensitive C and E neurons are also required for WISL behavior, we genetically ablated these neurons using a toxin, ricin A chain (Moffat et al., 1992). When ricin A chain is expressed in a cell, it blocks protein synthesis and these cells die consequently. Because the JO-CE-Gal4 driver is expressed not only in JO neurons but also in the central brain (Fig. 10a), we employed an intersectional strategy to restrict ablation to the antenna using an *eyeless-FLP* recombinase. The specificity of this manipulation was confirmed using a FLP-dependent mCD8GFP reporter (Wong et al., 2002) (Fig. 10b).

In this experiment, we hypothesized that if the wind-sensitive neurons (C and E) are ablated, while the sound-sensitive neurons (A and B) are kept intact, we should

expect to see a loss of WISL behavior but intact sound-induced behavior (courtship behavior). To test the sound-induced behavior, we measured the time it takes for a female (without JO-C and -E neurons) to copulate with a wild-type male who can sing a wild-type courtship song. The latency to copulation is a good measure of hearing ability because the time it takes for a female to copulate is greatly influenced by her ability to hear the courtship song.

Following ablation of C and E neurons, WISL behavior was eliminated (Fig. 10g), while basal locomotor activity (prior to wind exposure) and phototaxis behavior were unaffected (Fig. 10g,10i, and 11a). This result supports the calcium imaging data showing that JO neurons in zones C and E are necessary for wind detection. Importantly, female flies lacking JO-C and -E neurons had normal hearing, as evidenced by their unperturbed receptivity to courtship by wild-type males, a behavior that depends on the females' ability to hear male courtship song. In contrast, females lacking *nanchung*, a gene required for hearing (Kim et al., 2003) or whose aristae were glued to the head to block the firing of JO neurons (Manning, 1967), exhibited a greatly increased latency to copulation (Fig. 10h, Nan/Nan; Bi-Gl).

These data indicate that JO-CE neurons are necessary for WISL behavior, but dispensable for a hearing-dependent behavior. Thus, clearly supports the calcium response imaging data showing that JO-C and -E neurons (but not JO-A and -B neurons) are implicated in wind detection.

Distinct intrinsic response properties for wind- and sound-sensitive neurons

So far, we demonstrated that A and B neurons are sensitive to sound, while C and E neurons are sensitive to wind based on calcium response imaging and behavioral analyses. However, it is not clear what stimulus features are responsible for the selective activation of sound- vs. wind-sensitive neurons in the JO. We first asked whether these two classes of mechanoreceptors are sensitive to different stimulus amplitudes, i.e., air particle velocities (v_{air}). A pressure gradient microphone positioned at the antenna (Göpfert and Robert, 2002) yielded a v_{air} = 0.011 m/s for the 400 Hz sound stimulus played at 90 dB, which maximally activated JO-AB neurons (Fig. 6a). Yet this sound stimulus did not activate zone E neurons (Fig. 4g), even though these neurons are activated by airflow at a v_{air} as low as 0.005 m/s (Fig. 6b). Thus, the selectivity of JO-CE and -AB neurons for wind vs. sound is not simply due to differences in stimulus magnitude.

To understand the selective nature of these wind- and sound-responsive JO neurons, we investigated the intrinsic response properties of these distinct classes of neurons. To this end, we compared the threshold and response characteristics of sound- and wind-sensitive JO neurons in response to various magnitudes and patterns of aristae displacement controlled by a probe connected to a DC motor (Fig 12a–b). Sound-sensitive neurons in zone A (Fig. 12c, red traces), were activated by displacements as small as 0.01 mm (Fig. 12c, red hatched bars), while wind-sensitive neurons in zone E (Fig. 12e, green traces) were only weakly activated at displacements below 0.04 mm (Fig. 12c, green bars). Thus, zone A neurons have a lower activation threshold than zone E neurons (see also Fig. 12g, 12j).

Strikingly, we observed that zone E neurons remained active for as long as the aristae were displaced, while zone A neurons were only transiently activated at the onset and offset of the probe displacement (Fig. 12h, k). This suggested that zone E neurons might adapt slowly, and therefore respond tonically, while zone A neurons might adapt rapidly, and therefore respond phasically. To confirm this, we moved the aristae in three successive steps of 0.033 mm each (total displacement of 0.099 mm; Fig. 12i). Zone A neurons exhibited transient (phasic) responses after each displacement (Fig. 12l, red traces), while zone E neurons were tonically activated for the entire duration of three-step displacements, and were maximally activated after the second step (Fig. 12l, green traces).

These data indicate that sound-sensitive (A) and wind-sensitive (E) neurons respond phasically and tonically to arista displacement, with low vs. high activation thresholds, respectively (see Supplementary Footnote S3). Furthermore, zone A neurons were activated by bidirectional arista displacement, while zone E neurons were activated by only unidirectional arista diaplacement (Fig. 12h, k). It is important to note that the reason why wind-sensitive neurons respond only unidirectional arista deflection is because these C and E neurons are direction sensitive (as discussed above).

These different intrinsic response properties are well matched to the oscillatory arista movements caused by pulses of near-field sound vs. unidirectional arista deflections caused by wind. The fly's ability to discriminate wind vs. sound using a common sensory organ is thus explained by different populations of JO neurons with different intrinsic response properties, which project to distinct area of the AMMC in the brain.

Tonic vs. phasic response properties are conserved properties of mechanoreceptors

The identification of different sub-populations of JO neurons with tonic vs. phasic response properties illustrates a general and conserved feature of mechanosensation across evolution. In the superficial layer of mammalian skin, there are two types of mechanoreceptors that are used to encode for different aspects of light touch sensations. Slowly adapting, tonically activated Merkel cells are used to encode for the shape of an object causing the skin indentation, while rapidly adapting, phasically activated Meissner's corpuscles are used to encode for the movement of an object causing the skin indentation (Johnson and Hsiao, 1992). In the *Drosophila*, these two properties have been adapted to detect different types of bulk air particle movements by different subsets of JO neurons. In addition, Dickinson and Palka (1987) have also reported that *Drosophila* has slowly and rapidly adapting campaniform sensillae on their wings. It is hypothesized that the rapidly adapting campaniform sensillae are involved in the sensory feedback during flight while the slowly adapting campaniform sensillae are involved in the glooming behavior. Interestingly, slowly adapting Merkel cells have a higher activation threshold compared to rapidly adapting Meissner's corpuscles (Csillag, 2005; Muniak et al., 2007), which also resembles the slowly adapting, wind-sensitive JO neurons with a higher activation threshold compared to rapidly adapting sound-sensitive JO neurons. Since sensory information from different modalities is normally processed by separate sensory organs in most animals, it seems unusual for *Drosophila* to use a single sensory organ to mediate both wind and sound detection. It is possible that since sound frequency of *Drosophila* courtship song, the only known sound stimulus for *Drosophila*, is very low

(~280 Hz), it is not surprising that *Drosophila's* JO has evolved to respond to both wind and low-frequency sound stimuli.

Conclusions

The data presented here indicate that the JO is not simply a hearing organ (Kernan, 2007), but also mediates wind detection. A combination of electrophysiological recordings, calcium response imaging, and behavioral analyses of JO neurons reveal that there are distinct populations of sound- and wind-sensitive JO neurons. The stimulus selectivity of these distinct classes of JO neurons is due to different intrinsic response properties (i.e. activation threshold, adaptation rate, and the ability to respond to unidirectional vs. bidirectional aristae displacements), which serves as the bases for flies' ability to discriminate between wind and sound stimuli.

We have also identified the sensory map of wind direction within the AMMC of the brain. The underlying logic for the map of wind direction can be explained by the ability of C and E JO neurons to respond to arista displacements in a direction-sensitive manner. We hypothesize that this map of wind direction probably involves an internal comparison of activity patterns between zones C and E, both within and between each hemi-brain, which potentially provides a basis for computing wind direction in the *Drosophila* brain. It is also possible that a fly brain might use the activation timing differences between the right and left hemi-brains to compute the subtle variation of wind directions. For example, both 0^o and 45^o wind activate zone E JO neurons in both hemi-brains. However, flies could potentially use the interaural timing differences between the right and left hemi-brains to determine the differences between 0^o and 30^o wind

directions. This type of sensory map that involves the comparison of activity between the hemi-brains has been well characterized for the map of sound localization involving interaural time differences and interaural intensity differences described in the owl brain (Carr and Konishi, 1988; Knudsen and Konishi, 1978; Takahashi, 1989). Sensory maps are very old in evolutionary history as they are ubiquitous in many organisms in most sensory systems, because they seem to serve some functional advantages for neural computations. The functional significance of the map of wind directions in *Drosophila* remains to be investigated.

In the accompanying paper, Kamikouchi et al. (2009) show that zone C and E neurons are required for the behavioral response to gravity (negative geotaxis), a force that could also produce static deflection of arista, albeit of a smaller magnitude than those produced by wind (Supplementary Footnote S4). Based on our data, the wind-sensitive (C and E) neurons have a high activation threshold (compared to that of sound-sensitive JO neurons) and thus they do not seem to be involved in processing small arista deflection induced by gravity; however, this discrepancy can be explained: 1) if there are sub-populations of C and E neurons that are sensitive to wind vs. gravity, or/and 2) there is a gain control mechanism that can amplify the minute arista deflection caused by gravitational force. Whether there are distinct sub-populations of C and E neurons for wind vs. gravity detections and if there is a gain control mechanisms that can amplify the minute gravitational forces acting on aristae remain unknown.

Wind-activated neurons in the JO are, moreover, required for an innate behavioral response to wind. The function of WISL in nature is not clear. Field studies have suggested that wind is a major environmental factor affecting the dispersal of wild

Drosophila populations (Johnston and Heed, 1976; Johnston and Templeton, 1982; Richardson and Johnston, 1975). WISL may have evolved to control population dispersal, and thereby maintain genetic homogeneity (Johnston and Heed, 1976; Johnston and Templeton, 1982). Alternatively, WISL may represent a defense mechanism that serves to protect individual flies from injury, or to prevent dispersal from food resources. Identification of the sensory neurons that mediate WISL opens the way to a systematic analysis of the genes and neural circuitry that underlie this robust, innate behavioral response to wind.

MATERIALS AND METHODS

Fly stocks

Flies carrying *JO4-GAL4* (also called *JO-ACE*), *JO31-GAL4* (also called *JO-CE*), *JO15-GAL4* (also called *JO-AB*) were described in (Kamikouchi et al., 2006). *UAS-GCaMP* (Wang et al., 2003) and *UAS-mCD8-GFP* flies were obtained from Y. Wang (Wang et al., 2004) and R. Axel, *UAS-FRT-STOP-FRT-Ricin* flies were obtained from D. Berdnik (Berdnik et al., 2006), JO-CE-GAL4;eyFLP flies were obtained from H. Inagaki, *Canton-S* flies from J. Dubnau, and *UAS-hid* flies from B. Hay. Flies were maintained on corn meal-molasses food at 25°C on a (12/12) light-dark cycle.

WISL behavioral apparatus

The WISL assay was performed in a 6 x 6 x 1.5 cm transparent acrylic plastic box (WISL chamber), which has airflow inputs and outputs (1 cm diameter) on two of the four vertical sides of the box. The input tubing carries airflow from a tank containing

breathable air, connected to a flow regulator. The output tubing allows the airflow to escape from the box, and is connected to a flow meter that measures the speed of the airflow. The WISL chamber was mounted on a transparent plastic table and was trans-illuminated with a fluorescent light from underneath. A video camera (Sony, DCR-HC40 NTSC) was set up above the WISL chamber to record the flies' locomotor activity.

WISL assay protocol

20 flies per trial were sorted 36–48 hours prior to testing, using nitrogen gas or cold anesthesia. On the testing day, 20 flies were aspirated into the WISL chamber and allowed to acclimate for 7–8 min just before initiating the trial. A standard WISL trial lasts for 270 seconds. During the first 55 seconds of the trial period, the flies' baseline locomotor activity was recorded. At 55 seconds, a brief mechanical stimulation (5 manual strikes on the table that the WISL chamber was mounted on) was given to increase the flies' locomotor activity. The airflow exposure was initiated at 80 seconds and terminated at 200 seconds, for a total of 120 seconds (2 minutes) of exposure. Locomotor activity was recorded at 10 frames per second and average velocity was computed using custom software written in Matlab (MathWorks Inc.) (Lebestky et al., 2009).

Courtship (female receptivity) assay

Naive *Canton-S* males and virgin females of the genotype of interest were collected immediately after eclosion, using nitrogen or CO_2 gas anesthesia. Naive males were individually housed while virgin females were group housed for 6 days until the test day. Single naive *Canton-S* male and a single virgin female of the genotype of interest were

placed in a mating chamber (1 x 1 x 0.4 cm square chamber), and the time at which a successful copulation occurred was recorded for each mating pair. Successful copulation typically lasts 15–25 minutes.

Phototaxis assay

40 flies per trial were sorted 48 hours prior to testing, using nitrogen or CO_2 gas anesthesia. On the test day, 40 flies were tapped into the elevator of a T-maze and allowed to rest for 1 minute in a dark. Then, the elevator was lowered to the choice point where flies were given 1 minute to make a choice between a dark tube, or a tube illuminated with a 40 W fluorescent light, positioned approximately 20 cm away. The phototaxis response was analyzed by calculating the PI using the following formula: PI = [(2* COR) – 1] *100. COR = (number of flies that chose the illuminated tube/total number of flies). PI = 0 indicates an equal distribution of flies between the dark and illuminated tubes. PI = 100% indicates that all flies chose the illuminated tube.

Antenna manipulations

In order to test the role of the JO in wind detection, a3 segments were surgically removed using a pair of forceps 48 hours prior to the WISL testing. For the antennal gluing experiment, a small drop of UV-activated glue was placed at the junction between the a2 and a3 segments bilaterally, and cured with a UV lamp for 3–5 seconds, 48 hours before the testing. For the mechanical probe antennal displacement experiment, a sharpened tungsten needle was used to move the aristae in different direction and patterns. The probe was mounted on a DC motor/controller (LTA-HS and SMC100CC, Newport),

which was controlled by custom Matlab software (MathWorks Inc). To push the aristae backward, the probe was positioned anterior to the aristae; conversely, to push the aristae forward the probe was positioned posterior to the aristae. In the “push back” (and “push forward”) conditions, the aristae were pushed backward (and forward) in a single increment of varying distances (either 0.01, 0.02, 0.025, 0.03, 0.04, 0.05, 0.07, 0.09, or 0.11 mm), held for 8 seconds in the displaced position and then returned to the original position. In another experiment, the aristae were pushed backwards in three successive steps of 0.033 mm (a total of 0.099 mm), held in place for 2.9 seconds after each successive step, and then returned to the original position. In all conditions, the probe and aristae movements were verified using a video camera (GE680, Proscillica) that was set up underneath the fly preparation mounted on the microscope stage as described above.

Electrophysiology

Sample preparation and electrophysiological recording from the Johnston’s organ axons were performed as described in (Eberl et al., 2000). Briefly, extracellular recordings from the Johnston’s organ axons were recorded at the a1/a2 joint using a tungsten or glass electrode (0.5 MΩ). All recordings were carried out in a sound-proof chamber. Pulse song segments of recorded *D. melanogaster* courtship song [provided by J. Hall (Wheeler et al., 1988) and D. Eberl] were used as the sound stimulus and airflow rate between 0.3–0.9 m/second was used as wind stimulus.

Calcium response imaging and sample preparation

Flies were anesthetized in a plastic vial on ice for 15–20 sec, and were then gently

inserted into a hole of a thin plastic rectangular plate. Small drops of wax (55°C) were applied to prevent the fly from moving out from the hole. After the fly was stabilized in the plastic hole, the preparation was oriented in an up-side-down position (see Fig. 2b of the main text). The proboscis, ventral part of thorax and abdomen, and legs were protruding from the upper side of the horizontal plane of the plastic, while the rest of the fly head (including the antennae, but excluding the proboscis), thorax, and dorsal part of abdomen were protruding from the bottom side of the horizontal plane of the plastic. In a saline bath, the proboscis was cut off and the area surrounding the proboscis was surgically removed to expose the ventral side of the brain. Fat and air sacs were gently removed to have a clear view of the brain. For calcium response imaging, the water immersion objective lens (40X, N.A.=0.8, Olympus) was lowered near the exposed brain, while the underside of the plastic specimen mount, which contained the intact antennae, was kept dry and exposed to wind and sound stimuli.

Sound stimuli used in these experiments were recorded segments (provided by J. Hall and D. Eberl) of the pulse song portion of *D. melanogaster* courtship song, played at 75–100 dB at the aristae using a loudspeaker (ProMonitor 800 loudspeaker, Definitive Technology) and amplifier (P.A. amplifier, Radioshack) and was measured using a digital sound meter (DSM-325, Mannix). We tested the frequency tuning of zones A and B using narrowband signals derived from the original pulse-song. The original pulse-song was filtered in order to set the center of the frequency spectrum at a desired frequency between 100 and 2000 ± 200 Hz (using the Fourier transformation).

Wind stimuli used in imaging experiments were delivered at speeds between 0.005–15 m/sec. Wind speed was controlled by flow regulator (mass flow meters and controllers—Smart Trak series 100, Sierra Instrument Inc.) and was measured using an anenometer (Testo-435, Testo GmbH & Co.). VClamp software (Pairie Technology) was used to control all aspects of sound and wind stimuli used in the imaging experiments.

All imaging was performed on an Ultima two-photon laser scanning microscope (Prairie Technology). Live images were acquired at 6.1 frames per second using an Olympus 40X (N.A. = 0.8) water immersion objective at 128 x 128 resolution with an imaging wavelength at 925 nm. GCaMP responses were quantified using custom software written in Matlab. The relative change in fluorescence intensity ($\Delta F/F$) was computed by first calculating the average pixel values in the region of interest during the experimental period and applying a three frame moving average smoothing function. This average fluorescence value, F_{av}, was then converted to $\Delta F/F$ using the formula $\Delta F/F = (F_{av} - F_0)/F_0$, where F_0 is the baseline fluorescence value, measured as the average of frames 2–9. Average $\Delta F/F$ for specific stimulus period was compared between different JON zones to test for statistical significance by ANOVA.

ACKNOWLEDGEMENTS

We thank Ulrike Heberlein and Fred Wolf (UCSF) for hosting a sabbatical that led to the discovery of WISL; Lihi Zelnik, Michael Reiser and Pietro Perona for creating locomotor tracking software; Dan Eberl and Jeff Hall for *D. melanogaster* courtship song recordings; Gaby Maimon for making fly holders for imaging experiments; Mike Roy for

building behavioral chambers for WISL and female receptivity assays; Hidehiko Inagaki for sharing unpublished data and *JO-CE-GAL4;eyFLP* flies; Bruce Hay for *UAS-hid* flies; Daniela Berdnik for *UAS-FRT-STOP-FRT-Ricin* flies; Michael Dickinson for anemometers and helpful discussions; J. L. Anderson for advice on fluid mechanics; Martin Göpfert for providing a pressure gradient microphone; Mark Konishi for advice and use of lab facilities; and Gaby Mosconi for laboratory management. D. J. A. is an Investigator of the Howard Hughes Medical Institute. This work was supported in part by an NSF FIBR grant.

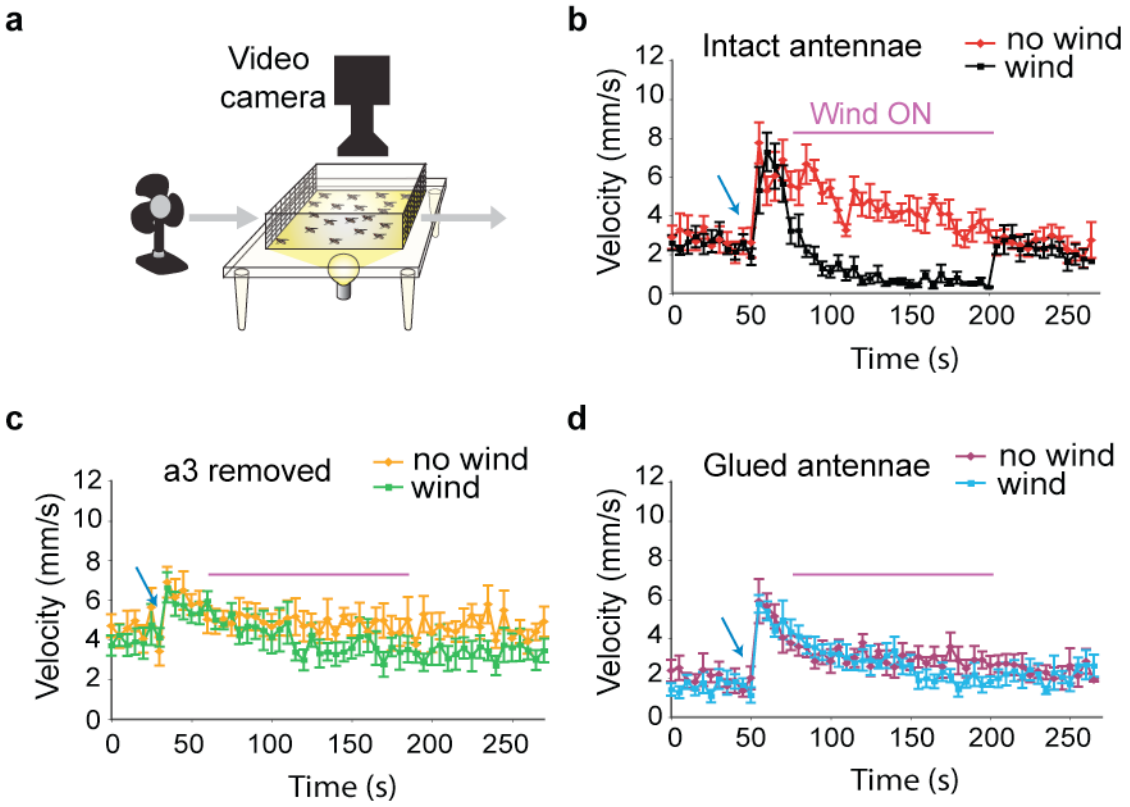

Figure 1. Wind-induced suppression of locomotion (WISL) behavior

(a) Schematic illustrating WISL assay apparatus (see Methods). (b) WISL behavior in CS flies. Data represent mean (±SEM) velocities (n=6). Blue arrow indicates brief mechanical startle. The "no wind" vs. "wind" curves are significantly different (p=.0001, Kruskal-Wallis ANOVA). (c, d) Elimination of WISL by removal of a3 (c) or gluing a3 to a2 (d). The "no wind" vs. "wind" curves are not significantly different (n=6).

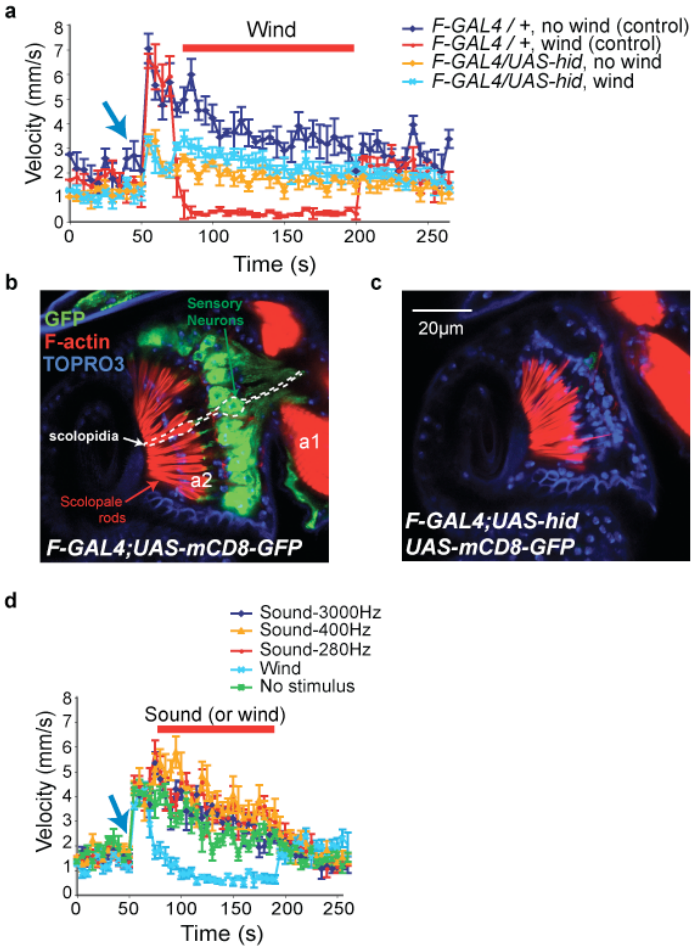

Figure 2. WISL behavior is dependent on chordotonal mechanosensory neurons in the Johnston's organ

(a) WISL behavior is lost in flies in which JO neurons are killed using nanchung (F)-Gal4 and UAS-hid. The light blue (wind) and orange (no wind) curves of F-Gal4; UAS-hid flies are not significantly different ($p>0.05$, Kruskal-Wallis ANOVA). Control F-Gal4/+ flies show a clear WISL effect: wind vs. no wind, $p<0.0001$ (Kruskal-Wallis ANOVA); $p=0.0006$ for comparison of average velocity during the "Wind ON" period of "no wind" vs. "wind" conditions (Mann-Whitney U-test). Control UAS-hid/+ flies also show a robust WISL effect; $p<0.0001$ (Kruskal-Wallis ANOVA; data not shown). (b, c) Confirmation that JO neurons in the antenna are ablated by F-Gal4; UAS-hid. (b) Control flies with F-Gal4; UAS-mCD8GFP. Scolopidia, the sensory organ unit of JO, are outlined (white dashed lines). Sensory neurons are green (GFP+). Scolopale rods are labeled by rhodamine F-actin (red). TOPRO3 is a nuclear counter-stain. (c) Similar view of JO from F-Gal4; UAS-hid/UAS-mCD8GFP flies. Note loss of sensory neurons. The scolopale rods remain because they are synthesized by scolopale cells that do not express the F-Gal4 driver and are therefore spared. Scale bar, 20 µm. (d) Average locomotor velocity vs. time plots for wild-type CS flies exposed to peak frequency-modified pulse-song derived from *D. melanogaster* courtship song recordings (Wheeler et al., 1988), presented at 90 dB (SPL) at the antenna. Blue arrows indicate brief mechanical startle; red line indicates duration of wind or sound exposure. Note that only wind causes locomotor suppression (light blue curve). "Wind" vs. "No stimulus" curves, $p=0.0002$ (Kruskal-Wallis ANOVA); $p=0.0013$ for comparison of average velocity during the wind ON period of "Wind" vs. "No stimulus" conditions (Mann-Whitney U-test). Data are mean ± SEM, n=10 (200 flies/condition).

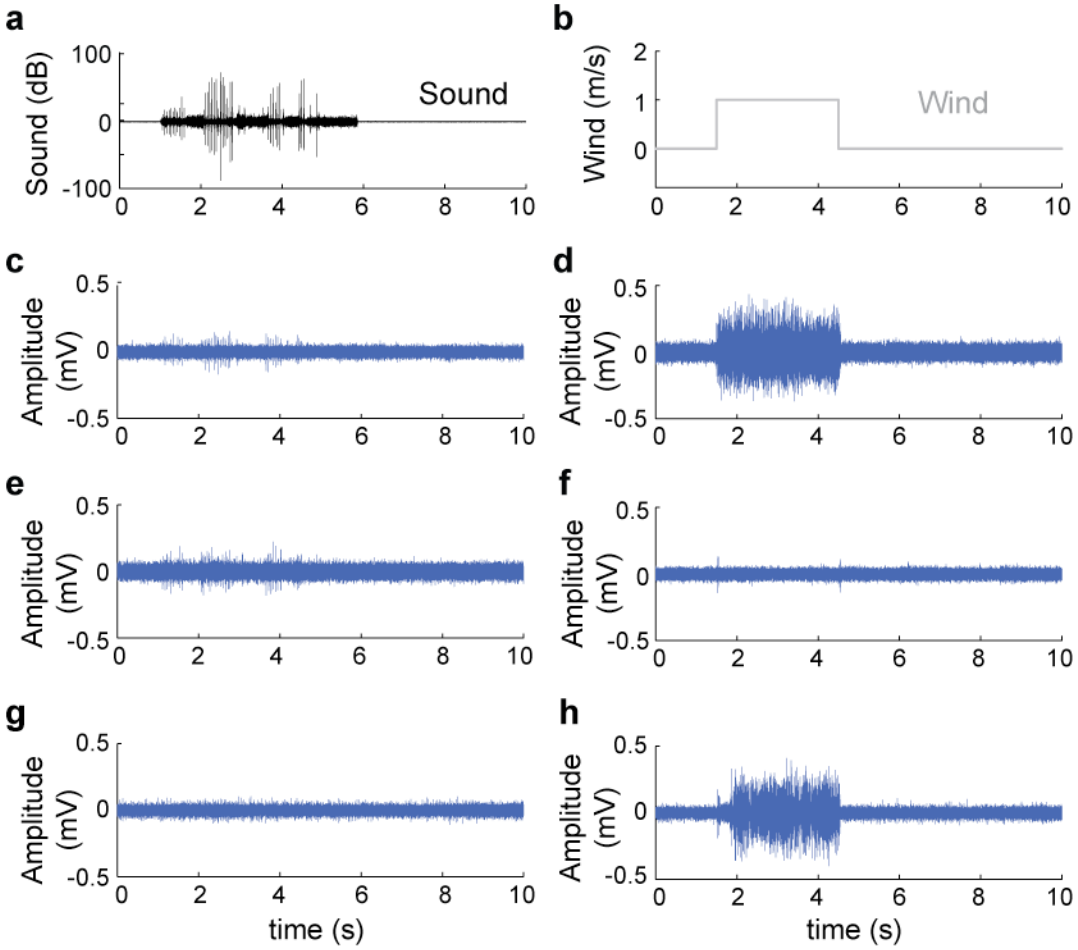

Figure 3. Electrophysioological analyses of wind- and sound-induced responses in *Drosophila*

(a) sound stimulus (courtship pulse-song) and (b) wind stimulus used for electrophysiological recording of the JO neurons. (c, d) Response of JO neurons to both sound (c) and wind (d). (e, f) Response of JO neurons to sound (e) but not wind (f). (g, h) Response of JO neurons to wind (g) but not sound (h).

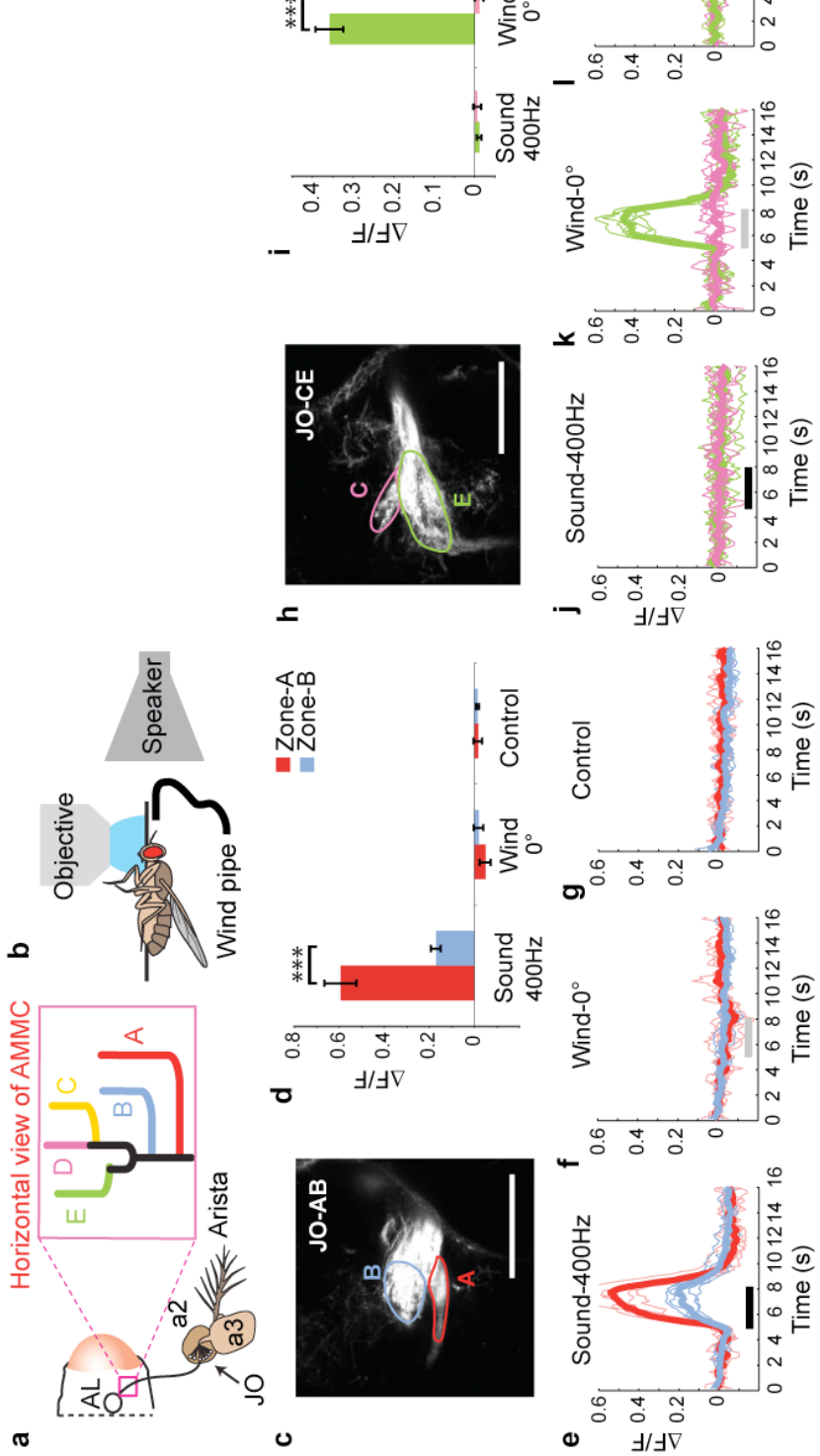

Figure 4. Different sub-populatons of JO neurons are activated by wind and sound

(a–b) Schematics illustrating (a) location of JO relative to a2 and a3, and five JO neuron axonal terminal zones (Kamikouchi et al., 2006) in the AMMC; (b) imaging set-up (see Methods for details). (c) Flies were exposed to peak frequency-modified pulse song (see Methods for details) at 400 Hz and 90 dB (as well as at 75 and 100 dB; not shown), or to wind (0.9 m/sec) delivered from the anterior (0°), in either flies expressing GCaMP in zones A and B (c–g), or in zones C and E (h–l). Zones A and B were activated by sound (d, e) but not wind (d, f), while zone E was activated by wind (i, k) but not sound (i, j). Zone C was also activated by wind, but only if presented from the posterior (180°; see Fig. 7). Data are mean ± SEM, n=6 experiments. Scale bars, 50µm. ***, $p<0.001$ (Repeated measure ANOVA and Bonferroni multiple comparisons).

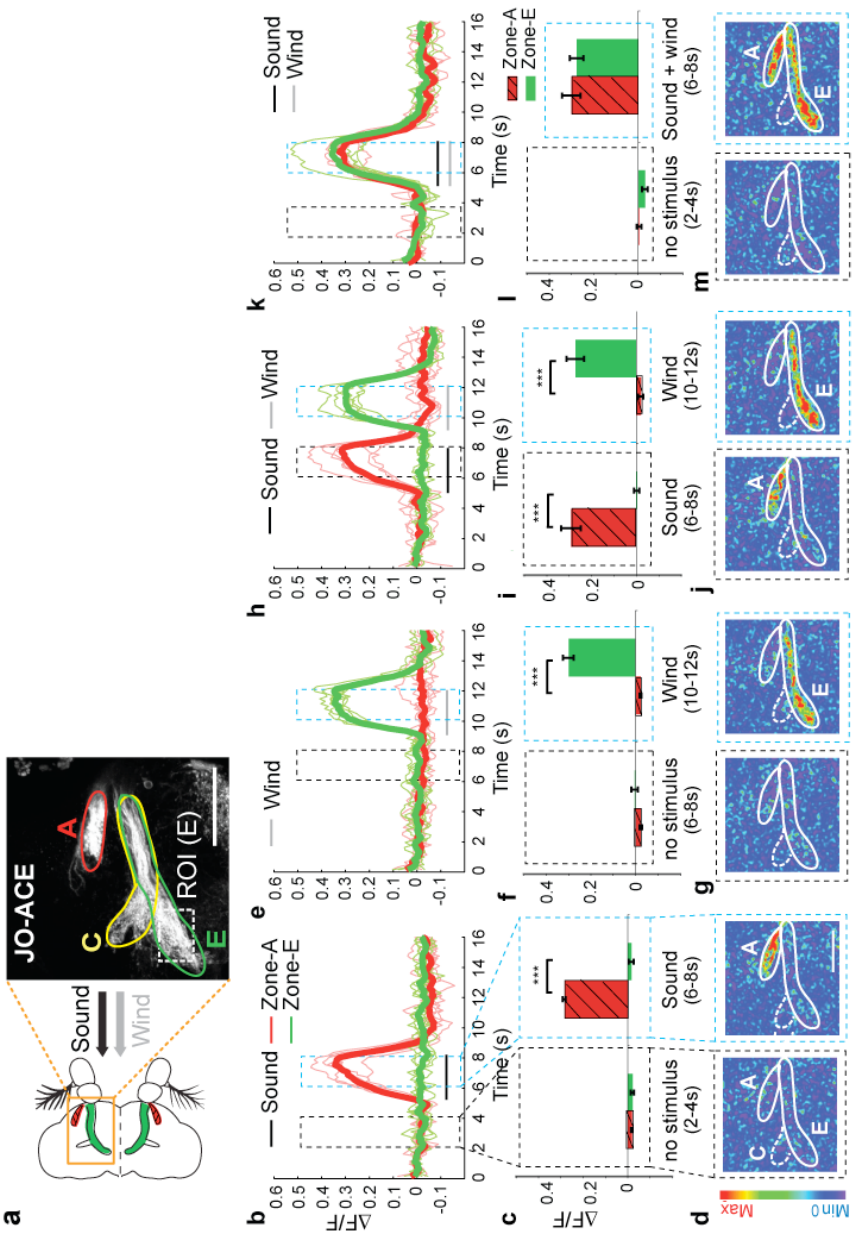

Figure 5. Calcium imaging reveals distinct populatons of wind- and sound-responsive JO neurons
(a) Zones A, C, and E are visualized using a UAS-mCD8-GFP reporter. ROI, region of interest for ΔF/F measurements in zone E. (b–m) Zones A (red traces, hatched bars) and E (green traces, bars) are activated by sound and wind, respectively, whether presented singly (b–g), sequentially (h–j) or simultaneously (k–m) (see Supplementary Movies 2a–e). Thick traces (b, e, h, k) represent average of the individual (thin) traces (n=6). (c, f, i, l) Bar graphs indicate the mean (±SEM) integrated ΔF/F in the time bins (dashed rectangles in b, e, h, k; see Methods). ***, $p<0.001$ (Repeated measure ANOVA and Bonferroni's planned comparisons). (d, g, j, m) ΔF images of GCaMP activation in zones A and E. Scale bars, 50μm.

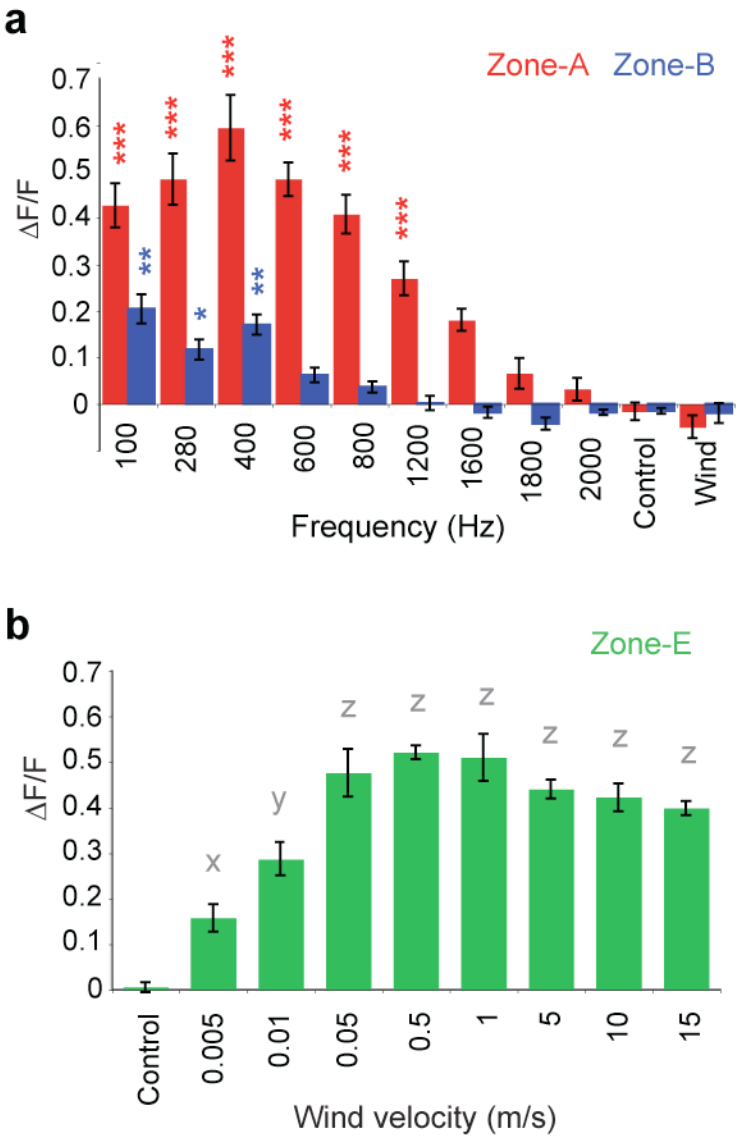

Figure 6. A and B neurons are sensitive to frequency, while E neurons are sensitive to a wide range of wind speeds

(a) Sensitivity of zones A and B neurons to different sound frequencies (mean±SEM, n=6). *** (red), $p<0.0001$; * (blue), $p<0.01$; ** (Blue), $p<0.001$ relative to control. (b) Sensitivity of zone E neurons to different wind speeds (n=5). Letters indicate significant differences relative to control (all $p<0.0001$ except "a," $p<0.001$).

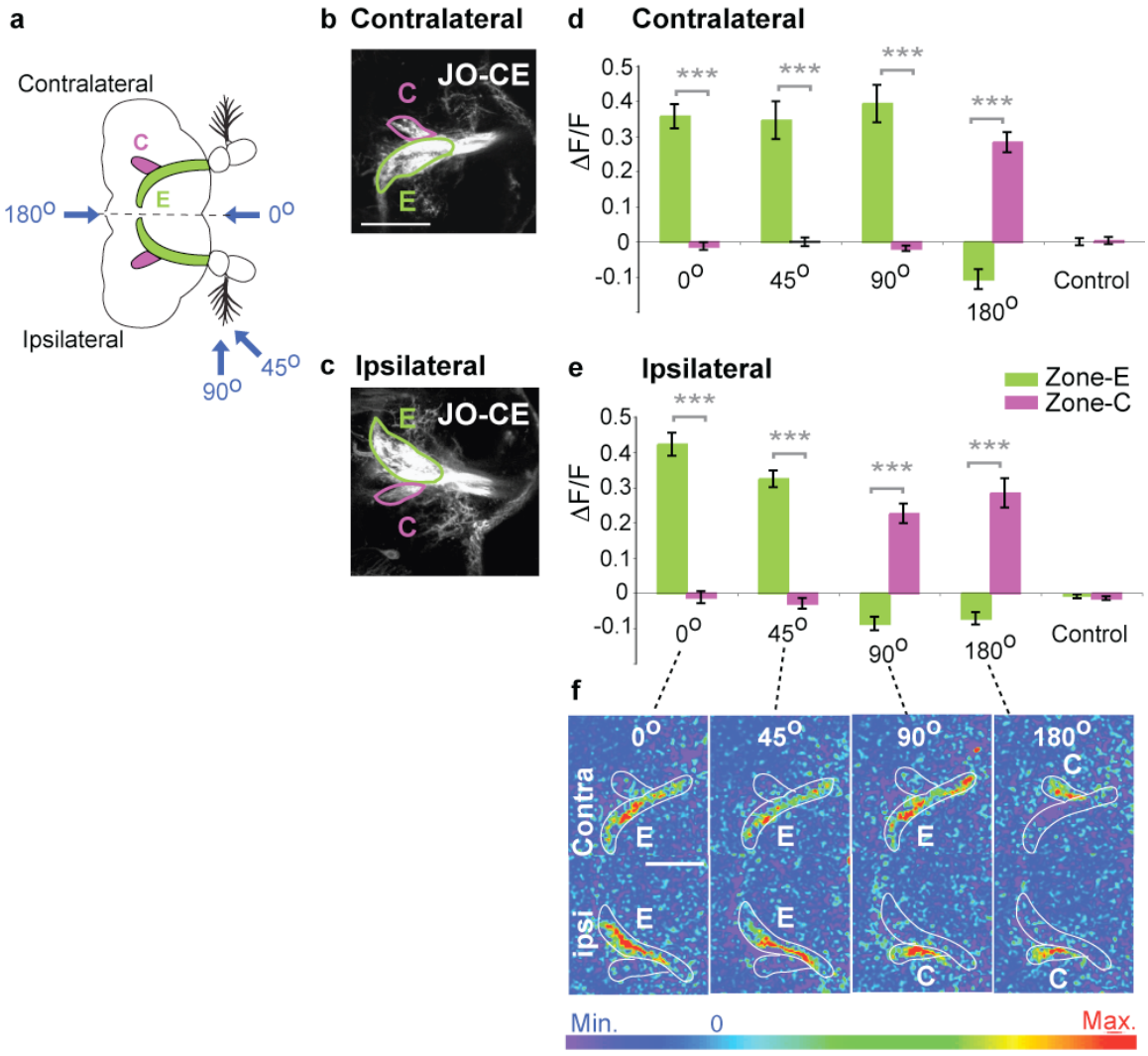

Figure 7. Map of wind directions in the AMMC

(a–c) Schematic (a) and mCD8-GFP expression (b, c) illustrating zones C and E in contralateral and ipsilateral hemi-brains. Blue arrows indicate wind direction. (d–f) Average (±SEM) ΔF/F signals integrated over the stimulus period for zones C and E in the contra- (d) and ipsi- (e) lateral hemi-brains, and corresponding ΔF images (f; see Supplementary Movies 3a–e).

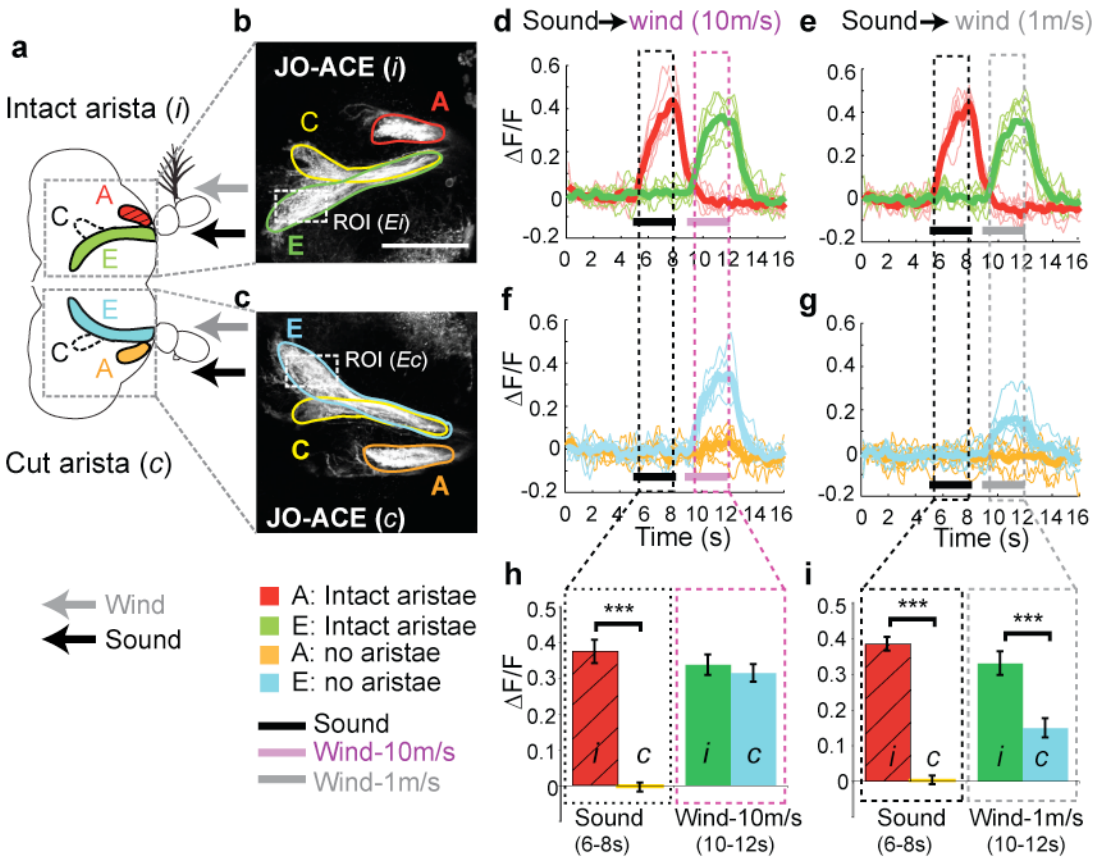

Figure 8. Effect of arista ablation on wind and sound sensitivity

(a–c), Schematic (a) and mCD8-GFP expression (b, c) illustrating zones A, C, and E in the right hemi-brain connected to the antenna without arista and in the left hemi-brain connected to the wild-type antenna, serving as a control side. d–I, Loss of arista causes complete loss of sound-induced responses in the zone A (d, e), while loss of arista causes partial reduction in wind-induced responses at wind speeds 10 m/s (f) and 1 m/s (g). Error bars are s.e.m. ***P<0.0001 (repeated measure ANOVA and Bonferroni planned comparisons).

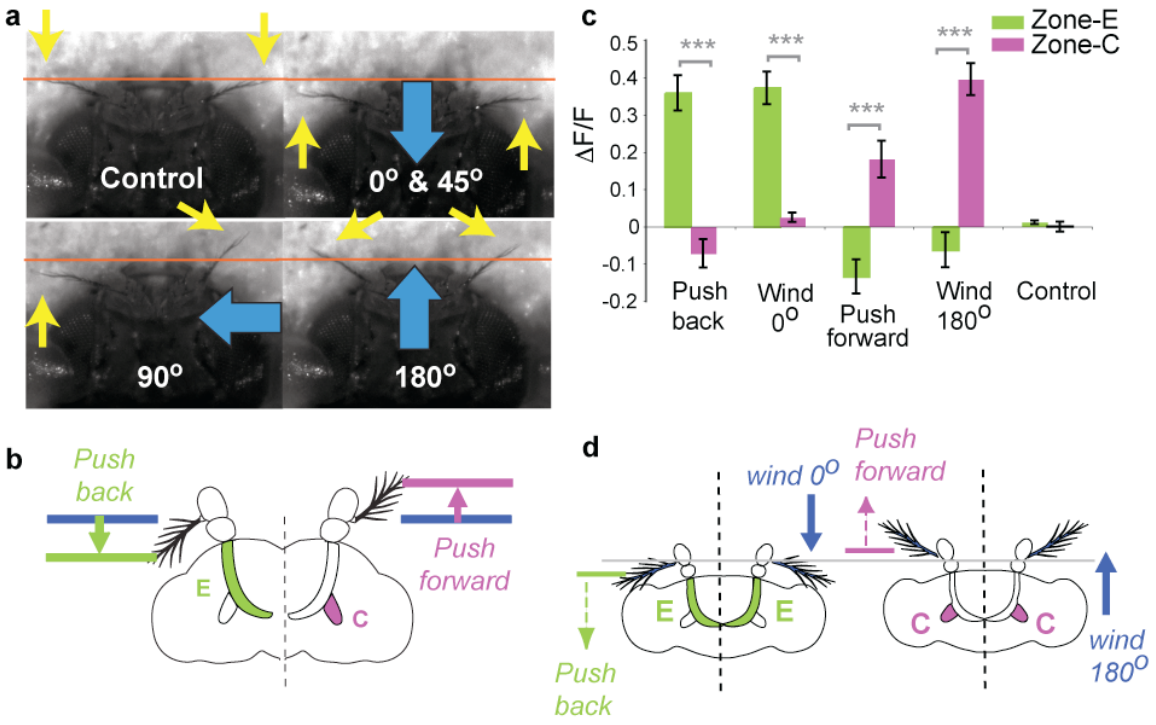

Figure 9. Anterial displacement of arista causes the activation of C neurons, while posterial displacement of arista causes the activation of E neurons

(a) Still frames from video recordings of aristae movements during wind stimulation (Supplementary Movies 4a–e). Yellow arrows indicate aristae position, orange line denotes rest position ("Control"). Blue arrows indicate wind direction. (b) Schematic illustrating predicted responses of zones C and E to directional, probe-driven aristae displacements. (c) Responses of the C and E neurons to wind and directional arista displacements. (d) Summary illustrating differential sensitivity of zones C and E to direction of arista displacement. Scale bars, 50μm. ***, $p<0.0001$ (Repeated measures ANOVA and Bonferroni planned comparisons).

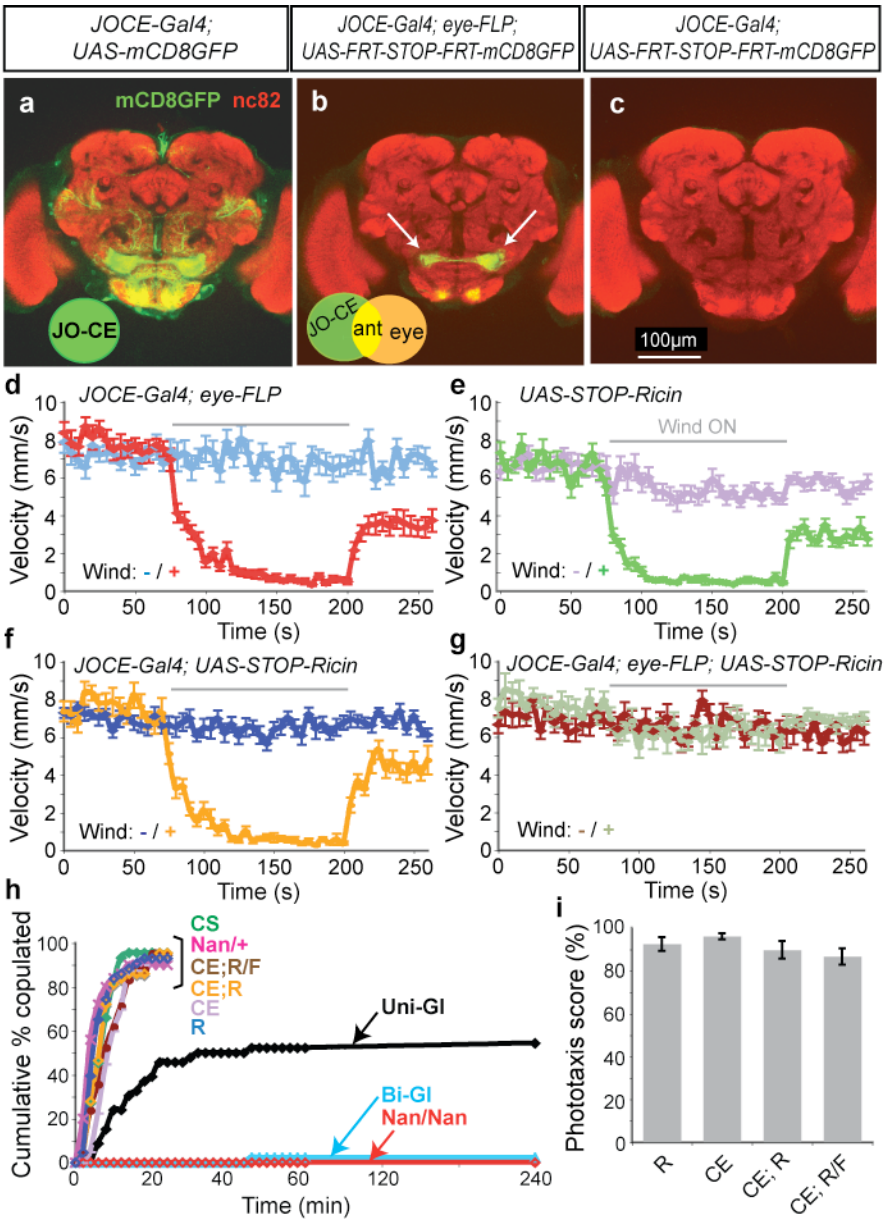

Figure 10. Ablation of wind-sensitive (C and E) neurons abolishes WISL behavior
(a–c) GFP expression patterns of the indicated genotypes, double-stained with antibodies to GFP (green) and nc82 (red). (a) Original JO-CE-Gal4 pattern. (b) Antennal-restricted JO-CE-Gal4 pattern using eye-FLP. Arrows indicate AMMC; underlying structures are gustatory neuron projections to the sub-oesophageal ganglia (Kamikouchi et al., 2006). (c) Control for (b) lacking eye-FLP. (d–g) WISL analysis. Curves represent mean velocity±SEM (n=15). (d–f) Genetic controls show robust WISL. The "wind-" vs. "wind+" curves are significantly different ($p<0.0001$). (g) Ablation of C and E neurons abolishes WISL. (h) Cumulative percentage of manipulated females copulating with CS males. >90% of all pairs in bracketed conditions exhibited successful copulation within 20 min (n=40–50 pairs). Genotypes: CE; R/F = JO-CEGal4; UAS<STOP<Ricin/eye-FLP; CE; R = JO-CEGal4; UAS<STOP<Ricin; CE = JO-CEGal4; R = UAS<STOP<Ricin. Unilateral ("Uni-Gl") or bilateral ("Bi-Gl") gluing of the aristae, or the nanchung mutation (Nan/Nan) (Kim et al., 2003) impaired copulation ($p<0.0001$). Ablation of JO-CE neurons ("CE; R/F") did not impair either copulation (h), or phototaxis (i). Phototaxis scores represent mean ±SEM (n= 7). P-values are shown by Kruskal-Wallis ANOVA.

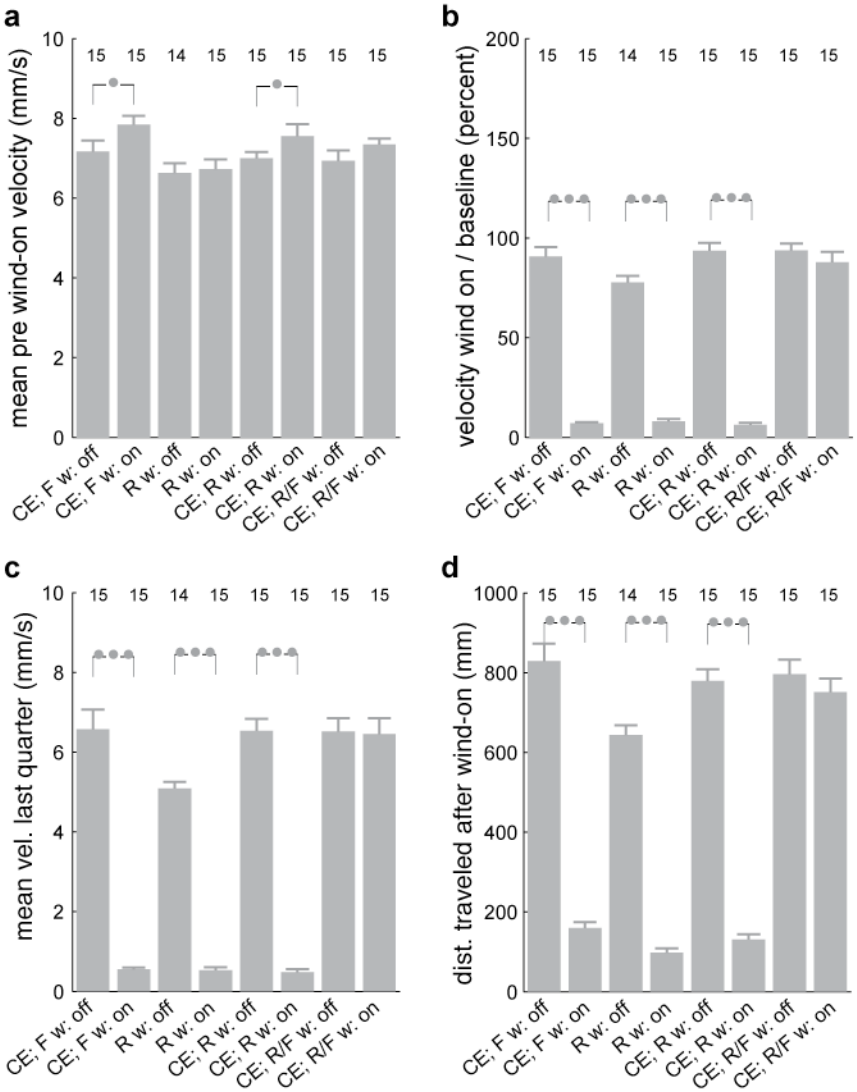

Figure 11. Quantification of WISL behavior in flies lacking JO-CE neurons

The parameters shown are calculated from the data in Fig. 3 (e–h). (a) Mean velocity prior to wind exposure. (b) Mean velocity during wind exposure, as a percentage of pre-wind baseline velocity. (c) Absolute mean velocity during the last quarter of the wind exposure period. (d) Distance traveled following the onset of wind exposure. •, $p<0.05$; •••, $p<.001$ (Kruskal-Wallis and Mann-Whitney U-test). Numbers above the bars indicate number of assays performed for each genotype or condition (20 flies/assay). Genotype abbreviations: "CE;F" = JO-CEGal4;eye-FLP; "R"= UAS-FRT-STOP-FRT-Ricin; "CE;R"= JO-CEGal4;UAS-FRT-STOP-FRT-Ricin; "CE;R/F" = JO-CEGal4;UAS-FRT-STOP-FRT-Ricin/eye-FLP. "w: off" and "w: on" indicate no wind applied during the experiment, vs. wind applied during the interval indicated by the gray bar in Fig. 3e–h, for each genotype.

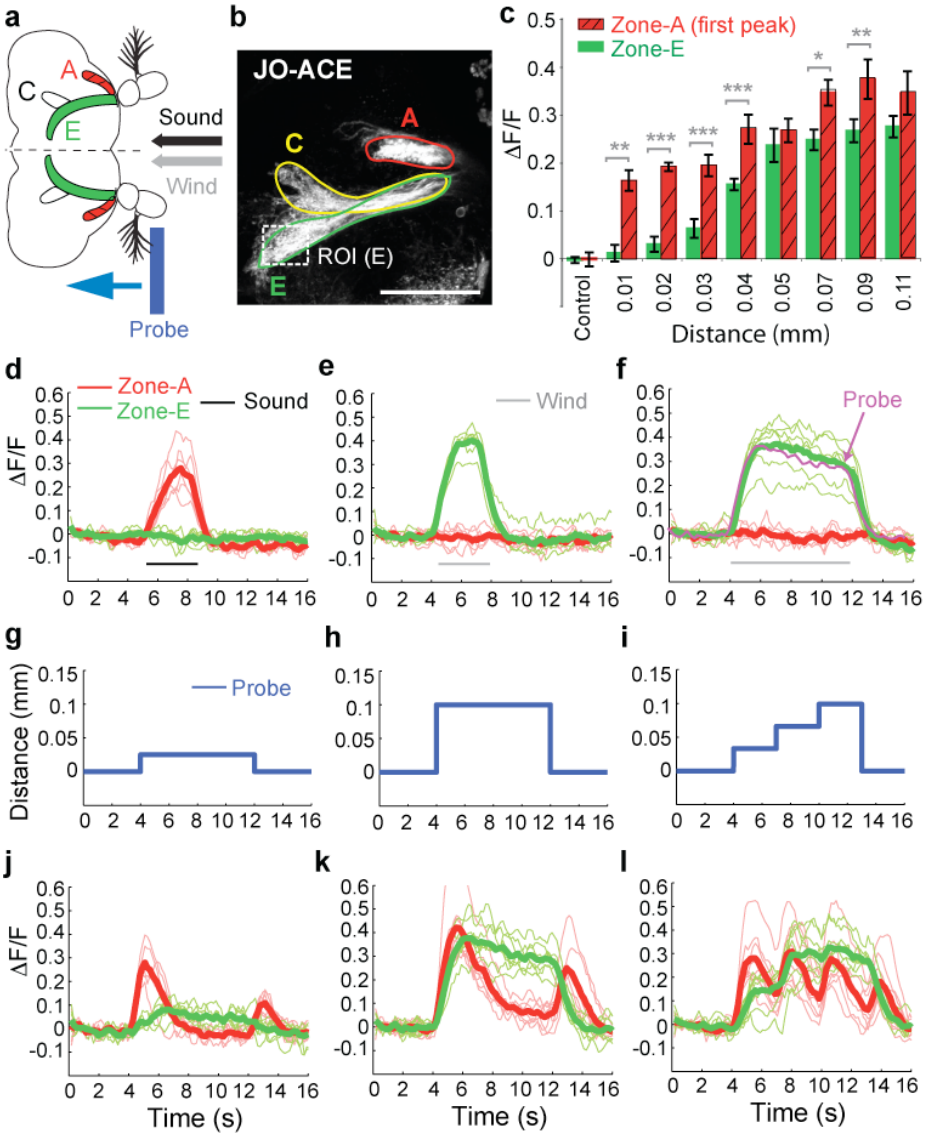

Figure 12. Wind- and sound-sensitive JO neurons have different intrinsic response properties

Comparison of sound-, wind-, and probe-evoked responses in zones A and E. (a, b) Schematic (a) and mCD8-GFP expression (b) illustrating zones A, C, and E. ROI, region of interest for ΔF/F measurements in zone E. Scale bar, 50µm. (c) Responses of zones A and E to different distances of probe-induced arista displacement. *, $p<0.01$; **, $p<0.001$; ***, $p<0.0001$; all zone A responses (relative to control), $p<0.0001$ except 0.01 mm ($p<0.001$); all zone E responses >0.04 mm, $p<0.0001$; zone E responses < 0.04 mm not significant. (d–f) Sound and wind responses. Thick lines represent average of the individual (thin) traces (n=6). (f) Superposition of the average responses of zone E to 8 seconds of wind (green trace) and mechanical probe displacement (magenta trace; see m). (g–l) Responses (j–l) of zones A and E to different distances and patterns of probe-induced arista displacement (g–i) (n=6). All p-values are shown by Repeated measure ANOVA and Bonferroni multiple comparisons.

Supplementary Footnote S1

J. S. Johnston and colleagues have measured wind speeds in the habitats of several wild-caught *Drosophila* species (Johnston and Heed, 1976; Johnston and Templeton, 1982), including both tropical and desert environments. In Kamuela, Hawaii, for example, *D. mercatorum* and *D. hydei* inhabit environments where trade winds blow in the range of 5–25 km/hr (1.4–6.9 m/s), with an average velocity of 15 km/hr (4.17 m/sec); gusts over 35 km/hr (9.72 m/s) are not uncommon (Johnston and Templeton, 1982). Wind speeds in the range of 0.46–4.64 m/s have been measured in the Arizona desert, the habitat of *D. nigrospiracula* (Johnston and Heed, 1976). We observed wind-induced suppression of walking in *D. melanogaster* between 0.7–1.6 m/s; these velocities are therefore well within the range of wind speeds measured in several *Drosophila* natural habitats. Wild-caught *D. mercatorum* and *D. hydei* exhibited locomotor arrest in the laboratory at wind speeds of 10 km/hr (2.8 m/sec) and greater (Johnston and Templeton, 1982), while wild-caught *D. mimica*, another Hawaiian species, exhibited locomotor arrest at air speeds between 6 and 7 km/hr (1.67–1.94 m/s) (Richardson and Johnston, 1975). Anecdotal evidence that wind suppresses *Drosophila* locomotor activity in the wild derives from the observation that during occasional days in Hawaii when the trade winds stop, called "Kona" weather (Johnston and Templeton, 1982), *Drosophila* in flight are abundant, while during the trade winds very few *Drosophila* are observed in flight because most of them are immobilized on their *Opuntia* substrate (J. S. Johnston, personal communication). These data suggest that WISL is a naturally occurring behavior exhibited by *Drosophila* at wind speeds normally encountered in their wild ecological habitat. Johnston and colleagues speculate that this behavior may be the dominant

environmental influence (rather than, e.g., temperature and humidity) affecting the dispersal of wild *Drosophila* populations, and thereby an important determinant of their "genoclines," geographic gradients in gene frequencies (Johnston and Templeton, 1982; Richardson and Johnston, 1975).

Supplementary Footnote S2

Our detection of distinct sound- and wind-evoked spiking responses in antennal nerve electrophysiological recordings (Fig. 3) argues that the differential activation of sound- vs. wind-sensitive axons observed by GCaMP imaging is unlikely to be explained by local circuit interactions within the AMMC. Electrophysiological recordings from sound-selective locations in the antennal nerve usually revealed one or two spikes at the onset and offset of the wind stimulus (Fig. 3e vs. f). These brief spiking responses probably reflect the fact that phasically responsive JO neurons can be transiently activated by deflections of the aristae caused by wind.

Supplementary Footnote S3

Our calcium imaging experiments indicate that arista movements triggered by the mechanical probe activate both wind- and sound-sensitive neurons (Fig. 12k, l), while the natural stimuli (wind and sound) activate these neurons in a mutually exclusive manner (Fig. 12d, e). Wind-sensitive neurons may not be activated by sound stimuli, because the magnitude of the antennal displacements produced by courtship song may be too small to

evoke a detectable response (see also Supplementary Footnote S4). This hypothesis is supported by the fact that short-distance mechanical displacements of the aristae activate sound- but not wind-sensitive neurons (Fig. 12e). Why, then, are sound-sensitive neurons not also activated by wind? In fact, our electrophysiological data indicate that they *are* activated, albeit very transiently: Brief spiking responses are observed in sound-sensitive JO neurons at the onset and offset of the wind stimulus (Fig. 3e, f, blue traces; see Supplementary Footnote S2). These transient spiking epochs are unlikely to produce sufficient accumulations of intracellular calcium to yield detectable GCaMP signals (Pologruto et al., 2004). In contrast, the GCaMP signals elicited in sound-sensitive JO neurons by controlled mechanical displacements (Fig 12g–l, red lines) may reflect more extended spiking responses caused by damped oscillatory vibrations of the probe as it pushes against the arista. Finally, it is possible that wind- and sound-selective neurons differ in their sensitivity to the position, velocity, or acceleration of the antenna caused by these different stimuli, as shown for limb chordotonal organs in the stick insect (Hofmann and Koch, 1985; Hofmann et al., 1985). The mechanical probe may not faithfully mimic these natural stimulus-specific differences in antennal movements.

Supplementary Footnote S4

We did not observe activation of zone C/E JO neurons by antennal deflections below ~30 μm, while Kamikouchi et al. observed activation with deflections as small as 1 μm, consistent with the estimated deflection caused by the earth's gravitational field acting on the mass of the antenna. This difference is probably due to differences in the calcium imaging methods used in the two studies. Our approach measures activity in JO neuron axon terminals, which most likely reflects influx of extracellular Ca^{2+} due to spike firing. In contrast, Kamikouchi et al. measure activity in JO cell bodies, which may reflect both Ca^{2+} influx and release from intracellular stores. In addition, the kinetics of the decay of Cam2.1 signal in response to transient Ca^{2+} increases is much slower (~2 s) than that of GCaMP (330 ms) (Mank et al., 2006), so that the method employed by Kamikouchi et al. integrates small changes in $[Ca^{2+}]_{in}$ over a longer period of time.

REFERENCES

Bennet-Clark, H. (1971). Acoustics of insect song. Nature *234*, 255-259.

Berdnik, D., Chihara, T., Couto, A., and Luo, L. (2006). Wiring stability of the adult *Drosophila* olfactory circuit after lesion. J Neurosci *26*, 3367-3376.

Budick, S. A., Reiser, M. B., and Dickinson, M. H. (2007). The role of visual and mechanosensory cues in structuring forward flight in *Drosophila melanogaster*. J Exp Biol *210*, 4092-4103.

Caldwell, J. C., and Eberl, D. F. (2002). Towards a molecular understanding of *Drosophila* hearing. J Neurobiol *53*, 172-189.

Carr, C. E., and Konishi, M. (1988). Axonal delay lines for time measurement in the owl's brainstem. Proc Natl Acad Sci USA *85*, 8311-8315.

Csillag, A. L., ed. (2005). Atlas of the sensory organs: functional and clinical anatomy (New Jersey: Humana press).

Dickinson, M. H. and Palka, J. (1987) Physiological properties, time of development, and central projection are correlated in the wing mechanoreceptors of *Drosophila*. J Neurosci *7*, 4201-4208.

Eberl, D. F., Hardy, R. W., and Kernan, M. J. (2000). Genetically similar transduction mechanisms for touch and hearing in *Drosophila*. J Neurosci *20*, 5981-5988.

Ewing, A. W. (1978). The antenna of *Drosophila* as a "love song" receptor. Physiol Entomol *3*, 33-36.

Göpfert, M. C., and Robert, D. (2002). The mechanical basis of *Drosophila* audition. J Exp Biol *205*, 1199-1208.

Göpfert, M. C., and Robert, D. (2002). The mechanical basis of *Drosophila* audition. J Exp Biol *205*, 1199-1208.

Hofmann, T., and Koch, U. T. (1985). Acceleration receptors in the femoral chordotonal organ of the stick insect, *Cuniculina Impigra*. J Exp Biol.

Hofmann, T., Koch, U. T., and Bassler, U. (1985). Physiology of the femoral chordotonal organ in the stick insect, *Cuniculina Impigra*. J Exp Biol.

Johnson, K. O., and Hsiao, S. S. (1992). Neural mechanisms of tactual form and texture perception. Annu Rev Neurosci *15*, 227-250.

Johnston, J., and Heed, W. (1976). Dispersal of desert-adapted *Drosophila*: the saguaro-breeding *D. nigrospiracula*. Am Nat *110*, 629-651.

Johnston, J., and Templeton, A. (1982). Dispersal and clines in *Opuntia* breeding *Drosophila mercatorum* and *Drosophila hydei* at Kamuela, Hawaii, In Ecological Genetics and Evolution, J. S. F. Barker, and W. T. Starmer, eds. (Sydney: Academic Press), pp. 241-256.

Kamikouchi, A., Shimada, T., and Ito, K. (2006). Comprehensive classification of the auditory sensory projections in the brain of the fruit fly *Drosophila melanogaster*. J Comp Neurol *499*, 317-356.

Kernan, M. J. (2007). Mechanotransduction and auditory transduction in *Drosophila*. Pflugers Arch *454*, 703-720.

Kim, J., Chung, Y. D., Park, D. Y., Choi, S., Shin, D. W., Soh, H., Lee, H. W., Son, W., Yim, J., Park, C. S., *et al.* (2003). A TRPV family ion channel required for hearing in *Drosophila*. Nature *424*, 81-84.

Knudsen, E. I., and Konishi, M. (1978). A neural map of auditory space in the owl. Science *200*, 795-797.

Lebestky, T., Chang, J. S., Dankert, H., Zelnik, L., Kim, Y. C., Han, K. A., Wolf, F. W., Perona, P., and Anderson, D. J. (2009). Two different forms of arousal in *Drosophila* are oppositely regulated by the dopamine D1 receptor ortholog DopR via distinct neural circuits. Neuron *64*, 522-536.

Mank, M., Reiff, D. F., Heim, N., Friedrich, M. W., Borst, A., and Griesbeck, O. (2006). A FRET-based calcium biosensor with fast signal kinetics and high fluorescence change. Biophys J *90*, 1790-1796.

Manning, A. (1967). Antennae and sexual receptivity in *Drosophila melanogaster* females. Science *158*, 136-137.

Moffat, K. G., Gould, J. H., Smith, H. K., and O'Kane, C. J. (1992). Inducible cell ablation in *Drosophila* by cold-sensitive ricin A chain. Development *114*, 681-687.

Muniak, M. A., Ray, S., Hsiao, S. S., Dammann, J. F., and Bensmaia, S. J. (2007). The neural coding of stimulus intensity: linking the population response of mechanoreceptive afferents with psychophysical behavior. J Neurosci *27*, 11687-11699.

Nakai, J., Ohkura, M., and Imoto, K. (2001). A high signal-to-noise Ca(2+) probe composed of a single green fluorescent protein. Nat Biotechnol *19*, 137-141.

Pologruto, T. A., Yasuda, R., and Svoboda, K. (2004). Monitoring neural activity and [Ca2+] with genetically encoded Ca2+ indicators. J Neurosci *24*, 9572-9579.

Richardson, R. H., and Johnston, J. S. (1975). Behavioral components of dispersal in *Drosophila mimica*. Oecologia *20*, 287-299.

Slatkin, M. (1985). Gene flow in natural populations. Annu Rev Ecol Syst *16*, 393-430.

Slatkin, M. (1987). Gene flow and the geographic structure of natural populations. Science *236*, 787-792.

Smith, C. I., and Farrell, B. D. (2006). Evolutionary consequences of dispersal ability in cactus-feeding insects. Genetica *126*, 323-334.

Takahashi, T. T. (1989). The neural coding of auditory space. J Exp Biol *146*, 307-322.

Tanouye, M. A., and Wyman, R. J. (1980). Motor outputs of giant nerve fiber in *Drosophila*. J Neurophysiol *44*, 405-421.

Wang, J. W., Wong, A. M., Flores, J., Vosshall, L. B., and Axel, R. (2003). Two-photon calcium imaging reveals an odor-evoked map of activity in the fly brain. Cell *112*, 271-282.

Wang, S. L., Hawkins, C. J., Yoo, S. J., Muller, H. A., and Hay, B. A. (1999). The *Drosophila* caspase inhibitor DIAP1 is essential for cell survival and is negatively regulated by HID. Cell *98*, 453-463.

Wang, Y., Guo, H. F., Pologruto, T. A., Hannan, F., Hakker, I., Svoboda, K., and Zhong, Y. (2004). Stereotyped odor-evoked activity in the mushroom body of *Drosophila* revealed by green fluorescent protein-based Ca2+ imaging. J Neurosci *24*, 6507-6514.

Wheeler, D. A., Fields, W. L., and Hall, J. C. (1988). Spectral analysis of *Drosophila* courtship songs: *D. melanogaster, D. simulans*, and their interspecific hybrid. Behav Genet *18*, 675-703.

Willis, M. A., and Avondet, J. L. (2005). Odor-modulated orientation in walking male cockroaches *Periplaneta americana*, and the effects of odor plumes of different structure. J Exp Biol *208*, 721-735.

Willis, M. A., Avondet, J. L., and Finnell, A. S. (2008). Effects of altering flow and odor information on plume tracking behavior in walking cockroaches, *Periplaneta americana* (L.). J Exp Biol *211*, 2317-2326.

Wong, A. M., Wang, J. W., and Axel, R. (2002). Spatial representation of the glomerular map in the *Drosophila* protocerebrum. Cell *109*, 229-241.

Wright, S. (1943). Isolation by distance. Genetics *28*, 114-138.

Chapter 3

Remaining outstanding questions and future directions

There is a tonotopic representation in the Johnston's organ

The basilar membrane of the mammalian cochlea is organized into a tonotopic map (Moller, 2003), which functions as an initial stage of spectral analyses even before acoustic energy reaches the auditory receptor cells, the inner hair cells. Thus, the tonotopic map in the basilar membrane provides a great functional advantage. Since sensory maps may serve adaptive advantage, and are found in auditory systems of various organisms (Mason and Faure, 2004; Stolting and Stumpner, 1998), we wanted to investigate if there is a tonotopic map in the *Drosophila* JO.

In order to investigate the location of cell bodies for all class of JO neurons (zones A, B, C, and E neurons) within the JO, I decided to use the genetically encoded photo-activatable GFP (PA-GFP) to photo-convert each class of JO neurons by illuminating their axon terminal zones in the AMMC. Illumination with 710 nm light cause photo-conversion of the PA-GFP to change its emission spectrum and become visible (Datta et al., 2008). The photo-converted GFP will eventually travel down to the cell body from the axon terminal zone by diffusion, which allows us to determine the relative location of the cell bodies of A, B, C, and E neurons in the JO.

PA-GFP experiments suggest that JO neurons are organized in a ring of arrays from the medial to lateral portion of the antenna in the JO (Fig. 13–h). The tip of the scolopedia is attached to the tip of the a3 segment and cell bodies are located at the outer ring of the array. Cell bodies of zone C neurons were located at the medial end of the array, while cell bodies of the zone E neurons were located at the lateral end of the arrays (Fig. 13 d–f, 13i). There was no overlap between the cell bodies of zones C and E neurons, since they were located at the opposite end of the array. Cell bodies of the zone

A neurons occupy the narrow midpoint area of the array, where axon bundles are exiting from the JO towards the brain (Fig. 13a–b). The cell bodies of zone A neurons never overlap with that of zone C or E neurons (Fig. 13–i). The cell bodies of zone B neurons occupy the wider area around the middle portion of the array compared to A neurons, thus they overlap with the cell bodies of zones A around the central potion (Fig. 13a, c, i). B neurons also overlapped with C neurons near the medial end, and E neurons near the lateral end (Fig. 13a–f, 13i).

As discussed in chapter 2, Zone A neurons respond to high frequency sound, while zone B neurons respond to low frequency sound (Fig. 6a). In contrast, zone C and E neurons respond to wind (Fig. 7). If we consider wind as an extremely low frequency "auditory" stimulus (~1 Hz), it looks like the JO neurons are organized in a tonopotic map: The cell bodies of C and E neurons, which respond to extremely low frequency stimulus (wind), are located at the extreme ends of the array, while the cell bodies of B neurons, which respond to lower frequency sound occupies the middle portion of the array. Finally, the cell bodies of A neurons, which respond to higher frequency sound, occupy the central portion of the array; thus from the direction of the medial to the central to the lateral end of the array, cell bodies are organized in the order of: C neurons (wind) → B (low frequency) → A (high frequency) → B (low frequency) → E (wind). It is important to note that there are no clear boundaries in this tonotopic map but the area occupied by A neurons never overlaps with the area occupied by C and E neurons. It is also interesting to note that cell bodies of A neurons are much larger (~6–7 μm, diameter) than these of B, C, and E neurons (~3–4 μm, diameter) (Fig. 14). Whether the size of cell body relates to any function is not known.

As discussed in Chapter 2, wind from the front (0^o) activated zone E neurons, and slightly inhibited C neurons, while wind from the rear (180^o) activated C neurons and inhibited E neurons in the AMMC. Thus, there are antagonistic activation patterns between C and E neurons (Fig. 7). At first, we thought that there is lateral inhibition between C and E neurons, however it is also possible to hypothesize that the structural arrangement of C vs. E neurons within the JO (medial vs. lateral end of the JO array) might also explain the antagonistic activation patterns between the C and E neurons. For example, when aristae are deflected posteriorly (by 0^o wind), the attachment sites of scolopedia for E neurons get tensioned, and cause activation of E neurons, while C neurons' scolopedia get relaxed, causing hyperpolalization of the C neurons (Fig. 13j). Conversely, when aristae is deflected anteriorly (by 180^o wind), the scolopedia for C neurons get tensioned, and activate C neurons, while E neurons' scolopedia get relaxed, causing hyperpolarization of E neurons (Fig. 13j).

The antagonistic activation patterns between C and E neurons are interesting from both functional and mechanistic perspectives. These antagonistic activation patterns remind us of lateral inhibition in the antennal lobes of olfactory system, which is known to sharpen the odor acuity. Whether these antagonistic relations between the C and E neurons are related to the acuity of the fly's wind detection system is not known. Also, whether these antagonistic relations are indeed due to their cell bodies' location within the JO or/and lateral inhibition also remains to be determined.

Full-length aristae are required for high frequency sound sensitivity

The sensitivity of a given sensory system determines the stimulus range and stimulus magnitude that an organism can detect. To increase sensitivity, many sensory systems in various organisms have evolved specialized structures that can magnify the stimulus range and magnitude. We reasoned that the arista is a specialized structure to amplify the stimulus sensitivity of JO. Thus, we investigated if the length of aristae influences the frequency sensitivity for sound detection using calcium response imaging in the zones A and B. We removed a half tip of arista from one antenna, and the full-length arista on the other antenna served as a control (Fig. 15a–b). Shortened arista causes loss of sensitivity for high frequency sound ($\leq$ 800 Hz) in zone A, while it has no effect for the sensitivity for the low frequency sound (Fig. 15c–d). The loss of sensitivity for high frequency sound is probably due to the change in the resonance frequency of an arista that is half the length of the original arista. It would be interesting to test if the length of aristae also affects the sensitivity for low speed wind or possibly gravity.

How do flies detect wind and gravity using C and E JO neurons?

Kamikouchi et al. (2009) in the accompanying paper showed that zone C and E neurons are required for the behavioral responses to gravity, while our study showed that C and E neurons respond to wind, based on electrophysiological recording, calcium response imaging, and behavioral analyses. The sensitivity of the JO, thus influences whether C and E neurons can respond to both gravity and wind.

According to our study, wind-responsive C and E neurons have a higher activation threshold (≥ 30 μm) compared to that of the sound responsive neurons based on the arista pushing experiments (Fig. 12c). Since arista deflection caused by gravitational force is estimated as approximately 1 μm (Kamikouchi et al., 2009), it is hard to imagine how C and E neurons could respond to a small forces such as gravity, in addition to wind stimuli. However, it is possible for C and E neurons to respond to both wind and gravity: 1) if the sensitivity of C and E neurons is enhanced by a structure-based amplification mechanism during signal transduction or by circuit-based gain control (i.e. spatial integration that allows the convergence of receptor neurons' outputs), or/and 2) if there are distinct sub-populations of C and E neurons that are wind- vs. gravity-sensitive.

Various amplification mechanisms for sensory systems are described in different sensory systems in various organisms. For example, the mammalian cochlea has outer hair cells that function as a structure-based mechanical amplifier to amplify small intensity sounds and reduce the sensitivity for very loud sound to protect our ear (Dallos, 2008; Hudspeth, 2008). Outer hair cells generate force to augment auditory sensitivity and frequency selectivity (Fettiplace and Hackney, 2006; Holley and Ashmore, 1988).

In the *Drosophila* JO, it is reported that sound-processing JO neurons have a structure-based amplification mechanism that can amplify low intensity sound and reduce the sensitivity for high intensity sound (Gopfert et al., 2006; Nadrowski et al., 2008; Nadrowski and Gopfert, 2009). A few genes, including *Nanchung* and *Inactive*, which encode TRP Vanilloid channels and *NompC*, which encodes the TRPN1 channel, have been implicated in the amplification mechanism in *Drosophila* (Gopfert et al., 2006).

Kamikouchi et al. (2009) have shown that *NompC*, a gene implicated in sound amplification, is not involved in the behavioral response to gravity. Thus, if there are amplification mechanisms for C and E neurons, they probably involve different sets of genes that contribute to gravity sensitivity. Whether there are amplification mechanisms that allow the same population of C and E neurons to respond to both wind and gravity remains unknown.

An alternative explanation for the involvement of C and E neurons for detection of wind and gravity is to have distinct sub-populations of C and E neurons that selectively respond to wind vs. gravity. Since it is technically challenging to evaluate the effect of gravity using calcium response imaging or electrophysiological recording, there are no data to support the existence of distinct sub-populations within the C and E populations at this point. It would be helpful to have GAL4 lines that are expressed in sub-populations of the C and E neurons, or intersectional strategies to manipulate sub-populations of C and E neurons.

How do flies distinguish wind from the front (0^o) and 45^o angle?

As discussed in chapter 2, we identified a sensory map of wind directions (Fig. 7), which potentially facilitates the discrimination of different wind directions. We hypothesized a model for the discrimination of wind directions involving the comparison of activation patterns between the zone C and E neurons within each heni-brains, and between the right and left hemi-brains. However, this model does not completely explain how flies can discriminate wind from the front (0^o) and 45^o angle, because they cause the same activation patterns in the *Drosophila* brain (Fig. 7d–f). However, if we modify this

model by including the comparison of activation timing or intensity in the left and right hemi-brains, this model can explain how flies could discriminate the wind from the front (0^o) and 45^o angle. For example, if we imagine that wind from the 45^o angle would activate E neurons in one side of hemi-brain before the other side, there are time differences between the activation of E neurons in the right and left hemi-brains. If the wind-sensitive JO neurons in the right and left antennae can encode for these time differences, this model can still explain the fly's ability to discriminate 0^o vs. 45^o wind.

Alternatively, it is also possible that there are differences in the speed of wind that reaches right and left antennae. The interaural intensity difference might affect the numbers of E neurons that are activated by 0^o vs. 45^o wind in the right and left hemi-brains. In this case, if we carry out calcium response imaging and compare the differences in the activation intensity in zone E between the right and left hemi-brains, we should see stronger increases in the fluorescence in the ipsilateral side compared to that of the contralateral side. Other insects, such as grasshoppers, indeed utilize interaural intensity differences between the right and left tympanal membranes to determine the location of a sound source (Hennig et al., 2004).

How do flies detect changes in wind direction or changes in speed?

In the *Drosophila*'s natural environment, the speed and direction of wind might change haphazardly; thus flies have to be able to detect the changes in speed and wind direction in order to navigate properly during flight or to avoid potential life threatening conditions. For example, what if the wind direction shifts from 45^o northeast to 45^o northwest? Either 45^o northeast or 45^o northwest wind would activate E neurons in both

hemi-brains, so how do flies detect this change in the wind direction? Furthermore, how do flies detect sudden changes in wind speed during flight? Our data suggest that wind and sound stimuli are processed by distinct populations of JO neurons, however it is possible that sound-sensitive A and B neurons might be able to provide useful information about wind. For example, if the wind is blowing from the front at 0.05 m/s and its speed changes suddenly from 0.05 m/s to 1 m/s, the E neurons continue to fire regardless of changes in wind speed. However, the arista might be deflected further posteriorly after wind speed increases from 0.05 m/s to 1 m/s. This condition reminds us of the probe experiment where aristae are pushed by a probe in three successive steps (Fig. 12i, 12l). In this experiment arista was deflected further posterially in three successive steps, and we observed that E neurons continued to fire (tonic response); in contrast A neurons responded at every successive deflection of the arista (phasic response). Thus, it is possible that A/B neurons might encode for changes in wind speed.

A similar scenario involving a potential role of A/B neurons in the detection of changes in wind directions can be hypothesized. When the wind direction changes slightly from 10^{o} to 45^{o}, the ipsilateral side (relative to wind stimulus) of arista might deflect further posteriorly after the wind direction shifts.

Since flies exhibit anemotaxis behavior, orientation behavior towards or away from wind (Budick et al., 2007), we can use this behavior to test a potential role of A/B neurons for detecting a change in wind direction from 10^{o} to 45^{o}. We can compare the fly's anemotaxis behavioral responses in wild-type flies and flies without A/B neurons. If flies without A/B neurons fail to show anemotaxis behavior, it suggests that A/B

neurons are essential for detecting changes in wind direction. This experiment is quite important to determine whether or not wind information processing involves population coding by A, B, C, and E neurons or by C and E neurons.

Where are the wind-sensitive second-order neurons?

A more comprehensive analysis of wind information processing and its circuit organization and the understanding of neural circuits controlling WISL behavior requires the identification of second and higher order neurons. Identifying the second order neurons is not only important for revealing the projection patterns of wind pathways, but it allows us to investigate how wind direction information is further transformed at the higher order neurons. To this end, we can also use the PA-GFP to identify the second order neurons, and possibly higher order neurons. For example, we can express the genetically encoded PA-GFP everywhere except in the primary JO neurons by genetically expressing the constructs: elav-GAL4; UAS-PA-GFP; nanchung-TDtomato-2A-GAL80. Expressing these constructs, we can selectively express the PA-GFP everywhere except the JO neurons and we can also express the red channel marker only in the JO neurons. Thus, activation of the JO neurons with 710 nm light within the AMMC allows us to activate the dendritic area of the second order neurons. There are so many exciting hypotheses that we can test if we can identify the second and higher order neurons.

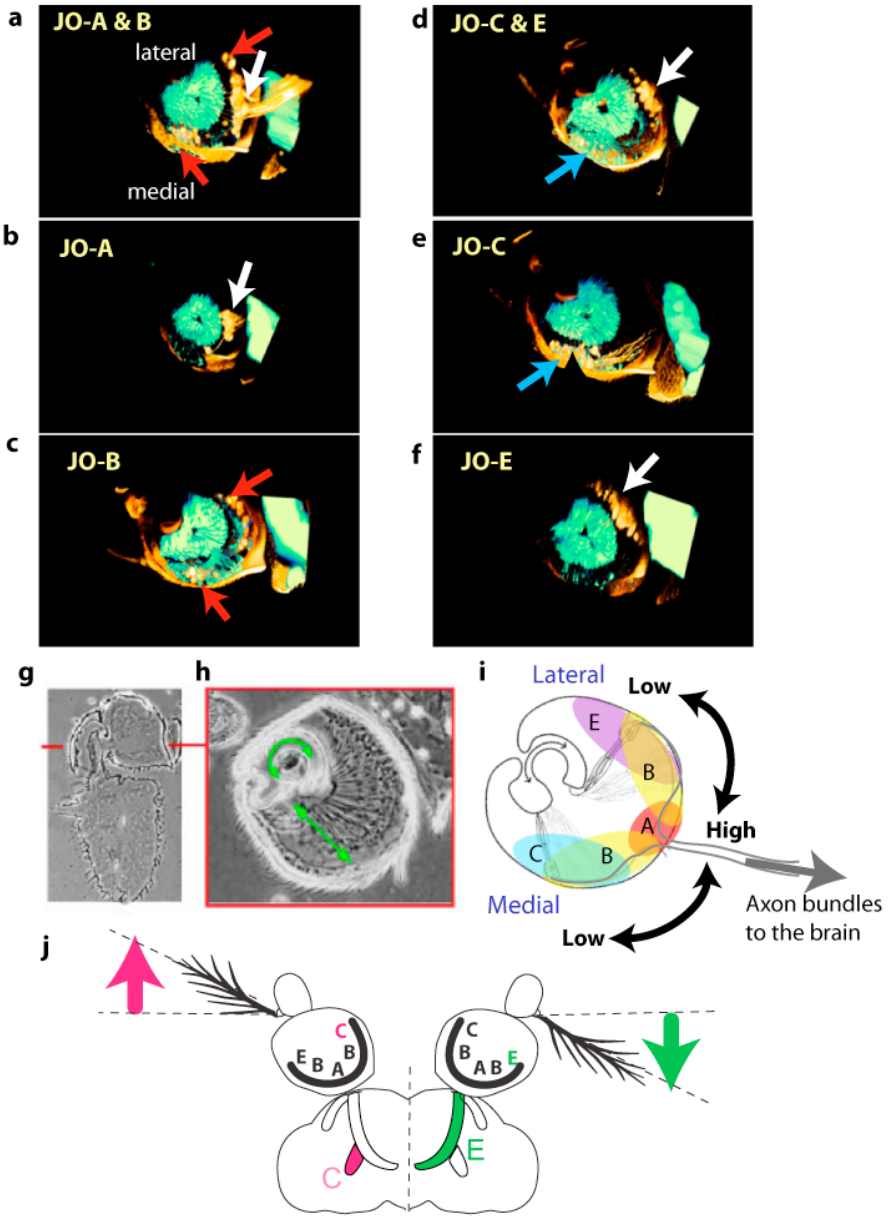

Figure 13. Tonopotic map in the Johnston's organ

a–f, The horizontal-plane view (see red line in g) of the location of cell bodies of Johnston's organ neurons in zone A, B, C, and E (orange) are visualized using photo-activatable-GFP with 710 nm illumination. Scolopale rods are labeled with F-actin rhodamine (green). The cell bodies of A neurons are located at the central position of the scolopedial arrays (white arrows in a, b), extending between the medial and lateral ends. The cell bodies of B neurons are located at the central portion towards the medial and lateral ends of the array (red arrows in a, c). The cell bodies of C neurons are located at the medial end of the array (blue arrows in d, e). The cell bodies of E neurons are located at the lateral end of the array (white arrows in d, f). (g–h) EM pictures of antenna (g) and horizontal section of Johnston's organ, showing scolopedial arrays (h). Note: g–h are modified from (Kernan, 2007). (i–j) Summary of the spatial relations between the cell bodies of Johnston's organ neurons in zone A, B, C, and E. Anterior displacement of arista causes the activation of zone C neurons, whose cell bodies are located at the medial end of the scolopedial arrays (pink in j), while posterial displacement of arista causes the activation of zone E neurons, whose cell bodies are located at the lateral end of scolopedial arrays (green in j).

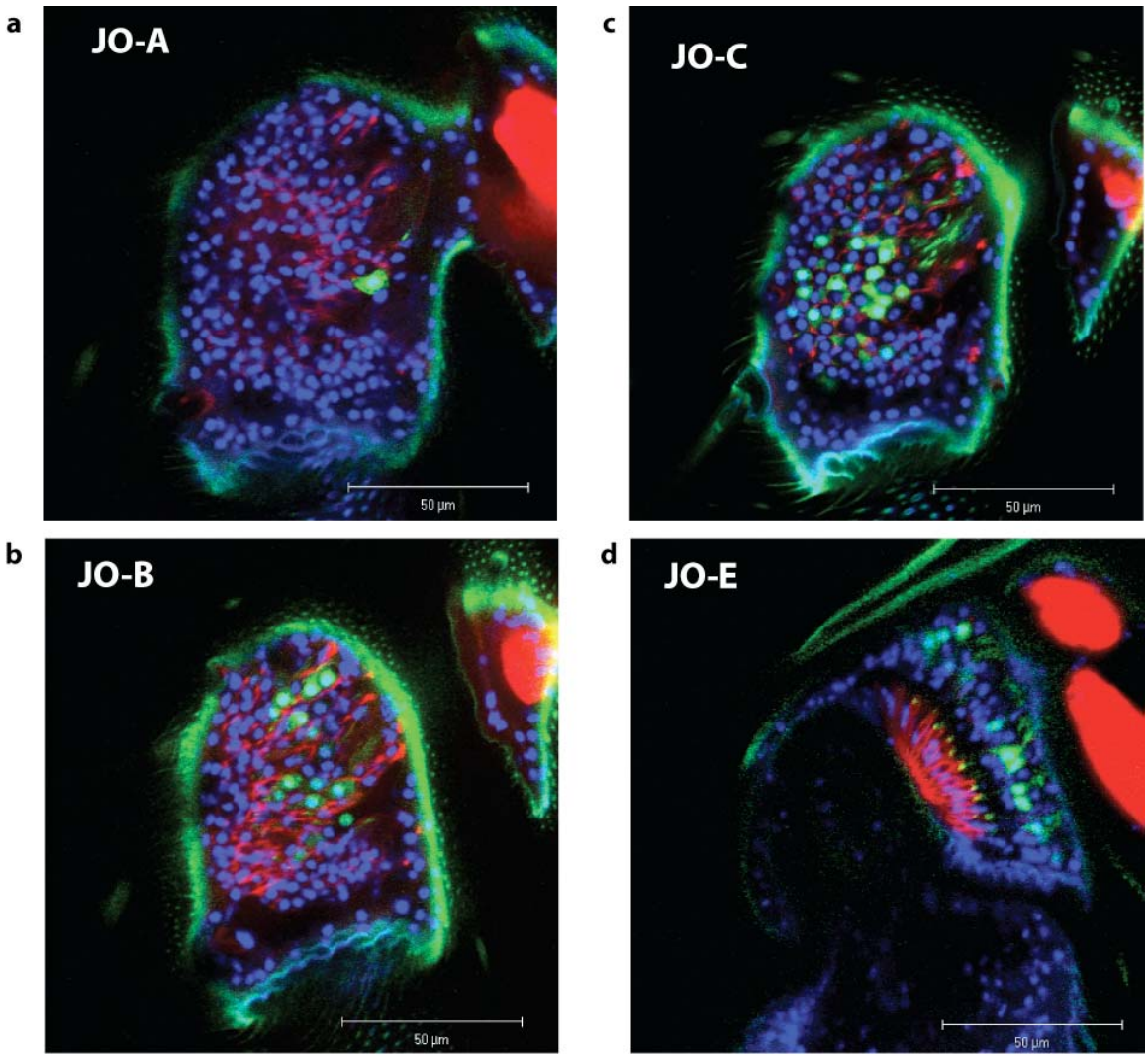

Figure 14. Cell body of A neurons are bigger than that of B, C, and E neurons

a–d, The cell bodies of Johnston's organ neurons in zone A, B, C, and E are visualized using photo-activatable GFP with 710 nm illumination. F-actin is labeled with rhodamine (red), TOPRO3 is a nuclear counter-stain (blue). The cell body of zone A neuron is larger (6–7 µm, a) than that of B (b), C (c), and E (d) neurons (3–4 µm). Scale bars, 50 µm.

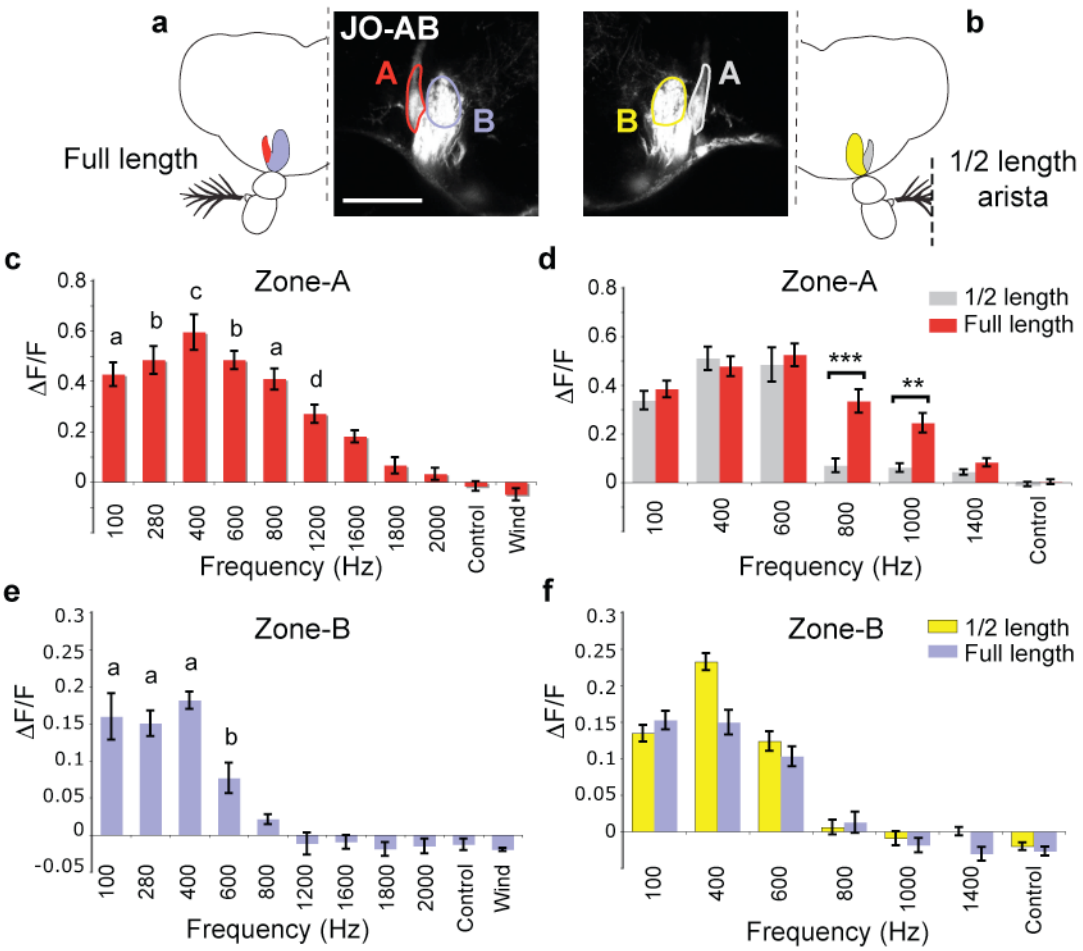

Figure 15. Full-length arista is required for the detection of high frequency sound but not for low frequency sound

a–b, Schematic and mCD8-GFP expression illustrating the zone A and B neurons in the left hemi-brain connected with a wild-type arista, serving as a control (a) and in the right hemi-brain connected with a half-length arista (b). c–f, The frequency tuning of the zone A (c) and zone B (e) neurons connected with the full-length arista. Shortened arista causes loss of sensitivity for high frequency sound (d), but it has no effect on the sensitivity for low frequency sound (f).

REFERENCES

Budick, S. A., Reiser, M. B., and Dickinson, M. H. (2007). The role of visual and mechanosensory cues in structuring forward flight in *Drosophila melanogaster*. J Exp Biol *210*, 4092-4103.

Dallos, P. (2008). Cochlear amplification, outer hair cells and prestin. Curr Opin Neurobiol *18*, 370-376.

Datta, S. R., Vasconcelos, M. L., Ruta, V., Luo, S., Wong, A., Demir, E., Flores, J., Balonze, K., Dickson, B. J., and Axel, R. (2008). The *Drosophila* pheromone cVA activates a sexually dimorphic neural circuit. Nature *452*, 473-477.

Fettiplace, R., and Hackney, C. M. (2006). The sensory and motor roles of auditory hair cells. Nat Rev Neurosci *7*, 19-29.

Gopfert, M. C., Albert, J. T., Nadrowski, B., and Kamikouchi, A. (2006). Specification of auditory sensitivity by *Drosophila* TRP channels. Nat Neurosci *9*, 999-1000.

Hennig, R. M., Franz, A., and Stumpner, A. (2004). Processing of auditory information in insects. Microsc Res Tech *63*, 351-374.

Holley, M. C., and Ashmore, J. F. (1988). On the mechanism of a high-frequency force generator in outer hair cells isolated from the guinea pig cochlea. Proc R Soc Lond B Biol Sci *232*, 413-429.

Hudspeth, A. J. (2008). Making an effort to listen: mechanical amplification in the ear. Neuron *59*, 530-545.

Kamikouchi, A., Inagaki, H. K., Effertz, T., Hendrich, O., Fiala, A., Gopfert, M. C., and Ito, K. (2009). The neural basis of *Drosophila* gravity-sensing and hearing. Nature *458*, 165-171.

Mason, A. C., and Faure, P. A. (2004). The physiology of insect auditory afferents. Microsc Res Tech *63*, 338-350.

Moller, A. R. (2003). Sensory systems: anatomy and physiology: Academic Press).

Nadrowski, B., Albert, J. T., and Gopfert, M. C. (2008). Transducer-based force generation explains active process in *Drosophila* hearing. Curr Biol *18*, 1365-1372.

Nadrowski, B., and Gopfert, M. C. (2009). Level-dependent auditory tuning: Transducer-based active processes in hearing and best-frequency shifts. Commun Integr Biol *2*, 7-10.

Stolting, H., and Stumpner, A. (1998). Tonotopic organization of auditory receptors of the bushcricket *Pholidoptera griseoaptera* (*Tettigoniidae*, *decticinae*). Cell Tissue Res *294*, 377-386.

Appendix

Distinct sensory representations of wind and near-field sound in the *Drosophila* brain

Suzuko Yorozu, Allan Wong, Brian J. Fischer, Heiko Dankert,

Maurice J. Kernan, Azusa Kamikouchi, Kei Ito, and David J. Anderson

Vol 458 | 12 March 2009 | doi:10.1038/nature07843 nature

LETTERS

Distinct sensory representations of wind and near-field sound in the *Drosophila* brain

Suzuko Yorozu[1,2], Allan Wong[1,2], Brian J. Fischer[1], Heiko Dankert[1,3], Maurice J. Kernan[4], Azusa Kamikouchi[5,6], Kei Ito[5] & David J. Anderson[1,2]

Behavioural responses to wind are thought to have a critical role in controlling the dispersal and population genetics of wild *Drosophila* species[1,2], as well as their navigation in flight[3], but their underlying neurobiological basis is unknown. We show that *Drosophila melanogaster*, like wild-caught *Drosophila* strains[4], exhibits robust wind-induced suppression of locomotion in response to air currents delivered at speeds normally encountered in nature[1,2]. Here we identify wind-sensitive neurons in Johnston's organ, an antennal mechanosensory structure previously implicated in near-field sound detection (reviewed in refs 5 and 6). Using enhancer trap lines targeted to different subsets of Johnston's organ neurons[7], and a genetically encoded calcium indicator[8], we show that wind and near-field sound (courtship song) activate distinct populations of Johnston's organ neurons, which project to different regions of the antennal and mechanosensory motor centre in the central brain. Selective genetic ablation of wind-sensitive Johnston's organ neurons in the antenna abolishes wind-induced suppression of locomotion behaviour, without impairing hearing. Moreover, different neuronal subsets within the wind-sensitive population respond to different directions of arista deflection caused by air flow and project to different regions of the antennal and mechanosensory motor centre, providing a rudimentary map of wind direction in the brain. Importantly, sound- and wind-sensitive Johnston's organ neurons exhibit different intrinsic response properties: the former are phasically activated by small, bi-directional, displacements of the aristae, whereas the latter are tonically activated by unidirectional, static deflections of larger magnitude. These different intrinsic properties are well suited to the detection of oscillatory pulses of near-field sound and laminar air flow, respectively. These data identify wind-sensitive neurons in Johnston's organ, a structure that has been primarily associated with hearing, and reveal how the brain can distinguish different types of air particle movements using a common sensory organ.

We observed that *Drosophila* exhibit a rapid and reversible arrest of walking activity under gentle air currents (0.7–1.6 m s^{-1}; Fig. 1a, b and Supplementary Movie 1). This behaviour is also exhibited by wild-caught *Drosophila* species at wind speeds (1.7–2.8 m s^{-1}) within the range measured in their natural habitats[1,2,4] (J. S. Johnston, personal communication; Supplementary Information footnote 1). This behaviour, called wind-induced suppression of locomotion (WISL), was observed in the presence or absence of mechanical startle applied to enhance locomotor activity, before the introduction of air flow (Figs 1b and 3d). Importantly, suppression of locomotion was not observed in response to near-field sound stimuli such as courtship song (280 Hz pulse song, 75–100 dB[9]; Supplementary Fig. 1a).

Recent antennal-gluing experiments have implicated the antenna, and by extension Johnston's organ (JO), in wind sensation in *Drosophila*[3,10]. Surgical removal of the third antennal segment (a3),

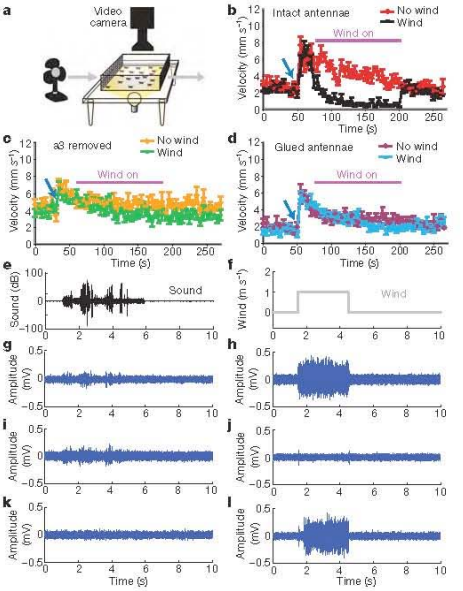

Figure 1 | Behavioural and electrophysiological analyses of wind responses in *Drosophila*. **a**, Schematic illustrating the WISL assay (see Supplementary Methods). **b**, WISL behaviour in Canton-S (CS) flies (Supplementary Movie 1). Data represent mean (± s.e.m.) velocities ($n = 6$). Blue arrow indicates a brief mechanical startle. The 'No wind' versus 'Wind' curves are significantly different ($P = 0.0001$, Kruskal–Wallis analysis of variance (ANOVA)). **c**, **d**, Elimination of WISL by removal of a3 (**c**) or gluing a3 to a2 (**d**). The 'No wind' versus 'Wind' curves are not significantly different ($n = 6$). Data represent mean (± s.e.m). **e**–**l**, Extracellular recordings of JO neuron responses (blue traces) to sound (**e**) or wind (**f**). **g**, **h**, Response to both sound (**g**) and wind (**h**). **i**, **j**, Response to sound (**i**) but not wind (**j**). **k**, **l**, Response to wind (**l**) but not sound (**k**).

[1]Division of Biology 216-76, [2]Howard Hughes Medical Institute, [3]Division of Engineering and Applied Sciences 136-93, California Institute of Technology, Pasadena, California 91125, USA. [4]Department of Neurobiology and Behavior, SUNY Stony Brook, Stony Brook, New York 11794-5239, USA. [5]Institute of Molecular and Cellular Biosciences, University of Tokyo, Yayoi, Bunkyo-ku, Tokyo 113-0032, Japan. [6]Sensory System Laboratory, Institute of Zoology, University of Cologne, 50923 Cologne, Germany.

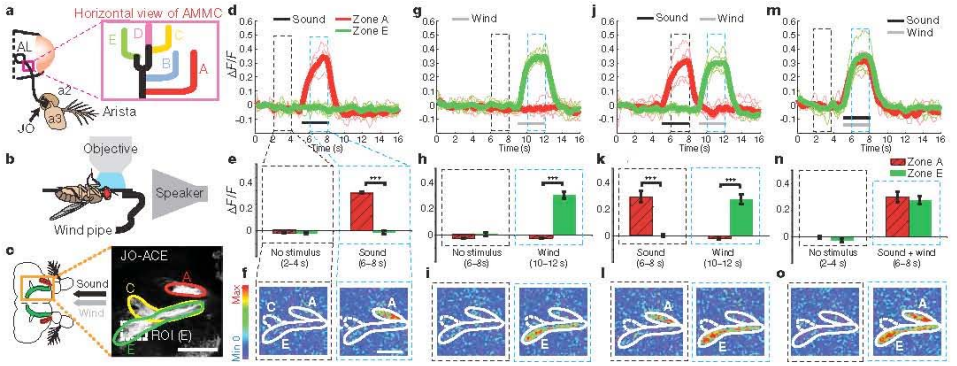

Figure 2 | Calcium imaging reveals distinct populations of wind- and sound-responsive JO neurons. **a–c**, Schematics illustrating location of JO relative to a2 and a3, and five JO neuron axonal terminal zones[7] in the AMMC (**a**), and imaging set-up (**b**). **c**, Zones A, C and E are visualized using a *UAS-mCD8-GFP* reporter. ROI, region of interest for $\Delta F/F$ measurements in zone E. **d–o**, Zones A (red traces, hatched bars) and E (green traces, bars) are activated by sound and wind, respectively, whether presented singly (**d–i**), sequentially (**j–l**) or simultaneously (**m–o**) (see Supplementary Movies 2a–e). Thick traces (**d**, **g**, **j**, **m**) represent the average of the individual (thin) traces ($n = 6$). **e**, **h**, **k**, **n**, Bar graphs indicate the mean (± s.e.m.) integrated $\Delta F/F$ in the time bins (dashed rectangles in **d**, **g**, **j**, **m**; see Methods). $^{***}P < 0.001$ (repeated measure ANOVA and Bonferroni's planned comparisons). **f**, **i**, **l**, **o**, ΔF images of GCaMP activation in zones A and E. Scale bars, 50 μm.

or gluing of a3 to the second antennal segment (a2), both of which cause a functional impairment of JO[11], eliminated WISL (Fig. 1c, d). Genetic ablation of mechanosensory chordotonal neurons using *nanchung-GAL4* (ref. 12) and *UAS-hid* (*head involution defective*, also known as *wrinkled*) a *Drosophila* cell death gene[13], also eliminated WISL (Supplementary Fig. 1b–d). Taken together, these results support the idea that JO is required for WISL, a conclusion confirmed by genetic ablation of specific JO subpopulations (see Fig. 3, later).

To investigate how wind and sound are discriminated by the brain, we first performed extracellular recordings from the antennal nerve[14]. In some electrode placements, spike trains were evoked by both wind (0.3–0.9 m s^{-1}) and courtship song (pulse song; Fig. 1e–h). The short duration of the wind-evoked action potentials (<1 ms) is consistent with neuronal, rather than muscle, action potentials[15]. In other cases, responses were evoked by sound but not wind (Fig. 1i, j; a few spikes were detected at the onset and offset of the wind stimulus), or by wind but not sound (Fig. 1k, l). These results indicate that different axons within the antennal nerve might respond differentially to wind versus sound.

To determine whether distinct subsets of JO neurons are activated by wind versus near-field sound, we performed functional imaging experiments using a genetically encoded calcium sensor (GCaMP-1.3; ref. 8), controlled by different Gal4 enhancer trap lines expressed in JO[7]. These lines identify five major groups of JO axonal projections in the antennal and mechanosensory motor centre (AMMC), called zones A, B, C, D and E (Fig. 2a, inset). Each Gal4 driver labels a subset of zones, but mosaic analysis has revealed that individual JO neurons innervate only one zone[7]. Because it is difficult to distinguish the cell bodies of these five groups of neurons in JO itself, we imaged activity in JO axon terminals in the AMMC, where the five zones are easily discriminated. To do this, we mounted live *Drosophila* in an inverted orientation under a two-photon microscope, while air flow and/or near-field sound were delivered from tubing and a speaker, respectively (Fig. 2b).

Using an enhancer trap line (JO-AB) that selectively labels neurons in zones A and B[7], we observed strong GCaMP activation by courtship song (pulse song; 400 Hz, 90 dB[16]), but not by wind (0.9 m s^{-1}) (Supplementary Fig. 2a–e). Conversely, using a different line (JO-CE) that selectively labels zones C and E[7], we observed responses to air flow, but not to courtship song (Supplementary Fig. 2f–j). To compare directly responses to wind and sound in the same preparation, we used a third line, which labels neurons in zones A, C and E[7] (Fig. 2c). These experiments confirmed that zone A was activated by sound but not by air flow, whereas zone E was activated by air flow but not by sound (Fig. 2d–i and Supplementary Movie 2a, b). The same selective responses were observed when the two stimuli were presented sequentially or simultaneously (Fig. 2j–o and Supplementary Movie 2c, d). Together, these data indicated that JO contains distinct populations of sound- and wind-responsive neurons that project to different regions of the AMMC[7] (Supplementary Information footnote 2).

To determine whether the wind-sensitive JO neurons are also required for WISL behaviour, we genetically ablated these neurons using a toxin, ricin A chain[17]. Because the *JO-CE-GAL4* driver is expressed not only in JO neurons but also in the central brain (Fig. 3a), we used an intersectional strategy to restrict ablation to the antenna using an *eyeless-flippase* (*eyFLP*) tissue-specific recombination system. The specificity of this manipulation was confirmed using an *eyFLP*-dependent mCD8–GFP reporter[18] (Fig. 3b).

Following ablation of JO-C and -E neurons, WISL behaviour was eliminated (Fig. 3g), whereas basal locomotor activity (before wind exposure) and phototaxis behaviour were unaffected (Fig. 3g, i and Supplementary Fig. 3a). Importantly, female flies lacking JO-CE neurons had normal hearing, as evidenced by their unperturbed receptivity to courtship by wild-type males, a behaviour that depends on the females' ability to hear male courtship song. In contrast, females lacking *nanchung*, a gene required for hearing[12], or whose aristae were glued to their head bilaterally[11] (Bi-Gl) exhibited a greatly increased latency to copulation (Fig. 3h, *nan/nan*; Bi-Gl). These data indicate that JO-CE neurons are necessary for WISL behaviour, but dispensable for a hearing-dependent behaviour.

We next investigated the functional significance of the two wind-sensitive JO subpopulations (C and E). Axons innervating zones C and E terminate in lateral versus medial domains of the AMMC, respectively (Fig. 4a–c). When air flow was applied to the front of the head (0°), or at 45°, there was strong activation in zone E and little activation in zone C. Conversely, air flow applied from the rear (180°) activated zone C, and slightly inhibited zone E (Fig. 4d–f and Supplementary Movie 3a–c). Air flow applied to the side of the head

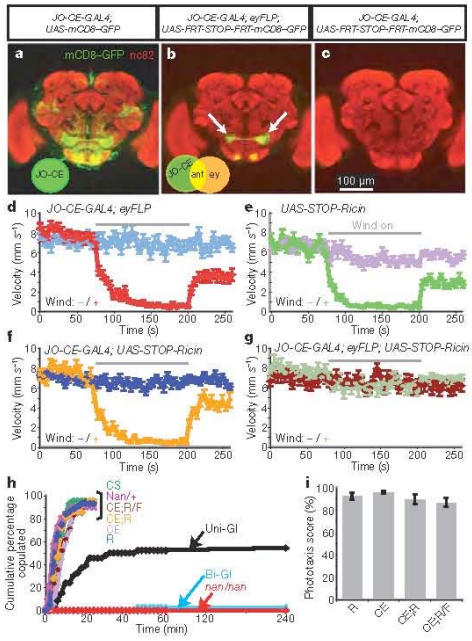

Figure 3 | Ablation of wind-sensitive (C and E) neurons abolishes WISL behaviour. **a–c**, GFP expression patterns of the indicated genotypes, double-stained with antibodies to GFP (green) and nc82 (red). **a**, Original *JO-CE-GAL4* pattern. **b**, Antennal-restricted *JO-CE-GAL4* pattern using *eyFLP*. Arrows indicate AMMC; underlying structures are gustatory neuron projections to the sub-oesophageal ganglia[7]. **c**, Control for **b** lacking *eyFLP*. **d–g**, WISL analysis. Curves represent mean velocity ± s.e.m. ($n = 15$). **d–f**, Genetic controls show robust WISL. The 'wind−' versus 'wind+' curves are significantly different ($P < 0.0001$). **g**, Ablation of C and E neurons abolishes WISL. **h**, Cumulative percentage of manipulated females copulating with CS males. >90% of all pairs in bracketed conditions exhibited successful copulation within 20 min ($n = 40$–50 pairs). Genotypes: CE:R/F, *JO-CE-GAL4; UAS<STOP<Ricin/eyFLP*; CE;R, *JO-CE-GAL4; UAS<STOP<Ricin*; CE, *JO-CE-GAL4*; R, *UAS<STOP<Ricin*. Unilateral ('Uni-GI') or bilateral ('Bi-GI') gluing of the aristae, or the *nanchung* mutation (*nan/nan*)[12] impaired copulation ($P < 0.0001$). Ablation of JO-CE neurons ('CE;R/F') did not impair either copulation (**h**) or phototaxis (**i**). Phototaxis scores represent mean ± s.e.m. ($n = 7$). *P* values are shown by Kruskal–Wallis ANOVA.

(90°) activated zone C ipsilaterally and zone E contralaterally (Fig. 4d–f, 90°; Supplementary Movie 3d). Thus, zone C and E neurons are differentially sensitive to air flow directionality.

High-magnification video analysis (Supplementary Movie 4a–c) revealed that air flow from different directions moves the aristae either anteriorly or posteriorly (Fig. 4g). We hypothesized that the direction of arista deflection determines whether zone C or E neurons are activated. Arista ablation experiments indicated that the activation of wind-sensitive JO neurons, like that of sound-sensitive JO neurons[11,19], is dependent on this structure (Supplementary Fig. 4). To test the hypothesis directly, we moved the aristae in different directions using a probe controlled by a DC motor (Fig. 4h). Displacing the arista posteriorly with a probe activated the E zone almost as strongly as wind delivered from the front, and weakly inhibited the C zone (Fig. 4i, 'Push back'), whereas displacing it anteriorly activated the C zone and inhibited the E zone (Fig. 4i, 'Push forward'). These data demonstrate that zones C and E are sensitive to different directions of arista deflection (Fig. 4j). This model can explain the asymmetric activation of zones C and E in ipsi- and contral-lateral hemi-brains during wind stimulation from 90° (Fig. 4f, g, 90°), because this stimulus produces opposite deflection of the aristae on the ipsi- and contra-lateral sides of the head (Fig. 4g, 90°, Supplementary Movie 4d). An internal comparison of activity between zones C and E, both within and between each hemi-brain, could provide a basis for computing wind direction[3].

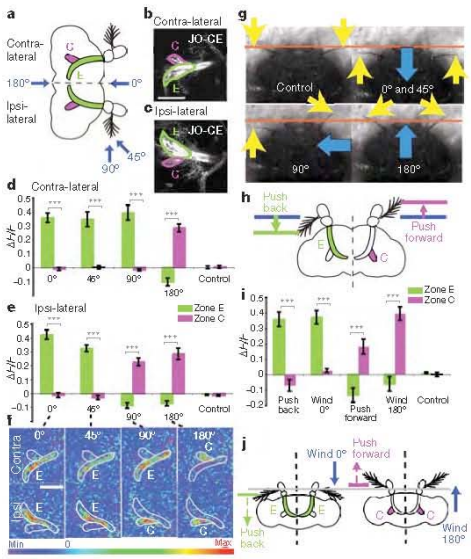

Figure 4 | Wind-direction-sensitivity of zones C versus E. **a–c**, Schematic (**a**) and mCD8–GFP expression (**b**, **c**) illustrating zones C and E in contra- and ipsi-lateral hemi-brains. Blue arrows indicate wind direction. **d–f**, Average (± s.e.m.) $\Delta F/F$ signals integrated over the stimulus period for zones C and E in the contra- (**d**) and ipsi- (**e**) lateral hemi-brains, and corresponding ΔF images (**f**; see Supplementary Movies 3a–e). **g**, Still frames from video recordings of aristae movements during wind stimulation (Supplementary Movies 4a–e). Yellow arrows indicate aristae position, orange lines denote the rest position ('Control') and blue arrows indicate wind direction. **h**, Schematic illustrating predicted responses of zones C and E to directional, probe-driven aristae displacements. **i**, Responses of the C and E neurons to wind and directional arista displacements. Error bars are s.e.m. **j**, Summary illustrating differential sensitivity of zones C and E to direction of arista displacement. Scale bars, 50 µm. ***$P < 0.0001$ (repeated measures ANOVA and Bonferroni's planned comparisons).

We investigated which stimulus features are responsible for the selective activation of sound- versus wind-sensitive neurons in JO. We first asked whether these two classes of mechanoreceptors are sensitive to different stimulus amplitudes, that is, air particle velocities (v_{air}). A pressure gradient microphone positioned at the antenna[9] yielded a v_{air} of 0.011 m s^{-1} for the 400 Hz sound stimulus played at 90 dB, which maximally activated JO-AB neurons (Fig. 5a). However, this sound stimulus did not activate zone E neurons (Supplementary Fig. 2g), even though these neurons are activated by air flow at a v_{air} as low as 0.005 m s^{-1} (Fig. 5b). Thus, the selectivity of JO-CE and -AB neurons for wind versus sound is not simply due to differences in stimulus magnitude.

We next asked whether JO-AB and -CE neurons might have different intrinsic sensitivities to different types of arista movements by moving

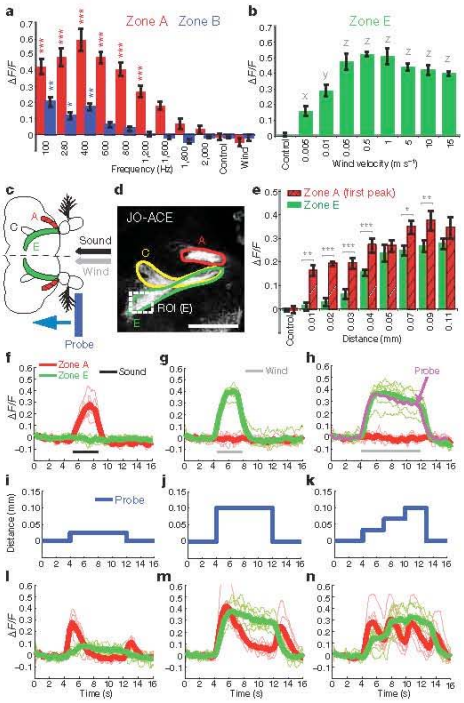

Figure 5 | Wind- and sound-sensitive JO neurons have different intrinsic response properties. **a**, Sensitivity of zones A and B to different sound frequencies (mean ± s.e.m., n 6). $^{***}P < 0.0001$ (red), $^{*}P < 0.01$ (blue) and $^{**}P < 0.001$ (blue) relative to control. **b**, Sensitivity of zone E to different wind speeds (n 5). Letters (x, y, z) indicate significant differences relative to control (all $P < 0.0001$ except 'x' ($P < 0.001$)). **c–n**, Comparison of sound-, wind- and probe-evoked responses in zones A and E. **c**, **d**, Schematic (**c**) and mCD8–GFP expression (**d**) illustrating zones A, C and E. ROI, region of interest for $\Delta F/F$ measurements in zone E. Scale bar, 50 μm. **e**, Responses of zones A and E to probe-induced arista displacements of different magnitudes. $^{*}P < 0.01$; $^{**}P < 0.001$; $^{***}P < 0.0001$ (zones A versus E comparisons). All zone A responses, $P < 0.0001$ (relative to control), except for 0.01 mm displacement ($P < 0.001$). All zone E responses ≥0.04 mm displacement, $P < 0.0001$; zone E responses <0.04 mm were not significantly different from control. **f–h**, Sound and wind responses. Thick lines represent average of the individual (thin) traces (n 6). **h**, Superposition of the average responses of zone E to 8 s of wind (green trace) and mechanical probe displacement (magenta trace; see **m**). **i–n**, Responses (**l–n**) of zones A and E to different distances and patterns of probe-induced arista displacement (**i–k**) (n 6). All P values are calculated by repeated measures ANOVA and Bonferroni multiple comparisons.

the aristae in steps of different magnitudes and patterns using a probe controlled by a DC motor (Fig. 5c, d). Sound-sensitive neurons in zone A (Fig. 5f, red traces) were activated by displacements as small as 0.01 mm (Fig. 5e, red hatched bars), whereas wind-sensitive neurons in zone E (Fig. 5g, green traces) were only weakly activated at displacements below 0.04 mm (Fig. 5e, green bars). Thus, zone A neurons have a lower displacement threshold than zone E neurons (see also Fig. 5i, l).

Strikingly, we observed that zone E neurons remained active for as long as the aristae were displaced, whereas zone A neurons were only transiently activated at the onset and offset of probe displacement (Fig. 5j, m). This suggested that zone E neurons might adapt slowly, and therefore respond tonically, whereas zone A neurons might adapt rapidly, and therefore respond phasically. To confirm this, we moved the aristae in three successive steps of 0.033 mm each (total displacement of 0.099 mm; Fig. 5k). Zone A neurons exhibited transient (phasic) responses after each displacement (Fig. 5n, red traces), whereas zone E neurons were tonically activated for the duration of each displacement, and were maximally activated after the second step (Fig. 5n, green traces). These data indicate that JO-AB and JO-CE neurons respond phasically and tonically to arista displacement, with low versus high activation thresholds, respectively (see Supplementary Information footnote 3). Furthermore, zone A neurons were activated by bi-directional movements, whereas zone E neurons were activated only unidirectionally (Fig. 5j, m). These different intrinsic response properties are well matched to the oscillatory arista movements caused by pulses of near-field sound versus uni-directional arista deflections caused by wind. The ability of flies to discriminate wind versus sound using a common sensory organ is thus explained by different populations of JO neurons with different intrinsic response properties, which project to distinct areas of the AMMC.

The identification of different subpopulations of JO neurons with tonic versus phasic response properties illustrates a general and conserved feature of mechanosensation. In mammalian skin, slowly adapting, tonically activated Merkel cells[20] and rapidly adapting, phasically activated Meissner's corpuscles[21] are used for different types of light-touch sensation. In *Drosophila*, these two properties have been adapted to detect different types of bulk air particle movements by different subsets of JO neurons. In the accompanying paper[22], the authors demonstrate, using complementary imaging methods, that zone AB neurons are activated by sound and required for hearing. They also show that zone CE neurons are required for the behavioural response to gravity (negative gravitaxis), a force that could also produce static deflections of the arista, albeit of a smaller magnitude than those produced by wind (Supplementary Information footnote 4).

The data presented here indicate that JO is not simply a hearing organ[6] but also mediates wind detection, in a direction-sensitive manner. Wind-activated neurons in JO are, moreover, required for an innate behavioural response to wind. The function of WISL in nature is not clear. Field studies have suggested that wind is a major environmental factor affecting the dispersal of wild *Drosophila* populations[1,2,4]. WISL may have evolved to control population dispersal, and thereby maintain genetic homogeneity[1,2]. Alternatively, WISL may represent a defence mechanism that serves to protect individual flies from injury, or to prevent dispersal from food resources. Identification of the sensory neurons that mediate WISL opens the way to a systematic analysis of the genes and neural circuitry that underlie this robust, innate behavioural response to wind.

METHODS SUMMARY

Behavioural assay. Twenty flies were used for each WISL trial. A standard WISL trial lasts for 270 s. During the first 55 s, the flies' baseline locomotor activity was recorded. Where indicated, at $t-55$ s, a brief mechanical stimulus was applied to transiently increase the flies' locomotor activity. Air flow exposure was then initiated at $t-80$ s, and terminated at $t-200$ s.

Electrophysiology. Sample preparation and electrophysiological recordings from JO axons were performed as described[14].

Calcium-response imaging. Flies were anaesthetized in a plastic vial on ice for 15–20 s, and then gently inserted into a hole of a thin plastic rectangular plate. After stabilizing the fly with a small drop of wax (55 °C), the proboscis and the area surrounding the proboscis were surgically removed, in a saline bath, to expose the ventral side of the brain. The preparation was then mounted on a microscope in an inverted orientation for calcium-response imaging. The antennae were kept intact and dry throughout the exposure to different stimuli (sound, wind and mechanical probe displacement).

Detailed descriptions of fly stocks, the WISL behavioural apparatus and assay, courtship and phototaxis assays, antennal manipulations, electrophysiology, calcium-response imaging and sample preparation, sound and wind stimuli and statistical methods are provided in the Supplementary Methods.

Full Methods and any associated references are available in the online version of the paper at www.nature.com/nature.

Received 25 November 2008; accepted 29 January 2009.

1. Johnston, J. & Templeton, A. in *Ecological Genetics and Evolution* (eds Barker, J. S. F. & Starmer, W. T.) 241–256 (Academic, 1982).
2. Johnston, J. & Heed, W. Dispersal of desert-adapted *Drosophila*: the saguaro-breeding *D. nigrospiracula*. *Am. Nat.* **110**, 629–651 (1976).
3. Budick, S. A., Reiser, M. B. & Dickinson, M. H. The role of visual and mechanosensory cues in structuring forward flight in *Drosophila melanogaster*. *J. Exp. Biol.* **210**, 4092–4103 (2007).
4. Richardson, R. & Johnston, J. Behavioral components of dispersal in *Drosophila mimica*. *Oecologia* **20**, 287–299 (1975).
5. Caldwell, J. C. & Eberl, D. F. Towards a molecular understanding of *Drosophila* hearing. *J. Neurobiol.* **53**, 172–189 (2002).
6. Kernan, M. J. Mechanotransduction and auditory transduction in *Drosophila*. *Pflügers Arch.* **454**, 703–720 (2007).
7. Kamikouchi, A., Shimada, T. & Ito, K. Comprehensive classification of the auditory sensory projections in the brain of the fruit fly *Drosophila melanogaster*. *J. Comp. Neurol.* **499**, 317–356 (2006).
8. Nakai, J., Ohkura, M. & Imoto, K. A high signal-to-noise Ca^{2+} probe composed of a single green fluorescent protein. *Nature Biotechnol.* **19**, 137–141 (2001).
9. Göpfert, M. C. & Robert, D. The mechanical basis of *Drosophila* audition. *J. Exp. Biol.* **205**, 1199–1208 (2002).
10. Mamiya, A. *et al.* Neural representations of airflow in *Drosophila* mushroom body. *PLoS ONE* **3**, e4063 (2008).
11. Manning, A. Antennae and sexual receptivity in *Drosophila melanogaster* females. *Science* **158**, 136–137 (1967).
12. Kim, J. *et al.* A TRPV family ion channel required for hearing in *Drosophila*. *Nature* **424**, 81–84 (2003).
13. Wang, S. L. *et al.* The *Drosophila* caspase inhibitor DIAP1 is essential for cell survival and is negatively regulated by HID. *Cell* **98**, 453–463 (1999).
14. Eberl, D. F., Hardy, R. W. & Kernan, M. J. Genetically similar transduction mechanisms for touch and hearing in *Drosophila*. *J. Neurosci.* **20**, 5981–5988 (2000).
15. Tanouye, M. A. & Wyman, R. J. Motor outputs of giant nerve fiber in *Drosophila*. *J. Neurophysiol.* **44**, 405–421 (1980).
16. Bennet-Clark, H. C. Acoustics of insect song. *Nature* **234**, 255–259 (1971).
17. Moffat, K. G. *et al.* Inducible cell ablation in *Drosophila* by cold-sensitive ricin A chain. *Development* **114**, 681–687 (1992).
18. Wong, A. M., Wang, J. W. & Axel, R. Spatial representation of the glomerular map in the *Drosophila* protocerebrum. *Cell* **109**, 229–241 (2002).
19. Ewing, A. W. The antenna of *Drosophila* as a 'love song' receptor. *Physiol. Entomol.* **3**, 33–36 (1978).
20. Ikeda, I. *et al.* Selective phototoxic destruction of rat Merkel cells abolishes responses of slowly adapting type I mechanoreceptor units. *J. Physiol. (Lond.)* **479**, 247–256 (1994).
21. Hoffmann, J. N., Montag, A. G. & Dominy, N. J. Meissner corpuscles and somatosensory acuity: the prehensile appendages of primates and elephants. *Anat. Rec. A Discov. Mol. Cell. Evol. Biol.* **281**, 1138–1147 (2004).
22. Kamikouchi, A. *et al.* The neural basis of *Drosophila* gravity-sensing and hearing. *Nature* doi:1010.1038/nature07810 (this issue).

Supplementary Information is linked to the online version of the paper at www.nature.com/nature.

Acknowledgements We thank U. Heberlein and F. Wolf for hosting a sabbatical that led to the discovery of WISL; J. S. Johnson for helpful discussions; L. Zelnik, M. Reiser and P. Perona for creating locomotor tracking software; D. Eberl and J. Hall for *D. melanogaster* courtship song recordings; G. Maimon for making fly holders for imaging experiments; M. Roy for building behavioral chambers for WISL and female receptivity assays; H. Inagaki for *JO-CE-GAL4;eyFLP* flies; B. Hay for *UAS-hid* flies; D. Berdnik for *UAS-FRT-STOP-FRT-Ricin* flies; M. Dickinson for anemometers and discussions; J. L. Anderson for advice on fluid mechanics; M. Göpfert for providing a pressure gradient microphone; M. Konishi for advice and use of laboratory facilities; and G. Mosconi for laboratory management. D.J.A. is an Investigator of the Howard Hughes Medical Institute. This work was supported in part by NSF grant EF-0623527.

Author Contributions S.Y. and D.J.A. designed experiments, S.Y. carried out all experiments reported in this paper and D.J.A. and S.Y. wrote the manuscript. A.W. wrote Matlab programs for $\Delta f/f$ measurements and mechanical probe actuation, B.J.F. assisted with computational filtering of song stimuli, H.D. assisted with computational and statistical analysis of data, M.J.K. provided facilities and support for electrophysiological experiments, and A.K. and K.I. provided Gal4 lines.

Author Information Reprints and permissions information is available at www.nature.com/reprints. Correspondence and requests for materials should be addressed to D.J.A. (mancusog@caltech.edu) or S.Y. (yorozu@caltech.edu).

doi:10.1038/nature07843 nature

METHODS

Fly stocks. Flies carrying *JO-ACE*, *JO-CE* and *JO-AB* were described previously[7]. *UAS-GCaMP*[23,24] and *UAS-mCD8-GFP* flies were obtained from Y. Wang and R. Axel. *UAS-FRT-STOP-FRT-Ricin* flies[25] were obtained from D. Berdnik. *JO-CE-GAL4; eyFLP* flies were obtained from H. Inagaki. Canton-S flies from J. Dubnau, and *UAS-hid* flies from B. Hay. Flies were maintained on corn meal and molasses food at 25 °C on a (12/12) light–dark cycle.

WISL behavioural apparatus. The WISL assay was performed in a 6 × 6 × 1.5 cm transparent acrylic plastic box (WISL chamber), which has air flow inputs and outputs (1 cm diameter) on two of the four vertical sides of the box. The input tubing carries air flow from a tank containing breathable air, connected to a flow regulator. The output tubing allows the air flow to escape from the box, and is connected to a flow meter that measures the speed of the air flow. The WISL chamber was mounted on a transparent plastic table and was trans-illuminated with a fluorescent light from underneath. A video camera (Sony, DCR-HC40 NTSC) was set up above the WISL chamber to record the flies' locomotor activity.

WISL assay protocol. Twenty flies per trial were sorted 36–48 h before testing, using nitrogen gas or cold anaesthesia. On the testing day, 20 flies were aspirated into the WISL chamber and allowed to acclimate for 7–8 min just before initiation of the trial. A standard WISL trial lasted for 270 s. Flies were given a brief mechanical stimulation (5 manual strikes on the table that the WISL chamber was mounted on) at 55 s, and air flow exposure began at 80 s and ended at 120 s. Locomotor activity was recorded at ten frames per second and average velocity was computed using custom software written in Matlab (MathWorks Inc.).

Courtship (female receptivity) assay. Naive Canton-S males and virgin females of the genotype of interest were collected immediately after eclosion, using nitrogen or CO_2 gas anaesthesia. Naive males were individually housed whereas virgin females were group-housed for six days until the test day. Single naive Canton-S male and a single virgin female of the genotype of interest were placed in a mating chamber (1 × 1 × 0.4 cm square chamber), and the time at which a successful copulation occurred was recorded for each mating pair. Successful copulation typically lasts 15–25 min.

Phototaxis assay. Forty flies per trial were sorted 48 h before testing, using nitrogen or CO_2 gas anaesthesia. On the test day, 40 flies were tapped into the elevator of a T-maze and allowed to rest for one minute in a dark. Next, the elevator was lowered to the choice point where flies were given one minute to make a choice between a dark tube and a tube illuminated with a 40 W fluorescent light, positioned approximately 20 cm away. The phototaxis response was analysed by calculating the performance index (PI) using the following formula: PI = [(2 × COR) − 1] × 100, where COR = (number of flies that chose the illuminated tube/total number of flies). PI = 0 indicates an equal distribution of flies between the dark and illuminated tubes. PI = 100% indicates that all flies chose the illuminated tube.

Antenna manipulations. To test the role of JO in wind detection, a3 segments were surgically removed using a pair of forceps, 48 h before the WISL testing. For the antennal gluing experiment, a small drop of ultraviolet-activated glue was placed at the junction between the a2 and a3 segments bilaterally, and cured with an ultraviolet lamp for 3–5 s, 48 h before the testing. For the mechanical probe antennal displacement experiment, a sharpened tungsten needle was used to move the aristae in different directions and different patterns. The probe was mounted on a DC motor/controller (LTA-HS and SMC100CC, Newport), which was controlled by custom Matlab software (MathWorks Inc.). To push the aristae backward, the probe was positioned anterior to the aristae; conversely, to push the aristae forward, the probe was positioned posterior to the aristae. In the 'push back' (and 'push forward') conditions, the aristae were pushed backward (or forward) in a single increment of varying distances (0.01, 0.02, 0.025, 0.03, 0.04, 0.05, 0.07, 0.09 or 0.11 mm), held for 8 s in the displaced position and then returned to the original position. In another experiment, the aristae was pushed backwards in three successive steps of 0.033 mm (a total of 0.099 mm), held in place for 2.9 s after each successive step, and then returned to the original position. In all conditions, the probe and aristae movements were verified using a video camera (GE680, Proscillica) that was set up underneath the fly preparation mounted on the microscope stage as described previously.

Electrophysiology. Extracellular recordings from JO axons were recorded at the a1/a2 joint using a tungsten or glass electrode (0.5 MΩ) as described previously[14] in a sound-proof chamber. Pulse-song segments of recorded *D. melanogaster* courtship song (provided by J. Hall[26] and D. Eberl) were used as the sound stimulus and an air flow rate between 0.3 and 0.9 m s^{-1} was used as the wind stimulus.

Calcium-response imaging and sample preparation. Flies were anaesthetized in a plastic vial on ice for ~15–20 s, and were then gently inserted into a hole of a thin plastic rectangular plate. Small drops of wax (55 °C) were applied to prevent the fly from moving out from the hole. After the fly was stabilized in the plastic hole, the preparation was oriented in an upside-down position (see Fig. 2b). The proboscis, ventral part of thorax and abdomen, and legs were protruding from the upper side of the horizontal plane of the plastic, while the rest of the fly head (including the antennae, but excluding the proboscis), thorax and dorsal part of abdomen were protruding from the bottom side of the horizontal plane of the plastic. In a saline bath, the proboscis was cut off and the area surrounding the proboscis was surgically removed to expose the ventral side of the brain. Fat and air sacs were gently removed to give a clear view of the brain. For calcium-response imaging, the water immersion objective lens (×40, NA = 0.8, Olympus) was lowered near the exposed brain, while the underside of the plastic specimen mount, which contained the intact antennae, was kept dry and exposed to wind and sound stimuli.

Sound stimuli used in these experiments were recorded segments (provided by J. Hall[26] and D. Eberl) of the pulse-song portion of *D. melanogaster* courtship song, played at 75–100 dB at the aristae using a loudspeaker (ProMonitor 800 loudspeaker, Definitive Technology) and amplifier (P.A. amplifier, Radioshack) and were measured using a digital sound meter (DSM-325, Mannix). We tested the frequency tuning of zones A and B using narrowband signals derived from the original pulse-song. The original pulse-song was filtered to set the centre of the frequency spectrum at a desired frequency between 100 and 2,000 ± 200 Hz (using the Fourier transformation).

Wind stimuli used in imaging experiments were delivered at speeds between 0.005 and 15 m s^{-1}. Wind speed was controlled by a flow regulator (mass flow meters and controllers, Smart Trak series 100, Sierra Instrument Inc.) and was measured using an anenometer (Testo-435, Testo GmbH & Co.). VClamp software (Pairie Technology) was used to control all aspects of sound and wind stimuli used in the imaging experiments.

All imaging was performed on an Ultima two-photon laser scanning microscope (Prairie Technology). Live images were acquired at 6.1 frames per second using an Olympus ×40 (NA = 0.8) water immersion objective at 128 × 128 resolution with an imaging wavelength at 925 nm. GCaMP responses were quantified using custom software written in MatLab. The relative change in fluorescence intensity ($\Delta F/F$) was computed by first calculating the average pixel values in the region of interest during the experimental period and applying a three-frame moving average smoothing function. This average fluorescence value, F_{av}, was then converted to $\Delta F/F$ using the formula $\Delta F/F = (F_{av} - F_0)/F_0$, where F_0 is the baseline fluorescence value, measured as the average of frames 2–9. Average $\Delta F/F$ for a specific stimulus period was compared between different JO neuron zones to test for statistical significance by repeated-measure ANOVA.

23. Wang, J. W., Wong, A. M., Flores, J., Vosshall, L. B. & Axel, R. Two-photon calcium imaging reveals an odor-evoked map of activity in the fly brain. *Cell* **112**, 271–282 (2003).
24. Wang, Y. *et al.* Stereotyped odor-evoked activity in the mushroom body of Drosophila revealed by green fluorescent protein-based Ca^{2+} imaging. *J. Neurosci.* **24**, 6507–6514 (2004).
25. Berdnik, D., Chihara, T., Couto, A. & Luo, L. Wiring stability of the adult *Drosophila* olfactory circuit after lesion. *J. Neurosci.* **26**, 3367–3376 (2006).
26. Wheeler, D. A., Fields, W. L. & Hall, J. C. Spectral analysis of *Drosophila* courtship songs: *D. melanogaster*, *D. simulans*, and their interspecific hybrid. *Behav. Genet.* **18**, 675–703 (1988).

doi: 10.1038/nature07843 nature

SUPPLEMENTARY INFORMATION

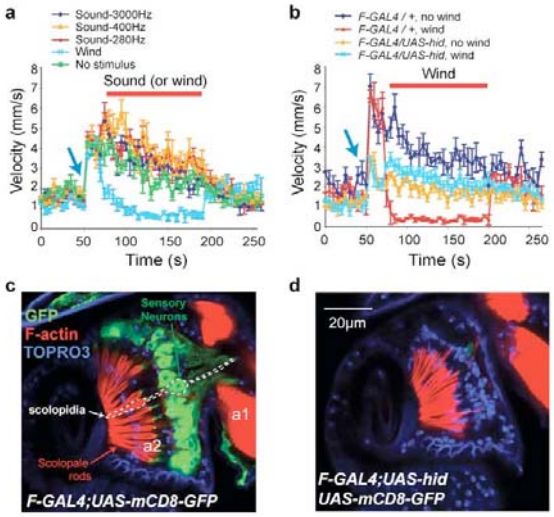

Supplemental Figure S1. WISL is not elicited by courtship song and is dependent on chordotonal mechanosensory neurons.

(a) Average locomotor velocity vs. time plots for wild-type CS flies exposed to recordings of peak frequency-modified (see Supplemental Methods) pulse song derived from *D. melanogaster* courtship song[23], presented at 90 dB (SPL) at the antenna. Blue arrows indicate brief mechanical startle; red line indicates duration of wind or sound exposure. Note that only wind causes locomotor suppression (light blue curve). "Wind" vs. "No stimulus" curves, p=0.0002 (Kruskal-Wallis ANOVA); p=0.0013 for comparison

doi: 10.1038/nature07843 SUPPLEMENTARY INFORMATION

of average velocity during the wind ON period of "Wind" vs. "No stimulus" conditions (Mann-Whitney U-test). Data are mean ± SEM, n = 10 (20 flies/assay). (b) WISL behavior is lost in flies in which JO neurons are killed using *nanchung (F)-Gal4* and *UAS-hid*. The light blue (wind) and orange (no wind) curves of *F-Gal4; UAS-hid* flies are not significantly different ($p>0.05$, Kruskal-Wallis ANOVA). Control *F-Gal4/+* flies show a clear WISL effect: wind vs. no wind, $p<0.0001$ (Kruskal-Wallis ANOVA); $p=0.0006$ for comparison of average velocity during the "Wind ON" period of "no wind" vs "wind" conditions (Mann-Whitney U-test). Control *UAS-hid/+* flies also show a robust WISL effect; $p<0.0001$ (Kruskal-Wallis ANOVA; data not shown). (c, d) Confirmation that JO neurons in the antenna are ablated by *F-Gal4; UAS-hid*. (c) Control flies with *F-Gal4; UAS-mCD8GFP*. A scolopidium, the sensory organ unit of JO, is outlined (white dashed lines). Sensory neurons are green (GFP^+). Scolopale rods are labeled by rhodamine F-actin (red). TOPRO3 is a nuclear counter-stain. (d) Similar view of JO from *F-Gal4; UAS-hid/UAS-mCD8GFP* flies. Note loss of sensory neurons. The scolopale rods remain because they are synthesized by scolopale cells which do not express the *F-Gal4* driver and are therefore spared. Scale bar, 20 μm.

doi: 10.1038/nature07843 SUPPLEMENTARY INFORMATION

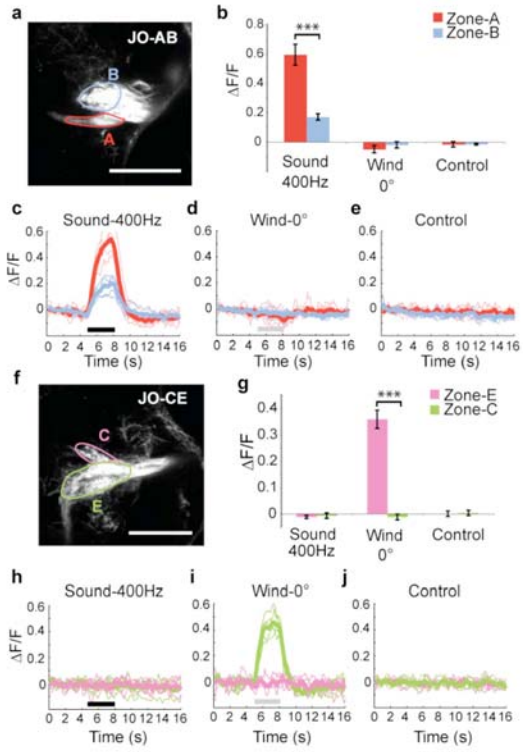

Supplemental Figure S2. Different subpopulations of JONs are activated by wind and sound.

Flies were exposed to peak frequency-modified pulse song (see Supplementary Methods) at 400 Hz and 90 dB (as well as at 75 and 100 dB; not shown), or to wind (0.9 m/sec; also 0.01m/s, data not shown) delivered from the anterior (0^{o}), in flies expressing GCaMP in either zones A and B (a-e), or in zones C and E (f-j). Zones A and B were activated by sound (b, c) but not wind (b, d), while zone E was activated by wind (g, i)

doi: 10.1038/nature07843 SUPPLEMENTARY INFORMATION

but not by sound (g, h). Zone C was also activated by wind, but only if presented from the posterior (180°; see Fig. 4). Data are mean ± SEM, n=6 experiments. Scale bars, 50µm. ***, $p<0.001$ (Repeated measure ANOVA and Bonferroni multiple comparisons).

doi: 10.1038/nature07843 SUPPLEMENTARY INFORMATION

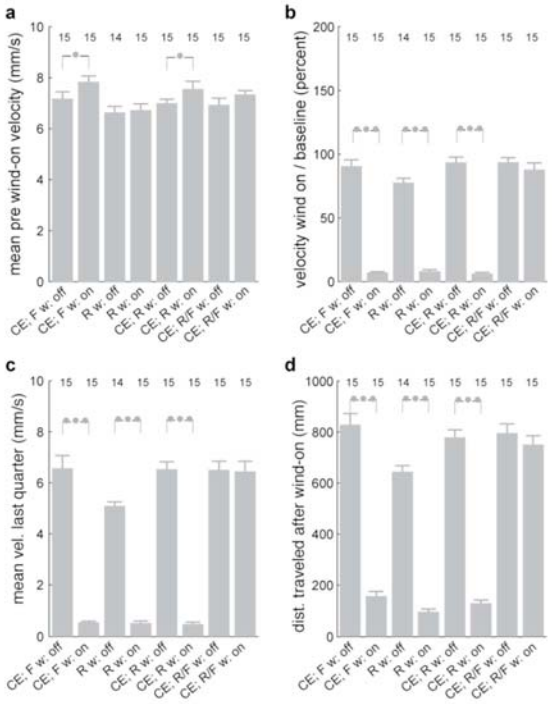

Supplemental Figure S3. Quantification of WISL behavior in flies lacking JO-CE neurons.

The parameters shown are calculated from the data in Fig. 3 (d-g). (a) Mean velocity prior to wind exposure. (b) Mean velocity during wind exposure, as a percentage of pre-wind baseline velocity. (c) Mean velocity during the last quarter of the wind exposure period. (d) Distance traveled following the onset of wind exposure. •, $p<0.05$; •••, $p<.001$ (Kruskal-Wallis and Mann-Whitney U-test). Numbers above the bars indicate number of assays performed for each condition (20 flies/assay). Genotype

doi: 10.1038/nature07843

abbreviations: *"CE; F" = JO-CEGal4; eye-FLP; "R" = UAS-FRT-STOP-FRT-Ricin; "CE; R" = JO-CEGal4; UAS-FRT-STOP-FRT-Ricin; "CE; R/F" = JO-CEGal4; UAS-FRT-STOP-FRT-Ricin/eye-FLP.* "w: off" vs. "w: on" indicate no wind applied during the experiment, vs. wind-applied during the interval indicated by the gray bar in Fig. 3 d-g, for each genotype.

doi: 10.1038/nature07843 SUPPLEMENTARY INFORMATION

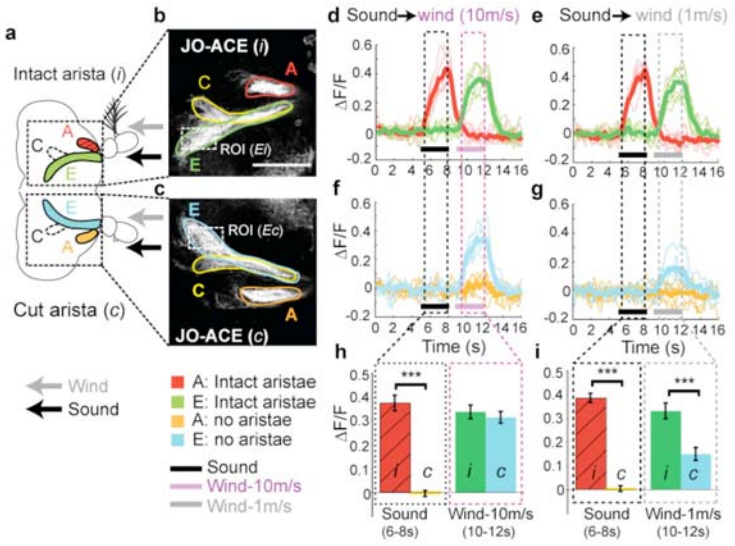

Supplemental Figure S4. Effect of arista ablation on wind and sound sensitivity.

(a) Schematic illustrating arista ablation experiment: The arista was ablated on one side and the contralateral arista was left intact and served as an internal control. (b,c) Expression of UAS-mCD8-GFP in zones A, C, and E on the arista-intact side (b) and arista-ablated side (c). ROI, region of interest for ΔF/F measurements in zone E, on either the arista-intact ("*Ei*") or arista-cut ("*Ec*") hemi-brains. Scale bar, 50μm. (d, f, h) Responses to sound (red and orange traces in dashed black box) and 10m/sec wind (green and blue traces in dashed purple box) in control (d) vs. arista-ablated (f) hemi-brains. (h) Comparison of integrated ΔF/F values in zone A vs. zone E in intact ("*i*") vs. cut ("*c*") hemi-brains during the stimulus periods (dashed black and purple box). Zone C is not activated because the wind is delivered from the front (0°). ***, $p<0.001$ (Repeated

doi: 10.1038/nature07843

measure ANOVA and Bonferroni multiple comparisons). (e,g,i) As in (d, f, h), except that wind was delivered at 1 m/s. Note that detection of airflow is less sensitive than that of sound to removal of the aristae. This could be because high velocity airflow (10m/s) can still move a3 relative to a2 in the absence of an arista, thus activating the JO-CE neurons.

doi: 10.1038/nature07843 SUPPLEMENTARY INFORMATION

Supplementary Footnote S1

J.S. Johnston and colleagues have measured wind speeds in the habitats of several wild-caught *Drosophila* species[1, 2] including both tropical and desert environments. In Kamuela, Hawaii, for example, *D. mercatorum* and *D. hydei* inhabit environments where trade winds blow in the range of 5-25 km/hr (1.4 m/s – 6.9 m/s), with an average velocity of 15 km/hr (4.17 m/sec); gusts over 35 km/hr (9.72 m/s) are not uncommon[1]. Wind speeds in the range of 0.46 – 4.64 m/s have been measured in the Arizona desert, the habitat of *D. nigrospiracula* [2]. We observed wind-induced suppression of walking in *D. melanogaster* between 0.7-1.6 m/s; these velocities are therefore well within the range of wind speeds measured in several *Drosophila* natural habitats. Wild-caught *D. mercatorum* and *D. hydei* exhibited locomotor arrest in the laboratory at wind speeds of 10 km/hr (2.8 m/sec) and greater[1], while wild-caught *D. mimica*, another Hawaiian species, exhibited locomotor arrest at air speeds between 6 and 7 km/hr (1.67 – 1.94 m/s)[4]. Anecdotal evidence that wind suppresses *Drosophila* locomotor activity in the wild derives from the observation that during occasional days in Hawaii when the trade winds stop, called "Kona" weather[1], *Drosophila* in flight are abundant, while during the trade winds very few *Drosophila* are observed in flight because most of them are immobilized on their *Opuntia* substrate (J.S. Johnston, personal communication). These data suggest that WISL is a naturally occurring behavior exhibited by *Drosophila* at wind speeds normally encountered in their wild ecological habitat. Johnston and colleagues speculate that this behavior may be the dominant environmental influence (rather than, e.g., temperature and humidity) affecting the dispersal of wild *Drosophila* populations,

doi: 10.1038/nature07843

and thereby an important determinant of their "genoclines," geographic gradients in gene frequencies[1, 4].

doi: 10.1038/nature07843 SUPPLEMENTARY INFORMATION

Supplementary Footnote S2

Our detection of distinct sound- and wind-evoked spiking responses in antennal nerve electrophysiological recordings (Fig. 1e-l) argues that the differential activation of sound- vs. wind-sensitive axons observed by GCaMP imaging is unlikely to be explained by local circuit interactions within the AMMC. Electrophysiological recordings from sound-selective locations in the antennal nerve usually revealed 1 or 2 spikes at the onset and offset of the wind stimulus (Fig. 1i, j). These brief spiking responses probably reflect the fact that phasically responsive JO neurons can be transiently activated by deflections of the aristae caused by wind (see Fig. 5).

doi: 10.1038/nature07843 SUPPLEMENTARY INFORMATION

Supplementary Footnote S3

Our calcium imaging experiments indicate that arista displacements triggered by the mechanical probe activate both wind- and sound-sensitive neurons (Fig. 5m, n), while the natural stimuli (wind and sound) activate these neurons in a mutually exclusive manner (Fig. 5f, g). Wind-sensitive neurons may not be activated by sound stimuli, because the magnitude of the antennal displacements produced by courtship song may be too small to evoke a detectable response (see also Supplementary Footnote S4). This hypothesis is supported by the fact that short-distance mechanical displacements of the aristae activate sound- but not wind-sensitive neurons (Fig. 5e, 0.01mm). Why, then, are sound-sensitive neurons not also activated by wind? In fact, our electrophysiological data indicate that they *are* activated, albeit very transiently: brief spiking responses are observed in sound-sensitive JO neurons at the onset and offset of the wind stimulus (Fig. 1j, blue traces). These transient spiking epochs are unlikely to produce sufficient accumulations of intracellular calcium to yield detectable GCaMP signals[24]. In contrast, the GCaMP signals elicited in sound-sensitive JO neurons by controlled mechanical displacements (Fig 5l-n, red lines) may reflect more extended spiking responses caused by damped oscillatory vibrations of the probe as it pushes against the arista. Finally, it is possible that wind- and sound-selective neurons differ in their sensitivity to the position, velocity or acceleration of the arista displacement caused by these different stimuli, as shown for limb chordotonal organs in the stick insect[25, 26]. The mechanical probe may not faithfully mimic these natural stimulus-specific differences in arista displacements.

doi: 10.1038/nature07843

Supplementary Footnote S4

We did not observe activation of zone C/E JO neurons by arista displacements below ~20 μm, while Kamikouchi et al.[22] observed activation with deflections as small as 1 μm, an estimated magnitude of the extent of deflection of the aristae that could be caused by the earth's gravitational field acting on the mass of the antenna. This difference is probably due to differences in the calcium imaging methods used in the two studies. Our approach measures activity in JO neuron axon terminals (using a GCaMP-1.3), which most likely reflects influx of extracellular Ca^{2+} due to spike firing. In contrast, Kamikouchi et al.[22] measure activity in JO cell bodies (using Cam2.1), which may reflect both Ca^{2+} influx and release from intracellular stores. In addition, the kinetics of the decay of Cam2.1 signal in response to transient Ca^{2+} increases is much slower (~2,000 ms) than that of GCaMP-1.3 (330 ms)[27], so that the method employed by Kamikouchi et al.[22] might integrates small changes in $[Ca^{2+}]_{in}$ and extend Cam2.1 responses over a longer period of time from the onset of the stimulus, than would GCaMP-1.3.

doi: 10.1038/nature07843 SUPPLEMENTARY INFORMATION

SUPPLEMENTARY MOVIE LEGENDS

Supplementary Movie 1

WISL behavior in *Drosophila melanogaster*. The movie shows the flies' baseline locomotor activity, followed by a brief mechanical startle, and finally wind-induced suppression of locomotion. The onset of mechanical startle and the onset and duration of wind treatment are indicated during the movie footage. 2x normal speed. (QuickTime (880KB).

Supplementary Movie 2 (a-e)

These movies show the responses of JO neurons to sound and wind stimuli in zones A, C and E, using the Gal4 line JO-ACE to drive expression of UAS-GCaMP. All movies are pseudo-colored to illustrate the magnitude of the calcium responses (ΔF) (red, green, and blue indicates the maximum, intermediate, and minimum, respectively). All movies are 3x normal speed. (a) Response of zone A neurons during modified courtship song presentation. Note that the zones C and E show no responses to song. (b) Response of zone E neurons during wind (0^{o}) stimulation. Zone C is not active because it responds to wind from 180^{o} (see Supplementary movie 3). Note that zone A is not activated during wind stimulation. (c) Response of zone A and E neurons to sequential presentation of courtship song and wind (0^{o}), respectively. (d) Response of zone A and E neurons to simultaneous presentation of courtship song and wind. (e) Control (neither courtship song nor wind presented). QuickTime (1.2MB/ each).

doi: 10.1038/nature07843 SUPPLEMENTARY INFORMATION

Supplementary Movie 3 (a-e)

These movies show the responses of zone C and E neurons to wind delivered from different directions, using the Gal4 line JO-CE to drive expression of GCaMP. See Supplementary Movie 2 legend for details. (a) Response during wind (0^o) presentation. Note that zone E is activated in both hemi-brains. (b) Response during wind (45^o) presentation. Zone E is activated in both hemi-brains, similar to the wind (0^o) responses. (c) Response during wind (180^o) presentation. Note that zone C is activated in both hemi-brains. (d) Response during wind (90^o) presentation. Note that zone C and E neurons are activated in the ipsi- and contra-lateral sides, respectively. (e) No stimulus control. QuickTime (2.7MB/ each).

Supplementary Movie 4 (a-e)

These movies were made to show the direction of aristae deflection during the presentation of wind stimuli, under the same conditions used to obtain the data illustrated in Supplementary Movie 3. The movies are played at actual (real-time) speed. (a) Both aristae move anteriorly when wind is presented from the posterior (180^o). (b) Both aristae move posteriorly when wind is presented from the front (0^o). (c) Both aristae move posteriorly when wind is presented at a 45^o angle. (d) The aristae move anteriorly on the hemi-brain ipsi-lateral to the stimulus and posteriorly on the contra-lateral side, when wind is presented at a 90^o angle (in this case from the right). (e) Control condition in which no wind is presented. QuickTime (450KB/each).